ABSTRACT

Title of Thesis: HYDROLOGIC DRIVERS OF SOIL ORGANIC CARBON STORAGE AND STABILITY IN FRESHWATER MINERAL WETLANDS

Anna I. Kottkamp, Master of Science in Marine, Estuarine, and Environmental Science, 2019

Thesis Directed by: Dr. Margaret Palmer, Department of Entomology, Co-Advisor
Dr. Kate Tully, Department of Plant Sciences and Landscape Architecture, Co-Advisor

Mineral wetlands comprise most of historic wetland loss, yet few studies focus on mineral wetland soil organic carbon (SOC). We explore SOC across continuous hydrologic gradients within and among seasonally flooded mineral wetlands. First, we quantify SOC stabilization (e.g., organo-mineral associations and aggregates) across a wetland–upland gradient. Second, we examine relationships between hydrologic regime and SOC stocks among wetlands. From wetland–upland, saturation was highly variable in the transition zone. Organo-mineral associations peaked in the transition zone while large macroaggregate SOC declined from wetland–upland. Across wetlands, indicators of drying (e.g., minimum water level and summertime recession rate) were more related to SOC than inundation duration. From wetland basin–upland, SOC stocks were significantly related to both mean water level and relative elevation. We highlight relationships between SOC and the dynamic hydrology of wetlands, emphasizing the need for research on how changing hydrologic regime may influence mineral wetland SOC.

HYDROLOGIC DRIVERS OF SOIL ORGANIC CARBON STORAGE AND STABILITY IN FRESHWATER MINERAL WETLANDS

by

Anna I. Kottkamp

Thesis submitted to the Faculty of the Graduate School of the
University of Maryland, College Park, in partial fulfillment
of the requirements for the degree of
Master of Science
2019

Advisory Committee:
Dr. Margaret Palmer, Co-Chair
Dr. Kate Tully, Co-Chair
Dr. Martin Rabenhorst
Dr. Patrick Megonigal

Dedication

This thesis is dedicated to the young scientists of the future, who will always build on and challenge the science of the past. I would also like to dedicate this thesis to my family. Thank you to my loving parents, Tam and Andy, for gently encouraging me in everything I do and for being my home, even from afar. Thank you to my siblings, Kate and John, for always listening and laughing with me. And, of course, I am endlessly grateful to my partner, Jason, for the love, joy, grace, and adventure you bring to our life together. This work would not be possible without all your love and faith in me.

Acknowledgements

Behind every sentence in this thesis is a team of people who worked alongside me, cheered me on, and offered their time and knowledge to make this research a reality. Thank you all.

I would like to thank my co-advisors, Kate and Margaret, for their support in the research process and for mentoring me as women in science. I also thank my committee members: Dr. Martin Rabenhorst for sharing his wetland wisdom with me and for supporting me in the lab, and Dr. Patrick Megonigal for his thoughtful suggestions and encouragement.

I would also like to thank the National Socio-Environmental Synthesis Center (SESYNC) for the many learning opportunities provided there, including funding and professional development.

Lastly, and most importantly, I would like to thank every person who accompanied me daily in the trenches of the lab, field, and office. I am especially grateful to Alec Armstrong, Graham Stewart, and Christine Maietta for their innumerable hours spent wondering, speculating, and chatting together about everything from “what is a wetland?” to what it means to be a good scientist to how to survive graduate school. Your time and thoughtfulness through this entire research process made this work possible and elevated it beyond anything I could have done alone. I am also thankful to the other sages of the Palmer Lab, Nate Jones and Kelly Hondula, for their advice and tireless work to bring my data standards up to code. I would also like to thank the Tully lab, especially Dani Weissman, Elizabeth de la Reguera, and Cullen McAskill, for their support in the lab and for the long chats about aggregates and iron. Finally, I am especially grateful to the undergraduate interns who brought their joyfulness and dedication to this project, especially Bianca Noveno, Maggie Tan, Abigail Toretsky, and Julianna Greenburg. I learned from each and every one of you, and I look forward to carrying your lessons to the next adventure.

Table of Contents

List of Tables

List of Figures

Chapter 1: Hydrologic drivers of soil organic carbon stabilization in freshwater mineral wetlands

Abstract

Freshwater mineral wetlands store significant soil organic carbon (SOC) globally yet are vulnerable to degradation or loss from land use and climate change. Though physiochemical protection is a dominant control on SOC residence time in upland soils, the role of stabilization mechanisms in wetland soils is understudied. Seasonally flooded freshwater mineral wetlands dry annually, which may promote physiochemical stabilization. We investigated the relationship between SOC stabilization and hydrology across the aquatic–terrestrial interface of five seasonally flooded freshwater mineral wetlands (Maryland, U.S.A.). At each wetland, we monitored water level and collected samples at five points along a transect spanning from wetland edge to upland. We quantified organo-mineral associations and aggregate stability in mineral horizons of each transect point to 50 cm depth. From wetland to upland SOC decreased but dithionite-extractable iron (Fe) concentrations increased. Organo-mineral associations were highest in the transition zone and upland, whereas large macroaggregates contained the most SOC in the wetland and transition zone. Macroaggregates were associated with a greater proportion of total SOC than organo-mineral associations. Overall, our results highlight differences in SOC stabilization mechanisms across the hydrologically dynamic transition zone between wetlands and uplands, with potential implications for wetland SOC vulnerability water levels are altered in future.

1. Introduction

Wetlands are a major component of the terrestrial carbon (C) cycle and sequester disproportionately high C stocks for their area (Mitsch et al. 2010, Mitsch and Gosselink 2015). Given the high C sequestration and potential to help offset rising C emissions, wetland soils are the focus of current conservation and restoration efforts (Griscom et al. 2017). Research to date has primarily focused on wetlands with organic soils, where continuously anoxic conditions suppress organic matter decomposition and are a strong environmental control on soil organic C (SOC) storage (Mitsch and Gosselink 2015). In contrast, less is known about the controls on SOC sequestration in mineral wetlands, which make up 38% of wetland area yet 80% of historic losses to wetland area globally (Bridgham et al. 2006). Some mineral wetlands are seasonally flooded and experience dry, oxic soil conditions on an annual basis (Brooks 2005, Cowardin et al. 2005). Soil C of mineral soil wetlands may be less vulnerable than organic soil wetlands to decomposition and loss during periodic drying if there are stabilizing interactions between SOC and mineral surfaces, as have been shown in upland soils (Kögel-Knabner et al. 2008). However, little is known about the role of SOC physiochemical stabilization in seasonally flooded mineral wetlands.

Research on physiochemical stabilization of SOC has almost entirely focused on terrestrial soils (Grandy and Robertson 2007; Six, Elliott, and Paustian 2000; Blankinship and Schimel 2018), and generally shows that interactions with soil structure and surfaces protect SOC from decomposition by restricting microbial access (Schmidt et al. 2011, Lehmann and Kleber 2015). For example, macro- (>250 μm) and micro- (<250 μm) aggregates of soil particles promote anoxic microsites within which SOC is occluded and rendered spatially inaccessible to microbial uptake (Ebrahimi and Or 2016, Keiluweit et al. 2018). In terrestrial soils, aggregate size classes have been linked to fractions of SOC with distinct ages and chemical composition; macroaggregates are a dynamic, younger fraction closely related to plant detritus while microaggregates represent a more biologically processed, older fraction (von Lützow et al. 2006;

von Lützow et al. 2007; Six et al. 2004). Within aggregates, SOC that may otherwise be readily mineralized can instead persist for years to centuries, though macroaggregates may stabilize SOC for shorter time periods than microaggregates (von Lützow et al. 2006; Puget, Chenu, and Balesdent 2000).

In terrestrial soils, organo-mineral associations are also known to play an important role in SOC physiochemical stabilization. Organo-mineral associations involve strong interactions between SOC and iron (Fe) or aluminum (Al) (hydr)oxides that stabilize SOC for up to centuries (Torn et al. 1997, Kleber et al. 2005, Mikutta et al. 2006, Wagai and Mayer 2007, Kögel-Knabner et al. 2008). The relative importance of organo-mineral associations in SOC stabilization is determined by the amount of reactive minerals in the soil and the distribution of mineral species which have distinct interactions with SOC. Different types of organo-mineral associations have varying stabilization strengths, ranging from strong adsorption of SOC to Fe (hydr)oxides to weaker chelation of SOC with Fe^{2+} (Kaiser and Guggenberger 2000; Coward, Thompson, and Plante 2017). Poorly crystalline Fe more readily forms organo-mineral complexes than crystalline Fe (Wahid and Kamalam 1993), but these associations are likely to be transient (Hall et al. 2018). Conversely, associations between crystalline Fe and SOC are more stable in the long-term, though much of this research comes from highly weathered tropical soils (von Lützow et al. 2006; Hall, Berhe, and Thompson 2018).

Physiochemical stabilization may be promoted by the dynamic hydrology and mineral soils of seasonally flooded wetlands, which may be especially relevant at wetland perimeters. The perimeters of seasonally flooded wetlands are at the aquatic–terrestrial interface and are better characterized as “transition zones” due to frequent seasonal changes in water levels. Previous work has shown that transition zone soils become dry with water table drawdown during the growing season and contain intermediate C storage compared to basin and upland soils, though these studies do not quantify physiochemically stabilized SOC (Webster et al. 2011; Fenstermacher 2012; LaCroix et al. 2019). While the transition zone makes up only a small

portion of the area of an individual wetland, the unique hydrology and high perimeter to area ratio of small wetlands may contribute to important biogeochemical functions on the landscape scale.

The dynamic hydrology of wetland transition zones may promote SOC persistence through aggregation and organo-mineral associations. Experiments with agricultural soils suggest that aggregate formation and stability are enhanced by alternating wet and dry conditions, organic matter inputs, roots and fungal hyphae, and clay content, all of which change across the transition zone of seasonally flooded wetlands (Denef et al. 2001; Park, Sul, and Smucker 2007; Blankinship et al. 2016). Dynamic hydrology also influences the strength of organo-mineral associations. For instance, poorly crystalline Fe species dominate in alternating wet-dry conditions (Wahid and Kamalam 1993). Poorly crystalline Fe species are also more likely to be solubilized and release C under reducing conditions than crystalline Fe, which may limit SOC stabilization with poorly crystalline Fe species to seasonally dry soil conditions. Physiochemical stabilization of SOC in transition zones of seasonally flooded wetlands may serve as an important yet currently unquantified SOC sink.

Given the gaps in understanding how physiochemical stabilization mechanisms influence SOC sequestration of seasonally flooded wetlands, our objectives were to (1) quantify SOC and hydrologic characteristics from wetland to upland and (2) examine the relative importance of aggregation and organo-mineral associations at the terrestrial-aquatic interface of seasonally flooded wetlands. We investigated the change in stabilized C fractions at five seasonally flooded wetlands across a gradient of decreasing mean water level using selective Fe extractions and aggregate sieving. We hypothesize that the proportion of total C associated with macroaggregates and Fe will be greatest in the transition zone where hydrologic characteristics are most variable.

2. Methods

2.1 Study sites

The study was located on the Delmarva Peninsula in eastern U.S.A., which is bordered by the Chesapeake Bay on the west and the Atlantic Ocean on the east. Mean monthly temperature

ranges from 1.3 °C (January) to 25.1 °C (July). Mean annual precipitation is 1105 mm (PRISM average from 1981-2010; Oregon State University 2019) and is distributed evenly through the year on average. Study wetlands are on two properties (<5 km apart) managed by The Nature Conservancy which contain numerous seasonally flooded freshwater wetlands. Water table fluctuations are primarily driven by seasonal changes in evapotranspiration, with maximum hydrologic expression in late spring and general wetland drawdown over the growing season from May through September (Brooks 2005).

We selected five seasonally flooded mineral wetlands with similar soils and vegetation (Fig. 1.1B). The dominant soil map unit is the Hammonton-Fallsington-Corsica complex, Order: Ultisols, Suborders: Udults and Aquults (Soil Survey Staff, Natural Resources Conservation Service). Preliminary work showed very acidic soils (pH: 3.4–4.3); therefore, calcium carbonates were assumed to be negligible. In a preliminary dithionite-citrate-bicarbonate extraction of total aluminum (Al; Darke and Walbridge 1994), we found low concentrations of Al which were relatively unchanged across the transect (mean ± standard error: 2.8 ± 0.3 mg Al g^{-1} soil; data not shown). Surrounding forest is comprised of *Acer rubrum*, *Quercus phellos, Liquidambar styraciflua*, and *Nyssa sylvatica* overstory with *Ilex opaca, Magnolia virginianica, Clethra alnifolia,* and *Vaccinium corymbosum* understory.

2.2 Field methods

2.2.1 Transect location selection

At each wetland, we established one 20–25 m transect with five evenly spaced points (4–5 m apart) extending from the "basin edge" (transect point A) to the "upland" (transect point E; Fig. 1.1A*).* The basin edge was designated as the minimum extent of ponded water observed during the 2017 water year. The upland was designated as the higher elevation sandy rim area around a wetland (Stolt and Rabenhorst 1987a); specifically, the upland transect point was located where (a) upland trees and understory vegetation were present and (b) no hydromorphic soil features were found in the upper 50 cm of the soil profile.

2.2.2 Hydrologic conditions

To characterize hydrologic conditions across the transition zone, we monitored water levels relative to soil surface in water year 2018 (October 1, 2017–September 31, 2018). Two wells were installed at each study wetland in September 2017, one to a depth of 2 m near the upland transect point and one to a depth of 1 m close to the wetland center. We collected water level data at 5 min intervals via HOBO water level data loggers (Onset Computer Corporation, Bourne, MA). Water levels from each well were averaged to daily timesteps and used to interpolate water level at each transect point, assuming a linear change in water table altitude from the point where water level intersects with ground surface to the upland well (Fig. 1.1A; Jones 2019). Though seasonally flooded wetlands are known to experience groundwater mounding and troughing throughout the year (Phillips and Shedlock 1993, Rosenberry and Winter 1997), we assumed linearity of water table altitude given the relatively small spatial scale and low-relief landscape. Interpolated water levels for each transect point were comparable to observed water levels measured at transect points biweekly from May to August 2018 (R^2=0.87, Supplemental S1). Higher, more positive values for water level indicate wetter conditions at the wetland edge, while lower, more negative water levels indicate drier conditions in the upland.

For the hydrologic analysis, we focus on continuous (i.e., mean water level) data instead of categorical transect point to more directly characterize the relationship between physiochemical stabilization and hydrologic conditions. All hydrologic metrics indicate consistently wet conditions at transect points A and B from 0–1.0 m soil depth, dry conditions at transect point D and E from 0–1.0 m soil depth, and variable hydrologic conditions consistent with a transition zone around transect point C (Fig. 1.1A; Table 1.2). Transect point A (wetland edge) was flooded (water level >0) for a mean of 56% of the year and transect point B was flooded for 20% of the year. At the upland end of the transect, points D and E were never flooded and water level was < -0.5 m below the soil surface for nearly the entire water year. Water level was > -0.5 m from the soil surface for one-third of the water year at transect point C (Table 1.2).

Mean water level at individual sample points ranged from -1.2 m at transect point E (below the soil surface; drier soil) to 0.1 m at transect point A (above the soil surface; wetter soil).

Reducing conditions were measured by installing Fe-oxide painted Indicator of Reduction In Soils (IRIS) films (Rabenhorst 2018). At transect points A–D, five replicate films were installed to 50 cm depth on April 5-6, 2019 and removed after 30 days. We conducted a preliminary study in April 2018 by installing IRIS films at all transect points and found no Fe oxide paint removal (i.e., no reducing conditions) at transect points D and E. Therefore, we assumed 0% oxide paint removal at transect point E in April 2019. For each film, we recorded the maximum percent paint removal within a 10 cm zone and took the mean of the three replicate films with the greatest oxide removal at each sample point, following Castenson and Rabenhorst (2006). Images were processed with Adobe Photoshop version 20.0.4 (Adobe Creative Cloud, 2019) and Matlab version 9.6 (Mathworks, 2019).

2.2.2 Soil sampling

Soils were sampled to 1.0 m depth in June 2018 at five transect points at each wetland and separated by pedogenic horizon (Supplemental S4). We collected soils with a gouge auger to 50 cm depth and with a bucket auger from 50–100 cm depth. Three replicate cores were taken within 0.5 m of established transect points and replicate horizon samples were gently homogenized to obtain a representative sample for each transect point. A 200 g subsample was removed from each horizon for aggregate analysis. The remaining horizon samples were fully homogenized and transported to lab in a cooler.

2.3 Soil chemical analysis

Soil samples were analyzed by pedogenic horizon (5–6 horizons at each transect point) for pH, texture, and bulk C and N. Field moist samples were stored in coolers and processed within 48 h of collection. Soil pH was measured on a field moist subsample in a 1:2 ratio of soil to 0.01 *M* calcium chloride solution (Maietta et al. 2019). Bulk soils were subsequently air dried, ground and sieved to 2 mm, and stored for analysis of texture and Fe. Texture was determined for

mineral horizons by Brookside Laboratories (New Bremen, OH) using the hydrometer method (Gee and Bauder 1986). Bulk C (C_{bulk}) and N were measured using dry combustion (LECO CHN-2000 analyzer; LECO Corp, St. Joseph, MI).

2.3.1. Soil Fe and C extractions to determine organo-mineral complexation

We measured total Fe concentration on all mineral horizon samples in the upper 50 cm using a dithionite-citrate-bicarbonate (DCB) extraction of total extractable Fe (hydr)oxides (Fe_{DCB}) following the method by Darke and Walbridge (1994). A separate extraction with acid ammonium oxalate (AAO) extracted poorly crystalline Fe (hydr)oxides (Fe_{AAO}; Darke and Walbridge 1994, Hall et al. 2018). For both extractions, supernatant was filtered through a 0.45 µm nylon filter (Tisch Scientific) and analyzed on an atomic absorption (AA) spectrometer on an air-acetylene flame (Perkin Elmer, Waltham, MA).

We analyzed mineral horizons from the upper 50 cm of soil for C associated with Fe (hydr)oxides using inorganic Fe extractions (Darke and Walbridge 1994, Lopez-Sangil and Rovira 2013, Wagai et al. 2013, Maietta et al. 2019). Protocols were developed from Maietta et al. (2019) to directly measure C associated with each solubilized Fe fraction. We conducted sequential extractions with potassium chloride (KCl) and sodium pyrophosphate (Pyro; $Na_4P_2O_7$) on the same 0.5 g soil sample. A dilute KCl solution was used to prevent-overestimating organo-mineral associations by removing labile organic matter from exchangeable sites; however, these data are not discussed further as the amount of C was associated with this fraction was negligible (range: <0.4 mg C g^{-1} soil). Sodium pyrophosphate solubilizes Fe complexed with organic matter (Fe_{Pyro}), which is considered chelated Fe (e.g., Coward, Thompson, and Plante 2017). On a separate 0.5 g dried soil we conducted a sodium dithionite-HCl (Dit-HCl) extraction (Maietta et al., 2019). Sodium dithionate with HCl is an inorganic method to remove total Fe oxides ($Fe_{Dit-HCl}$) and is intended to mimic the DCB extraction of total Fe without using an organic buffer that would prevent us from measuring C in the extractant (Supplemental S5). Extractant C concentrations represent the amount of C associated with each Fe species (Table 1.1).

Extraction procedures were as follows: a 0.5 g subsample of dried, ground soil was combined with 25 mL of extractant by shaking at 47 rpm for 16 h on a reciprocal shaker table (Model E6000, Eberbach Corporation, Ann Arbor, MI). Extractions were centrifuged for 5 min at 12,000 rpm and supernatants were poured into clean HDPE bottles. The same subsample was extracted at least one additional time by adding 25 mL of the extractant and shaking on high for 1 h to ensure total Fe removal. Extractions were centrifuged again, and the second supernatant was combined with the first. The volume of the combined supernatants was measured via a serological pipette and then syringe filtered to 0.45 μm using a nylon filter (Tisch Scientific, North Bend, OH). Combined, filtered supernatants were stored at 4 °C until analysis of total organic C concentration with a TOC/TN Analyzer (Shimadzu Corporation, Kyoto, Japan; Sugimura and Suzuki 1988) and Fe concentration with AA spectrometry as above.

2.3.2 Water-stable aggregate fractionation to determine physical protection of C in soils

We examined water-stable aggregates within mineral soils of the upper 50 cm of the soil profile across transect points via the wet sieving protocol established by Six et al. (2000) and modified for use in wetland soils by Maietta et al. (2019). Across the transect, some soils were relatively dry while others were saturated at the time of collection. Dry soils were passed through a 4.75 mm sieve within 24 h of sampling and dried for 7 days at room temperature (Six et al., 2000). Wet soils were dried for three days at room temperature before passing through a 4.75 mm sieve. After 3 days, soils were solid enough to be broken gently by hand, yet soft enough to pass through the sieve without excessive force or rewetting. Very large macroaggregates that formed during the drying process were gently broken by hand to pass through the sieve. Soils were dried for 7 days at room temperature and stored for analysis.

Soils were wet-sieved following Six et al. (2000) within two months of collection. This procedure separated four size classes: (1) large macroaggregates ($\geq$ 2000 μm), (2) small macroaggregates (250-2000 μm), (3) microaggregates (53-250 μm), and (4) silt/clay minerals (<53 μm). Briefly, soils were slaked by submerging in deionized water for 5 min. Soils were then

sieved 50 times throughout 2 min on a 2 mm sieve. Water-stable aggregates remaining on top of the sieve were retained as the size class larger than the sieve (i.e., >2000 μm), while soil and water that passed through the sieve were carried to the next step. We repeated this sieving process with sequential sieves of 250 μm and 53 μm. Floating particulate organic matter was skimmed off the surface of the large and small macroaggregate size classes. Samples were dried at room temperature with fans until all water evaporated, then dried in a 65 °C oven for 7 days before weighing. Large and small macroaggregates were gently crushed, and rocks and roots were separated with a 1 mm sieve. The remaining mass for each size class was weighed and analyzed for total C and N using dry-combustion (LECO CHN-2000 analyzer; LECO Corp, St. Joseph, MI). Finally, we measured sand content in large macroaggregates, small macroaggregates, and microaggregates on a 5 g subsample from using the pipette method and subtracted sand mass to avoid overestimation of aggregate mass (Elliott et al. 1991, Six et al. 2002).

2.4. Calculations

We calculated the percent of total soil Fe (Fe_{DCB}) that is poorly crystalline (Fe_{AAO}), where higher Fe_{AAO}/Fe_{DCB} indicates that a greater proportion of Fe species are poorly crystalline and therefore more likely to be involved in organo-mineral associations (Hall et al. 2018; Coward et al. 2017; Table 1.1)

$$\text{Percent poorly crystalline Fe} = \frac{Fe_{AAO}}{Fe_{DCB}} \times 100 \quad \text{Eq. 1}$$

We also calculated the proportion of C in bulk soil (C_{bulk}) extracted by either Pyro (C_{Pyro}) or Dit-HCl ($C_{Dit\text{-}HCl}$; Table 1.1). This normalized value allowed us to compare the relative proportion of C stabilized by organo-mineral associations while accounting for the differences in C_{bulk} across samples.

$$\text{Normalized Pyro-extracted C (mg C g-1 C)} = \frac{C_{Pyro}}{C_{bulk}} \quad \text{Eq. 2}$$

$$\text{Normalized Dit-HCl-extracted C (mg C g}^{-1}\text{ C)} = \frac{C_{Dit-HCl}}{C_{bulk}} \quad \text{Eq. 3}$$

The ratio of extracted C to extracted Fe for each extraction indicates the type of organo-mineral association. The maximum ratio of C:Fe for sorptive associations is 0.22 g C g^{-1} Fe; therefore, C:Fe <0.22 indicates C sorbed to Fe (Kaiser and Guggenberger 2007; Wagai and Mayer 2007). Conversely, co-precipitation and chelation of organic materials with Fe oxides produce organic associations with higher C:Fe (Wagai and Mayer 2007, Coward et al. 2017).

$$C_{Pyro}{:}Fe_{Pyro}\ (g\ C\ g^{-1}\ Fe) = \frac{C_{Pyro}}{Fe_{Pyro}} \quad \text{Eq. 4}$$

$$C_{Dit\text{-}HCl}{:}Fe_{Dit\text{-}HCl}\ (g\ C\ g^{-1}\ Fe) = \frac{C_{Dit-HCl}}{Fe_{Dit-HCl}} \quad \text{Eq. 5}$$

For aggregates, we calculated both aggregate mass ($mass_{aggregate}$) and sand-corrected aggregate mass ($mass_{aggregate,\ sand\text{-}free}$). Aggregate associated C ($C_{aggregate}$) is expressed on a mass basis out of bulk soil excluding rocks >1 mm ($mass_{total}$), equivalent to the concentration of aggregate-associated C (Eq. 6).

$$C_{aggregate}\ (g\ C\ g^{-1}\ soil) = \frac{Aggregate\ C \times mass_{aggregate}}{mass_{total}} \quad \text{Eq. 6}$$

We corrected aggregate C measured by dry-combustion ("Aggregate C" in Eq. 6) for sand content (Aggregate $C_{sand\text{-}free}$). Sand correction is useful to interpret C across samples of varying sand content (Márquez et al. 2004); however, we decided not to use sand-free values in calculations to compare C with organo-mineral association data, which is out of bulk soil (e.g., not g C per g "sand-free" soil).

Finally, we again calculated the proportion of total C_{bulk} for the sample that was associated with each aggregate size class. First, we calculated Aggregate C * $mass_{aggregate}$ for each size class, then we divided by the sum (total) of Aggregate C * $mass_{aggregate}$ for the entire sample ("$C_{aggregate}/C_{bulk}$", Table 1.1). This normalized value allows us to compare the proportion of C in each aggregate size class out of total C, relativized to differences in C_{bulk} of each sample across the transect.

$$\text{Normalized aggregate-associated C (mg C } g^{-1}\text{ C)} = \frac{Aggregate\ C \times mass_{aggregate}}{\sum Aggregate\ C \times mass_{aggregate}} \quad \text{Eq. 7}$$

2.5 Use of methods from upland soils to characterize physiochemical stabilization in wetland soils

Organo-mineral extractions and aggregate size class separation are operationally defined, as such, there are caveats to their use in wetland soils. Drying soils before aggregate analysis standardizes soils and allows soils to be stored before analysis while avoiding the effects of freezing on SOC. Standardization is necessary because aggregate stability in field-moist soils may be a function of antecedent water content (Gollany et al. 1991). However, soil drying may favor the stability of macroaggregates (Beare and Bruce 1993). Sample drying may also cause rapid abiotic oxidation of reduced Fe, which may strengthen organo-mineral interactions by forcing contact between soil particles (Kaiser, Kleber, and Berhe 2015). These methods were selected for reproducibility and comparison with non-wetland soils; however, method development is necessary to understand the ecological significance in wetland soils of C fractions studied here. While stabilization analysis must be understood in the context of sample pretreatment, the real-world importance of these mechanisms may be greatest when wetland soils are seasonally dry and are not protected by the environmental stabilization of anoxic conditions.

2.6 Statistical approach

We conducted an analysis of variance (ANOVA) test to determine how hydrologic variables change across categorical transect points from wetland to upland. Separate ANOVAs were conducted to determine the effect of transect point on elevation, mean water level, maximum and minimum water level, duration of water level > -0.5 m, saturation events to -0.5 m, and IRIS removal (Table 1.2). We tested differences between transect points with Tukey's honestly significant differences (HSD) test.

While we collected soils across a transect at specific points from the wetland basin to the upland edge (e.g., A–E; Fig. 1.1), simply comparing differences across categorical transect points fails to capture the unique hydrologic conditions and variations that drive soil chemical and physical changes at each point. Therefore, we used mean water level at each transect point as a

continuous hydrologic variable to explicitly test the role of hydrology in C stabilization across wetlands. Our main effect for statistical testing was mean water level during water year 2018. A higher mean water level indicates wetter soils; a lower, more negative water level indicates drier soils. We also tested the effect of horizon depth. As the exact depth of each soil horizon varied, we categorized horizons in order of increasing depth: organic horizons (O); first mineral horizon (1); second mineral horizon (2); third mineral horizon (3); fourth mineral horizon (4). O horizons were excluded from this analysis because O horizons are relatively high in fresh organic matter inputs and low in mineral matrices necessary for stabilization.

To test the effect of hydrology and soil horizon depth (e.g., differences among horizons 1–4) on % C_{bulk} and $C:N_{bulk}$, we used linear mixed effects (LME) models with the *lmer* package in R (Bates et al. 2015). In each case, mean water level (continuous) and horizon depth (categorical) were fixed effects and wetland was the random effect. For each LME, degrees of freedom for the conditional F-test were calculated with the *lmerTest* package using the Kenward-Roger approximation from the package *pbkrtest* (Halekoh and Højsgaard 2014, Kuznetsova et al. 2017). We used backwards model selection following Zuur et al. (2009) to determine the best fixed effects structure. Random intercepts by wetland were included as part of the study design (Barr et al. 2013). Assumptions of normality and homogeneity of variance of model residuals were checked graphically. Full model results are in Supplemental Materials (Supplemental S6).

We focused the remainder of our analysis of Fe and C dynamics within the upper two mineral soil horizons (i.e., 1 and 2), which comprise the top 50 cm of soil and experience the largest fluctuations in water level (Fig. 1.1A). We henceforth refer to these two mineral horizons as "upper soils." To test the effect of water level and soil horizon depth (e.g., difference between horizon 1 and horizon 2) on organo-mineral associations and aggregate-associated C, we again used LME models following the steps detailed above. Separate LMEs were conducted on upper soils for pH, clay (%), poorly crystalline Fe (Fe_{AAO}/Fe_{DCB}), normalized organo-mineral associated

C (C_{Pyro}/C_{bulk}, $C_{Dit\text{-}HCl}/C_{bulk}$), aggregate-associated C and C:N ($C_{aggregate}$, $C{:}N_{aggregate}$), and normalized aggregate-associated C ($C_{aggregate}/C_{bulk}$; Table 1.1).

Initial analysis revealed that Fe dynamics in the upper soils (0–50 cm) showed different patterns between soils that experienced wet conditions throughout the year ("wet upper soils;" mean water level > -0.5 m) and soils that experienced dry conditions throughout the year ("dry upper soils;" mean water level ≤ -0.5 m). Thus, for soil Fe species and associated C (e.g., Fe_{AAO}, Fe_{DCB}, Fe_{Pyro}, $Fe_{Dit\text{-}HCl}$, C_{Pyro}, $C_{Dit\text{-}HCl}$), we performed LMEs on these two groups separately to better describe the effects of hydrology on Fe species.

To test the association between Fe and C extracted by the inorganic Fe extractions (e.g., Dit-HCl or Pyro), we used a multiple linear regression, again conducting separate analysis for wet upper soils and dry upper soils. The global model consisted of predictor variables of either $Fe_{Dit\text{-}HCl}$ or Fe_{Pyro}, horizon depth, and the interaction, with the response variable of either $C_{Dit\text{-}HCl}$ or C_{Pyro}. We conducted a backwards selection by removing nonsignificant terms and refitting the model to the final, reduced model ($P < 0.05$).

Finally, we tested the effect of aggregate size class on aggregate-associated C ($C_{aggregate}$, $C{:}N_{aggregate}$, $C_{aggregate}/C_{bulk}$) in upper horizons with ANOVA and post-hoc Tukey's HSD tests.

Statistical analysis was conducted using R statistical software v3.5.3 (R Development Core Team). Data organization and plotting was conducted with the packages *tidyverse* and *cowplot* (Wickham 2017, Wilke 2019).

3. Results

3.1 Hydrologic variables across transect points.

Temperature in water year 2018 was within 30-year means. Mean monthly temperature ranged from -1 °C (January) to 26 °C (July; Fig. 1.2A). Precipitation was higher than average, with 1366 mm precipitation over the year. Low precipitation in November and December led to a relatively dry fall, while high precipitation in July and September led to a relatively wet summer.

During springtime peak water levels, soil reducing conditions (measured by reduction of Fe oxides on IRIS films in April 2019) were highest at transect points A and B (>95% reduction; Table 1.2). The range of reducing conditions at transect point C (range: 0.2–65% reduction) indicates the heterogeneity of oxygen availability within the soil profile in the transition zone. Reducing conditions were lowest at transect point D (<1% Fe oxide reduction) and were assumed to be 0 at transect point E.

Water level at each sample point varied approximately 1 m over the year, indicating dynamic inundation typical for seasonal wetlands of this region (Fig. 1.2B). Across all wetlands, water levels rose from November to February and remained high until May. Water levels fell with summer drawdown from June to September, though water levels rose sharply in response to large storm events in July and September. Saturation within the upper 0.5 m of the soil profile was most variable across wetlands at transect points B and C (the transition between wetland and upland; P=0.00088; Table 1.2). Specifically, the number of individual saturation events within the upper 0.5 m was highest at transect points with a mean water level of -0.5 m (Supplemental S2). Since water level varied not only among transect points but within a given transect point (e.g., all C transect points), we present results as a function of mean water level instead of transect point for the remainder of this paper. Thus, when we refer to "dry upper soils", we include the upper two mineral horizons (above 50 cm) at wetland sample points with mean water level ≤ -0.5 m, which include samples from transect points C, D, and E. In contrast, "wet upper soils" come from sample points with mean water level > -0.5 m, which includes samples from transect points A, B, and C.

3.2 Basic soil properties

Soil C_{bulk} concentration decreased with decreasing mean water level (i.e., drier soils; P <0.0001, Supplemental S6A; Supplemental S3A). In contrast, soil C:N_{bulk} increased with decreasing water level (P <0.0001, Supplemental S6B; Supplemental S3B). Toward the upland,

clay (%) decreased (P <0.0001, Supplemental S6C; Supplemental S3B) while % sand tended to increase (i.e., decreasing mean water level).

Bulk soil C (%) decreased down the soil profile, as is typical for soils not affected by fluvial processes (P <0.0001, Supplemental S6A). There were no significant differences in clay content between upper soil horizons (i.e., horizon 1 and 2). There was no significant interaction between mean water level and soil horizon for C_{bulk} concentration or clay content, but there was a significant interaction for soil pH (P=0.0017, Supplemental S6D; Supplemental S3D). In horizon 1, soil pH decreased with decreasing mean water level (i.e., drier soils), but in horizon 2, pH increased along the same gradient.

3.3 Soil Fe and C dynamics

The effect of water level on the mineral soil Fe species was analyzed separately for wet upper soils and dry upper soils. In wet upper soils, both poorly crystalline Fe_{AAO} and total Fe_{DCB} concentrations were low and were not related to mean water level (Fig. 1.3A). In dry upper soils, total Fe (Fe_{DCB}) concentrations were higher than in wet upper soils, but total Fe decreased with decreasing mean water level (i.e., drier soils; P<0.0001, Supplemental S6E; Fig. 1.3A). Similarly, poorly crystalline Fe_{AAO} concentrations were highest where mean water level was -0.5 m below the soil surface and decreased toward the upland (i.e., drier soils, P <0.0001, Supplemental S6F; Fig. 1.3A).

The percent poorly crystalline Fe (Fe_{AAO}/Fe_{DCB}) declined with decreasing mean water level (P <0.0001, Supplemental S6G; R^2=0.68, Fig. 1.3B). When mean water level was above soil surface (>0 m), nearly 100% of total Fe (Fe_{DCB}) was poorly crystalline (Fe_{AAO}), but only 25% of total Fe was poorly crystalline where mean water levels fell to -1.5 m below the soil surface (Fig. 1.3B).

For inorganic extractions, total $Fe_{Dit\text{-}HCl}$ and chelated Fe_{Pyro} followed similar patterns as total Fe_{DCB} and were again separated into wet upper soils and dry upper soils for analysis. In wet upper soils, chelated Fe_{Pyro} and total $Fe_{Dit\text{-}HCl}$ concentrations were low (<0.5 mg Fe g^{-1} soil; Fig.

1.4A–B). In dry upper soils, Fe_{Pyro} and $Fe_{Dit\text{-}HCl}$ concentrations were highest where mean water level was -0.5 m from the soil surface and declined toward the upland ($P < 0.0001$ both cases; Supplemental S6H; Fig. 1.4A–B).

Mineral-associated C followed similar patterns as extracted Fe (Fig. 1.4C–D). In wet upper soils, chelated C_{Pyro} and mineral-associated $C_{Dit\text{-}HCl}$ showed no significant changes with decreasing water level. In dry upper soils, both chelated C_{Pyro} and mineral-associated $C_{Dit\text{-}HCl}$ concentrations in soils were higher where mean water level was at least -0.5 m from the soil surface and decreased with decreasing water level ($P=0.001$ and $P=0.00035$ respectively, Supplemental S6I).

To understand the proportion of total C associated with Fe across the entire wet to dry gradient, we calculated normalized C_{Pyro}/ C_{bulk} and $C_{Dit\text{-}HCl}/ C_{bulk}$ proportions (mg C g^{-1} bulk C; Eq. 4–5; Table 1.1). Both normalized C_{Pyro}/C_{bulk} and $C_{Dit\text{-}HCl}/C_{bulk}$ proportions increased with decreasing mean water level ($P < 0.0001$ both cases, Supplemental S6J; Fig. 1.4E–F).

The relationship between extracted C and Fe was positive and linear in dry upper soils only, so these datasets were again separated for analysis. In dry upper soils, C_{Pyro} increased at approximately twice the rate of Fe_{Pyro} ($P < 0.0001$, Supplemental S6K; Fig. 1.4G). For the dithionite-HCl extraction, $C_{Dit\text{-}HCl}$ increased at approximately the same rate as $Fe_{Dit\text{-}HCl}$ in dry upper soils ($P=0.0001$, Supplemental S6L; Fig. 1.4H). The ratio of C:Fe in the extractant indicates the type of organo-mineral association. For wet upper soils, C_{Pyro}:Fe_{Pyro} was almost entirely >10. For dry upper soils, C_{Pyro}:Fe_{Pyro} was between 1 and 10. In wet upper soils, $C_{Dit\text{-}HCl}$:$Fe_{Dit\text{-}HCl}$ was again high, but in dry upper soils $C_{Dit\text{-}HCl}$:$Fe_{Dit\text{-}HCl}$ was <2.0.

3.4 Aggregate Fractionation

Upper soils (0–50 cm) were separated into four size classes (large macroaggregates, small macroaggregates, microaggregates and silt/clay) to determine the effect of hydrology on SOC protection within aggregates. Aggregate C concentrations ($C_{aggregate}$) significantly decreased with decreasing water level in the large macroaggregate size class only ($P=0.00098$,

Supplemental S6N; Fig. 1.5A-D). Among size classes, small and large macroaggregates contained the highest $C_{aggregate}$ concentrations, while microaggregates and silt/clay contained lower $C_{aggregate}$ concentrations ($P < 0.0001$, Supplemental S6P).

With decreasing mean water level (i.e., drier soils), $C:N_{aggregate}$ increased, as was observed in the bulk soil ($P < 0.0001$ for all tests, Supplemental S6M). Among size classes, $C:N_{aggregate}$ was lowest in silt/clay size class, and highest for the macroaggregate and microaggregate size classes ($P<0.0001$, Supplemental S6P).

Normalized $C_{aggregate}/C_{bulk}$ proportions (mg C g^{-1} bulk C) decreased with decreasing water level (i.e., drier soils) in the large macroaggregates, but increased with decreasing water level in all smaller size classes ($P < 0.05$ for all tests, Supplemental S6O; Fig. 1.5E-H). Among size classes, normalized $C_{aggregate}/C_{bulk}$ proportions were highest in small macroaggregates, lower in large macroaggregates, and lowest in the smallest size classes ($P < 0.0001$, Supplemental S6P).

Aggregate-associated C concentrations declined or did not change down the soil profile (Supplemental S6N; Fig. 1.5A–D). Normalized $C_{aggregate}/C_{bulk}$ proportions declined in large macroaggregates but increased in microaggregates down the soil profile ($P < 0.05$, Supplemental S6O; Fig. 1.5E–H).

4. Discussion

This study is the first to quantify aggregates and organo-mineral associations of SOC within seasonally flooded freshwater mineral wetlands across a continuous wetland–upland gradient. Our results demonstrate that mean water level is a strong predictor of organo-mineral associations and large macroaggregate-associated SOC. Additionally, we show that organo-mineral associations change nonlinearly across transects from wetland basins towards upland (drier) sampling points where wetland water levels are most dynamic (hereafter, transition zone). Large macroaggregates may be especially important in reducing loss of wetland SOC during dry periods, evidenced by our finding that the proportion of total C in large macroaggregates increased from upland drier regions toward the wetland basin. In the wettest transect positions,

large macroaggregates contained a higher proportion of total C (average 50% of total C at wetland edge) than organo-mineral associations (up to 30% of total C in upland soils), which suggests that significant amounts of SOC is in organo-mineral associations and macroaggregates in the transition zone around the wetland perimeter. Potentially stabilizing associations with SOC in the transition zone may influence C processing at landscape scales since this zone constitutes a relatively high proportion of the total area in regions dominated by small wetlands with high perimeter-to-area ratios. By examining a continuous hydrologic gradient from wetland to upland, our study identifies linear and nonlinear trends in aggregation and organo-mineral associations across mean water level that may be overlooked by studying categorical wetland–transition–upland. Overall, this research highlights the potential role of physiochemical stabilization freshwater mineral soil wetlands and indicates a need for more research on SOC stability during dry periods in these abundant yet anthropogenically vulnerable systems.

4.1 Organo-mineral associations were highest in the wetland transition zone and uplands

Our data suggest that organo-mineral associations between C and Fe are present across the transition zone at the wetland perimeter but not within in the wetland basin. We observed the highest accumulations of both total Fe (Fe_{DCB}) and poorly crystalline Fe (Fe_{AAO}) species in the transition zone (Fig. 1.3). In contrast, total Fe concentrations fell to the lowest levels in soils with an average water level within -0.5 m of the soil surface (above the soil sampling depth), which was unsurprising as Fe is likely to become reduced and translocated under these conditions (Fiedler and Sommer 2004, Chen et al. 2017). Recent research suggests that Fe accumulates at redox interfaces (Herndon et al. 2017), indicating that Fe–C associations may be abundant in hydrologically dynamic areas such as the transition zone. Prior research in seasonally flooded wetlands of the Delmarva Peninsula also found high Al and Fe concentrations in wetland "margins," likely due to periods of transient groundwater mounding that cause Al and Fe to flow from uplands towards ponds (Phillips and Shedlock 1993). Because the transition zone is rarely flooded to the soil surface, Fe is more likely to be retained and contribute to organo-mineral

associations in upper transition zone soils than in flooded soils. A study of similar seasonally flooded wetlands found that Al was a stronger predictor of C content in lowlands than Fe (LaCroix et al. 2019); however, we focused on Fe in this research because preliminary sampling of study wetlands showed no change in Al concentrations across the wetland–upland gradient.

Accordingly, C associated with Fe was highest in the transition zone (Fig. 1.4D). Both chelated C (C_{Pyro}) and total organo-mineral associated C ($C_{Dit\text{-}HCl}$) were highest in the transition zone and decreased linearly towards the upland. This finding adds to existing evidence that the accumulation of Fe increases Fe–C associations at redox interfaces (e.g., Riedel et al. 2013). While Fe–C associations were highest in the transition zone, the proportion of bulk soil C that was associated with total Fe ($C_{Dit\text{-}HCl}/C_{bulk}$) increased moving toward the upland (Fig. 1.4F). In uplands, up to 30% of bulk soil C was associated with total Fe ($Fe_{Dit\text{-}HCl}$), but in wetter soils less than 10% of bulk soil C was associated with total Fe, suggesting that SOC in uplands is more likely to be in organo-mineral associations than SOC in wetter soils. Our work corroborates other studies finding organo-mineral associations at low Fe concentrations and high C:Fe ratios (1–20 mg Fe g^{-1} soil; Moore and Turunen 2004, Kleber et al. 2005, Lopez-Sangil and Rovira 2013, Cloy et al. 2014, Maietta et al. 2019). For instance, Kleber et al. (2005) found stabilized C in acid subsoil horizons with poorly crystalline Fe concentrations in a similar range to those found in our study (1.0–3.0 mg Fe_{AAO} g^{-1} soil), indicating that the concentration of poorly crystalline Fe_{AAO} promotes SOC stabilization. Overall, our results add evidence that Fe-C associations exist non-upland.

In contrast to the transition zone and upland, Fe–C associations are much lower in wetland basin soils, which contained low Fe concentrations (<1 mg Fe g^{-1} soil) and only 10% of bulk soil C was associated with $Fe_{Dit\text{-}HCl}$. Additionally, we found poor relationships between C and Fe in the wettest soils, suggesting that extracted C is likely not associated strongly with Fe. These results corroborate other work in mineral wetlands finding a lack of (hydr)oxides in the wetland basin by LaCroix et al. (2019), suggesting that wetland basin SOC is largely unprotected

by organo-mineral associations. LaCroix et al. (2019) also found that SOC in upper horizons of basin soils is more chemically reduced than upland soils. Therefore, we expect relatively reduced SOC in basin soils to be more susceptible to microbial decomposition under seasonally oxic conditions than transition zone soils.

Though organo-mineral associations between C and Fe are prevalent in the transition zone, three lines of evidence from our results suggest these associations are relatively transient. First, the percent of poorly crystalline Fe (Fe_{AAO}/Fe_{DCB}) declined linearly from wetland to upland. Poorly crystalline Fe has a higher surface area than crystalline Fe and more effectively sorbs SOC (Kaiser and Guggenberger 2000), but also tends to be readily reducible and forms only transient associations with C that do not promote long-term C stabilization (Hall et al. 2018). Second, chelated C_{Pyro} was higher than total $C_{Dit\text{-}HCl}$, indicating a higher proportion of SOC in weaker organo-mineral associations. In contrast, the smaller pool of $C_{Dit\text{-}HCl}$ is likely more strongly associated with Fe oxides (Coward et al. 2017; Heckman et al. 2018). Third, we found high ratios of extracted C to Fe in all samples (C:Fe > 1). The ratio of extracted C to Fe (C:Fe) indicates the type of organo-mineral association, where C:Fe <0.22 indicates strong sorption while C:Fe >>0.22 indicates weaker co-precipitation or chelation between SOC and Fe (Kaiser and Guggenberger 2007; Wagai and Mayer 2007; Coward, Thompson, and Plante 2017). We observed lower C:Fe in uplands than in wetlands, indicating that organo-mineral associations are stronger in upland forested soils (e.g., Kaiser and Guggenberger 2000; Zhao et al. 2016). However, high overall C:Fe in the present study suggests that associations are Fe-limited and coprecipitation or chelation is the primary mechanism of organo-mineral association (Wagai and Mayer 2007). Coprecipitation and chelation are typically transient associations which have high organic C content but are also more reactive and likely do not persist during seasonal flooding (Mikutta et al. 2014, Coward et al. 2017, Sodano et al. 2017). As the transition zone soils contain relatively high amounts of SOC, seasonal dynamics in organo-mineral associations may have unexplored implications for wetland C at the landscape scale.

4.2 Large macroaggregates contain the most SOC in wetland soils

Large macroaggregates (>2 mm diameter) contained the most SOC in wetland soils and were most responsive to hydrologic gradients, indicating the potential for large macroaggregates to play a dominant role in physiochemical stabilization of C in wetland soils. Both C concentration ($C_{aggregate}$) and the proportion of total C ($C_{aggregate}/C_{bulk}$) in large macroaggregates were higher in basin wetland soils than upland soils (Fig. 1.5). While few studies have quantified macroaggregates in natural mineral wetlands, Maietta et al. (2019) and Hossler and Bouchard (2010) found that large macroaggregates store significantly more SOC than other aggregate size class in natural organic wetland soils. Large macroaggregates are a dynamic size class that have been shown to be responsive to changes in soil moisture in non-wetland soils (Blankinship et al. 2016). Several of the wettest soils in this study did not contain large macroaggregates, which may be because macroaggregates to not form under continuously flooded conditions. Therefore, while hydrology is an important factor in macroaggregate C content, other variables not studied here, such as root activity, microbial biomass, and wet-dry cycles may also contribute to aggregation (Blankinship et al. 2016; Wright and Inglett 2009).

Large macroaggregate formation and persistence in mineral soil wetlands may be promoted by both the influx of water with high dissolved organic C and seasonally dynamic water tables. The seasonal influx of C-rich water provides organic constituents that may increase macroaggregate stability through increased sorption between organic matter and minerals at aggregate surfaces, as has been shown in microcosm experiments on agricultural soils (Park et al. 2007). Other research in our study wetlands has reported high dissolved organic C concentrations of 30 mg C L^{-1} on average and as high as 45 mg C L^{-1} (Armstrong, in prep.). Additionally, fluctuating moisture conditions promote macroaggregate stability in agricultural soils, as macroaggregates may reform to more stable conformations with wet-dry events (Kemper and Rosenau 1984, Denef et al. 2001). Further research explicitly studying the relationship between seasonal fluctuations in saturation and macroaggregates is necessary in wetland soils.

We found that smaller aggregate size classes (small macroaggregates, microaggregates, silt/clay) were associated with the majority of SOC in drier conditions but were generally less variable across the hydrologic gradient than large macroaggregates. The proportion of total C ($C_{aggregate}/C_{bulk}$) associated with smaller aggregate size classes increased from wetland to upland, but the concentration of C in smaller size classes did not change across the gradient. As expected, smaller aggregate size classes contained lower C:N and C concentrations than macroaggregates, consistent with evidence that microaggregates and silt/clay consist of older, microbially derived C (Jastrow et al. 1996; Six, Elliott, and Paustian 2000). Importantly, SOC associated with smaller aggregate size classes in uplands may still be stabilized by strong adsorption reactions on mineral surfaces; however, the ecological significance of microaggregates and smaller size classes remains unresolved (Totsche et al. 2018). For example, one study found microaggregates contained some plant-derived C molecules which were not microbially processed, challenging the theory that microaggregates only contain highly processed SOC (Arachchige et al. 2018). Additionally, microaggregate C may be stabilized for longer time periods in soils than more dynamic macroaggregate C (von Lützow et al. 2007). Therefore, C in smaller aggregate size classes may still contribute to upland SOC stabilization despite a lower abundance of macroaggregates.

Generally, relationships between aggregate-associated C and water level were weaker than relationships between organo-mineral associated C and water level. However, the proportion of total C in macroaggregates ($C_{aggregate}/C_{bulk}$) was higher than the proportion of total C associated with Fe (C_{Pyro}/C_{bulk} and $C_{Dit\text{-}HCl}/C_{bulk}$), indicating that macroaggregates are a more important than associations with Fe for C storage in wetland basins and transition zones. Overall, the abundance of aggregates and organo-mineral associations in wetland and transition zone soils highlight the need for more research on the ecological significance of these fractions for wetland SOC storage, especially during seasonally dry conditions.

4.3 The significance of terrestrial-aquatic interfaces for wetland SOC storage at the landscape scale

Our research suggests that transition zone of seasonally flooded freshwater mineral soil wetlands is a hydrologically dynamic aquatic-terrestrial interface with unique conditions that promote SOC storage and stability. Our research adds SOC physiochemical stabilization to the body of ecosystem processes (e.g. denitrification, gas fluxes) that may be enhanced at the edges of wetlands (Hefting et al. 2004, Creed et al. 2013, Ligi et al. 2014, Capps et al. 2014, LaCroix et al. 2019). More broadly, ecohydrological interfaces such as the transition zone experience increased rates of biogeochemical processing and, as such, are critical in determining ecosystem response to environmental change (Krause et al. 2017). Since small depressional wetlands contribute a greater fraction of total perimeter than total area, the transition zone may have implications for SOC storage and stability on the landscape scale.

Further, our research indicates that examining a continuous hydrologic gradient across the wetland transition zone may reveal new insights into SOC processing. While several studies define the wetland-transition–upland as three categorical variables (e.g., LaCroix et al. 2019; Webster et al. 2008; Pearse et al. 2018), we found that mean water level was a useful continuous indicator of hydrologic conditions that allowed us to examine linear and nonlinear trends in SOC processes across wetlands. Importantly, our study defined the transition zone as the non-upland area with mean water level below 0.5 m soil depth and fluctuating saturation in the top 0.5 m of soil (Supplemental S2). Recent research in similar depressional wetland systems found low Fe where water levels rise to just below the soil surface and concluded that soils lacked mineral protection (LaCroix et al. 2019). However, by examining the entire wetland–upland gradient, our results show organo-mineral associations in soils that are influenced by wetland hydrology but are, on average, not inundated. Quantifying the hydrological variables in the transition zone is necessary for future work on this heterogeneous aquatic-terrestrial interface, particularly in low-relief areas where local groundwater tables may cause periodic shallow saturation (e.g., within 50

cm below the soil surface) but not flooding across the transition zone (Phillips and Shedlock 1993).

Our work provides evidence that hydrology is a sensitive indicator of SOC characteristics across the wetland–upland transition. Clay has historically been used as proxy for SOC stabilization with mineral surfaces (Oades 1988), but recent research suggests that Fe and Al (hydr)oxides are better predictors of SOC in high moisture, acidic soils (Rasmussen et al. 2018). While both clay and hydrology change across the transect and are likely to influence SOC stability, hydrology exerts a strong control on wetland SOC dynamics (Mitsch and Gosselink 2015) and also influences the distribution of both clay and Fe (hydr)oxides (Arndt et al. 2016). Further, hydrology and SOC are likely to change across similar, relatively short scales of time and space. Therefore, an explicitly hydrologic gradient provides insight into how SOC processing might change over time which may be useful to future studies of SOC.

The future of stabilized SOC in the wetland and transition zone is uncertain because the hydrologic regime of seasonally flooded wetlands is vulnerable to changes in land use and climate (Kolka et al. 2018). Under current hydrologic conditions, transition zone SOC is expected to be stabilized by organo-mineral associations and aggregation as observed in this study. However, as more extreme weather events are predicted for the Mid-Atlantic with climate change (Boesch et al., 2015), increased incidence of severe precipitation, droughts, and warmer temperatures may lead to longer dry periods and more rapid transitions between wet and dry conditions. We expect SOC in the transition zone and upland to be relatively protected by associations with Fe, which may partially offset the effects of increased oxic conditions. However, the low abundance of Fe in wetland basin soils may lead to increased SOC loss in the future (e.g., Fissore et al. 2009), though macro-aggregation may mitigate some of these effects. Stability of SOC in the transition zone may not be resilient to all kinds of hydrologic change; for example, if the frequency of saturation and flooding within the upper 0.5 m of transition zone soils increases due to increased incidence of large storm events, leaching loss of Fe in the

transition zone may render SOC less stable during seasonal drying. Our work highlights the complex and uncertain influence of future hydrologic change on SOC loss, C emissions, and SOC sequestration in freshwater mineral wetlands (Bridgham et al. 2006, Kolka et al. 2018). As freshwater mineral wetlands emit 70% more methane than North American peatlands but potentially sequester C at equivalent rates (Bridgham et al. 2006), understanding the effects of changing hydrology on SOC stability and loss in mineral wetlands is critical.

5. Conclusions

Our results indicate that hydrologic conditions influence aggregation and organo-mineral associations, which may play an underestimated role in SOC storage and stability in seasonally flooded mineral wetlands. Overall, our results highlight distinct patterns in aggregates and organo-mineral associations across the hydrologically dynamic transition zone, suggesting that these mechanisms play unique roles in wetland perimeters and in wetlands that experience seasonal changes in redox conditions (e.g., floodplain wetlands).

While the wetlands in this study are relatively small in area, the Delmarva Peninsula alone is estimated to contain 17,000 such wetlands (Fenstermacher et al. 2014). Therefore, the perimeters of many small wetlands are likely to have a significant cumulative impact on SOC stocks on the landscape scale. Mineral soil wetlands, particularly forested wetlands, are ubiquitous throughout the U.S. but are also highly vulnerable to loss due to climate change (Kolka et al. 2018) as well as development, silviculture, and agriculture (Dahl 2011). While wetland conservation and restoration tends to focus on restoring flooding to large wetlands, our results indicate that small, seasonally flooded wetlands have unique capacity for SOC storage. Our research emphasizes perimeters of seasonally flooded freshwater mineral wetlands as a critical but understudied component of landscape-scale wetland SOC storage that may be particularly vulnerable to future degradation.

Acknowledgements

We thank Alec Armstrong, Graham Stewart, Kelly Hondula, and Dr. Christine Maietta for their support throughout research process. We thank Dr. C. Nathan Jones for collecting and processing water level data at wetland sites and for his thoughtful contributions to drafts. We thank Dr. Martin Rabenhorst for his expertise and the use of his lab. Finally, we thank Bianca Noveno and Maggie Tan, whose tireless work as interns in the field and lab made this research possible. This work was completed with a Graduate Research Assistantship from the National Socio-Environmental Synthesis Center (SESYNC) in Annapolis, MD.

Tables

Table 1.1

Table 1.1. Description of soil characteristics.

Property	Response Variable	Abbreviation	Unit	Source or Equation	Description
Bulk soil C	Bulk soil C concentration	C_{bulk}	%; g C · g^{-1} soil	CHN Analyzer	Concentration of C in the bulk soil sample.
	Bulk soil C:N	$C:N_{bulk}$	ratio; g C · g^{-1} N	CHN Analyzer	Ratio of C:N in bulk soil.
Bulk soil Fe	Non-crystalline Fe	Fe_{AAO}	mg Fe · g^{-1} soil	Atomic absorption spectrometer	Concentration of non-crystalline Fe species, extracted by AAO.
	Total Fe	Fe_{DCB}	mg Fe · g^{-1} soil	Atomic absorption spectrometer	Concentration of total (both crystalline and non-crystalline) Fe species, extracted by DCB.
	Percent non-crystalline Fe	Fe_{AAO}/Fe_{DCB}	%	Fe_{AAO}/Fe_{DCB}*100 (Eq. 1)	Percent of total Fe that is non-crystalline.
Organo-Mineral Association	Chelated C	C_{Pyro}	mg C · g^{-1} soil	TOC Analyzer	Concentration of C extracted with Pyro, associated with chelated mineral species.
	Chelated Fe	Fe_{Pyro}	mg Fe · g^{-1} soil	Atomic absorption spectrometer	Concentration of Fe extracted with Pyro, associated with chelated mineral species.
	Total mineral-associated C	$C_{Dit\text{-}HCl}$	mg C · g^{-1} soil	TOC Analyzer	Concentration of C extracted with Dit-HCl, an inorganic extraction for total Fe.
	Total Fe	$Fe_{Dit\text{-}HCl}$	mg Fe · g^{-1} soil	Atomic absorption spectrometer	Concentration of Fe extracted with Dit-HCl.
	Normalized chelated C	C_{Pyro}/C_{bulk}	mg C · g^{-1} C	C_{Pyro}/C_{bulk} (Eq. 2)	Proportion of C associated with Fe_{Pyro} normalized to bulk soil C. Indicates the relative proportion of chelated organo-mineral association across the transect, normalized for differences in bulk soil C across the transect.
	Normalized mineral-associated C	$C_{Dit\text{-}HCl}/C_{bulk}$	mg C · g^{-1} C	$C_{Dit\text{-}HCl}/C_{bulk}$ (Eq. 3)	Proportion of C associated with $Fe_{Dit\text{-}HCl}$ normalized to bulk soil C. Indicates the relative proportion of C in organo-mineral associations across the transect, normalized for differences in bulk soil C across the transect.
	Extractant C:Fe	C:Fe	ratio; g C · g^{-1} Fe	C_{Pyro}/Fe_{Pyro} (Eq. 4); $C_{Dit\text{-}HCl}/Fe_{Dit\text{-}HCl}$ (Eq. 5)	Ratio of extracted C to extracted Fe; indicates the type of association between C and Fe.
Aggregate Size Class	Aggregate fraction mass		g aggregate	$mass_{aggregate}$	Mass of aggregate size class after air drying and removal of rocks (>1 mm). $Mass_{aggregate,\ sand\text{-}free}$ is corrected for sand.
	Aggregate C:N	$C:N_{aggregate}$	ratio; g C · g^{-1} N	CHN Analyzer	Ratio of C:N within an aggregate size class.
	Aggregate C concentration	$C_{aggregate}$	mg C · g^{-1} soil	CHN Analyzer; $(C*mass_{aggregate})/mass_{total}$ (Eq. 6)	Concentration of C in each aggregate size class per gram of bulk soil, excluding rocks (>1 mm).
	Normalized aggregate-associated C	$C_{aggregate}/C_{bulk}$	mg C · g^{-1} C	$(C*mass_{aggregate})$ / $\Sigma(C*mass_{aggregate})$ (Eq.7)	Proportion of C associated with an aggregate fraction, normalized to C of the entire sample. Indicates the relative proportion of C in each aggregate fraction, normalized for differences in bulk soil C across the transect.

Table 1.2

Table 1.2. Hydrologic data across transects for water year 2018, presented as means (standard error). Elevation is surveyed elevation relative to the center of the wetland. Days water level > -0.5 quantifies duration of saturation within the upper 0.5 m of soil surface (water level > -0.5 m). Saturation events to -0.5 m is the number of instances that water level came within -0.5 m below the soil surface, indicating how dynamic saturation within sampling zone is at each transect point. Maximum percent IRIS removal is the maximum percent of reduced iron oxide paint by area within a 10 cm zone within the upper 0.5 m of soils, indicating relative reducing conditions in the upper soil profile. Lowercase letters represent significant differences among transect points (ANOVA and Tukey's HSD, $P<0.05$).

Transect Point	Elevation relative to center of wetland (m)	Mean water level (m)	Minimum water level (m)	Maximum water level (m)	Days water level > -0.5 m	Saturation events to -0.5 m	Maximum Percent IRIS removal (2019)
A	0.4 (0.1)^{c}	0.1 (0.1)^{a}	-0.5 (0.1)^{a}	0.4 (0.1)^{a}	353.4 (9.7)^{a}	1.8 (0.6)^{bc}	96.6 (1.9)^{a}
B	0.8 (0.1)^{c}	-0.3 (0.0)^{b}	-0.8 (0.1)^{bc}	0.1 (0.1)^{b}	279.6 (21.3)^{a}	3.4 (0.7)^{ab}	99.6 (0.4)^{a}
C	1.2 (0.1)^{b}	-0.7 (0.1)^{c}	-1.3 (0.1)^{c}	-0.2 (0.1)^{c}	137 (43.7)^{b}	4.6 (0.7)^{a}	21.6 (13.9)^{b}
D	1.6 (0.1)^{ba}	-1.0 (0.1)^{d}	-1.6 (0.1)^{cd}	-0.5 (0.0)^{d}	7.4 (6.2)^{c}	1.4 (0.7)^{bc}	0.4 (0.1)^{b}
E	1.8 (0.1)^{a}	-1.2 (0.1)^{d}	-1.8 (0.1)^{d}	-0.6 (0.1)^{d}	0.2 (0.2)^{c}	0.2 (0.2)^{c}	NA
ANOVA, Tukey's HSD	F(4, 20)=38.4, P<0.0001	F(4, 20)=47.3, P<0.0001	F(4, 20)=30.7, P<0.0001	F(4, 20)=42.2, P<0.0001	F(4, 20)=50.6, P<0.0001	F(4, 20)=7.3, P=0.00088	F(3, 16)=66.3, P<0.0001

Figures

Figure 1.1

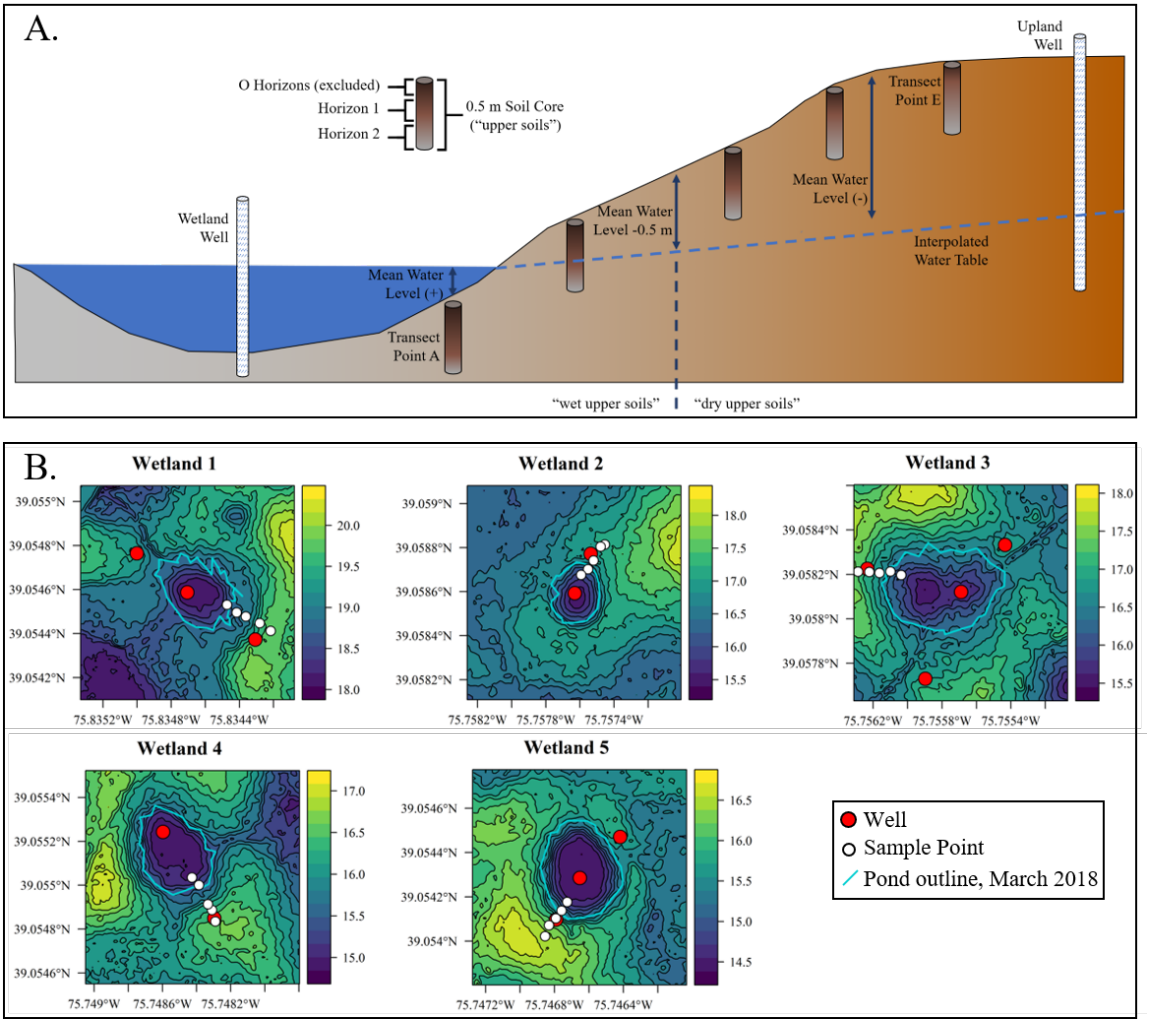

Figure 1.1. Cross-section schematic of sampling design (Panel A). Elevation gradient shown is exaggerated to fit on the page; accurate elevation gradient shown in Supplemental S2. Panel B shows actual location of wells and transects in wetlands that vary in topographic relief.

Figure 1.2

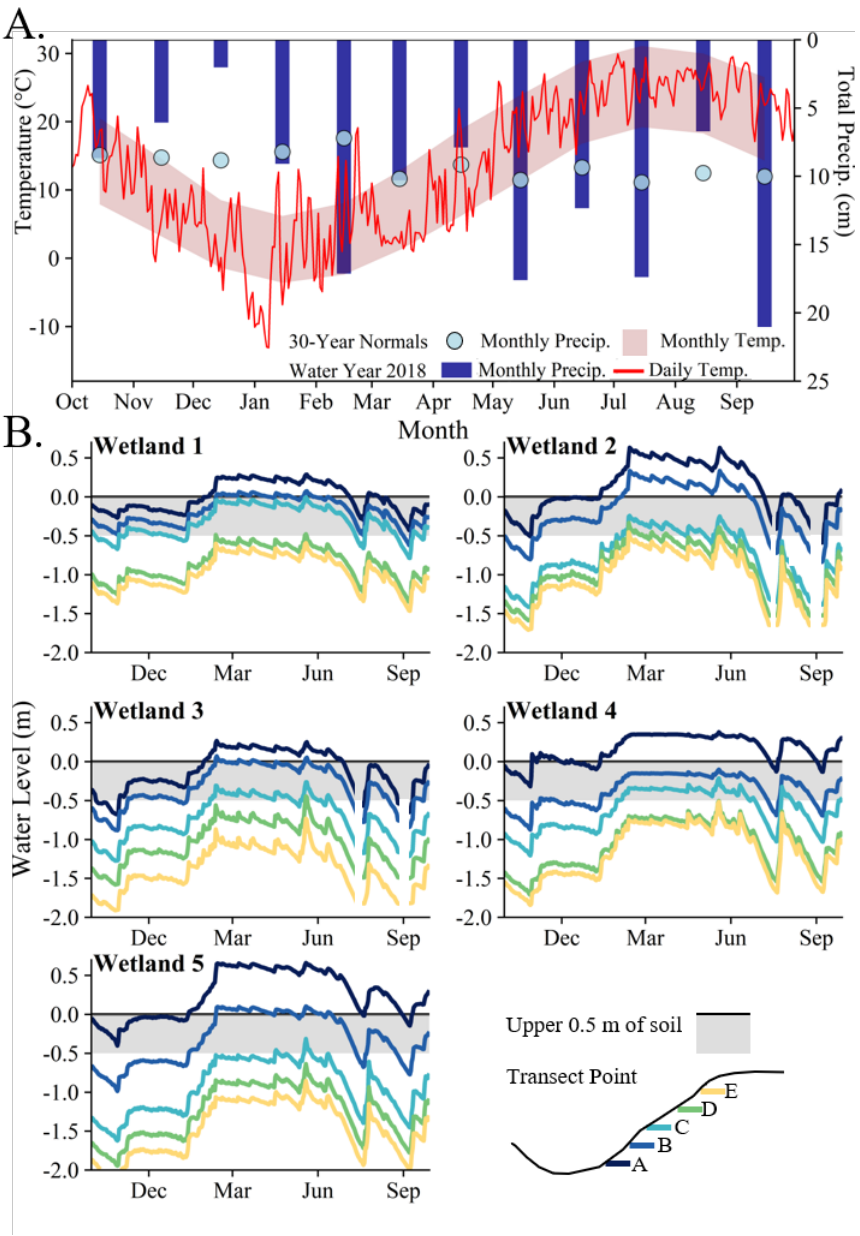

Figure 1.2: Temperature and precipitation were within expected 30-year normals, though rainfall was slightly higher than expected in summer (Panel A). Daily water levels at each wetland show differing hydrologic conditions across categorical transect points, with particularly variable hydrologic conditions at transect point C (Panel B). The black line indicates the soil surface, and the shaded grey band indicates the top 0.5 m of the soil profile.

Figure 1.3

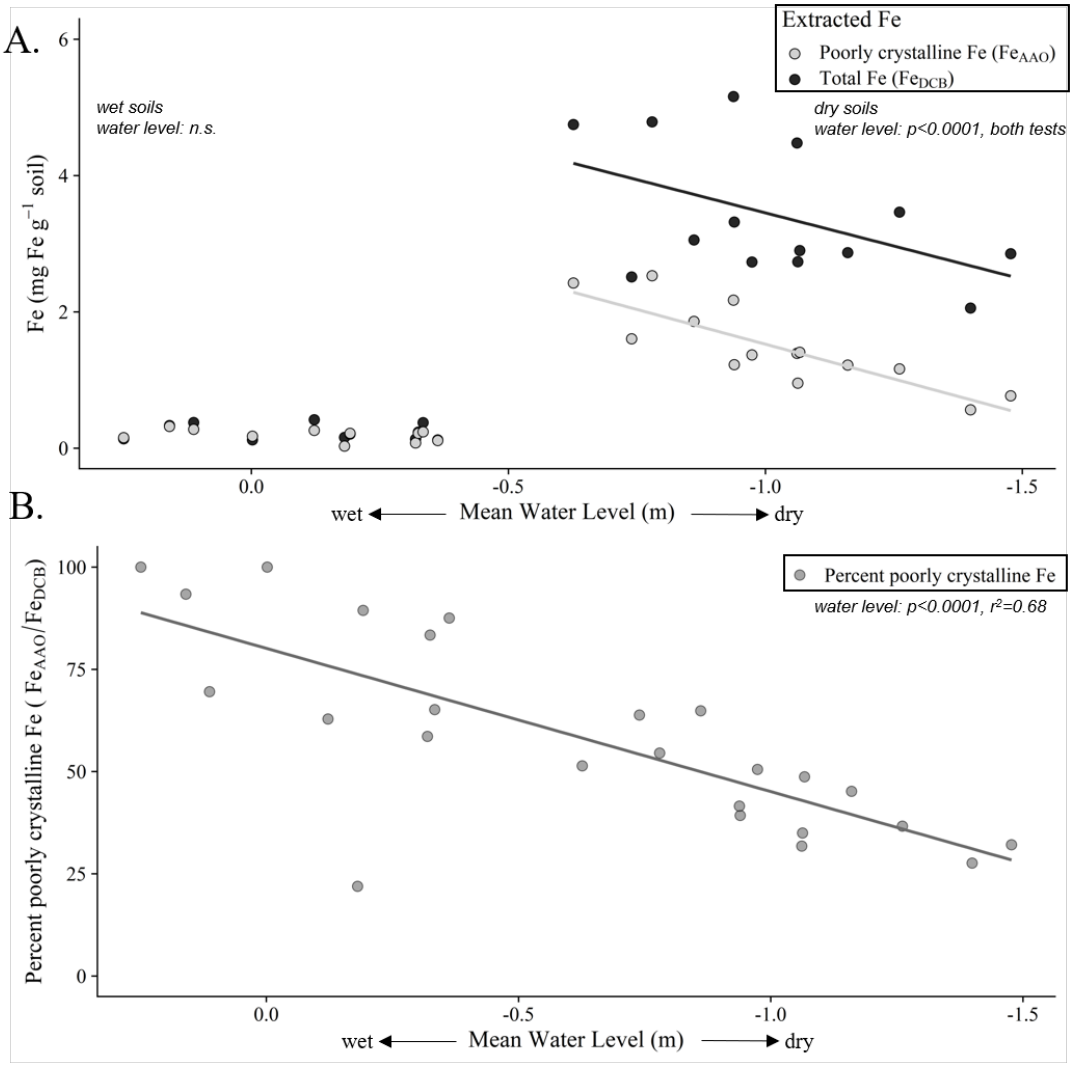

Figure 1.3. Mean Fe_{AAO} and Fe_{DCB} concentrations for upper horizons (Panel A). Data was separated into two groups for analysis: samples from soils with a mean water level >-0.5 m (wet upper soils) and samples from soils with mean water level ≤ -0.5 m (dry upper soils). Panel B shows the percent poorly crystalline Fe (Fe_{AAO}/Fe_{DCB}). Non-significant models not shown

Figure 1.4

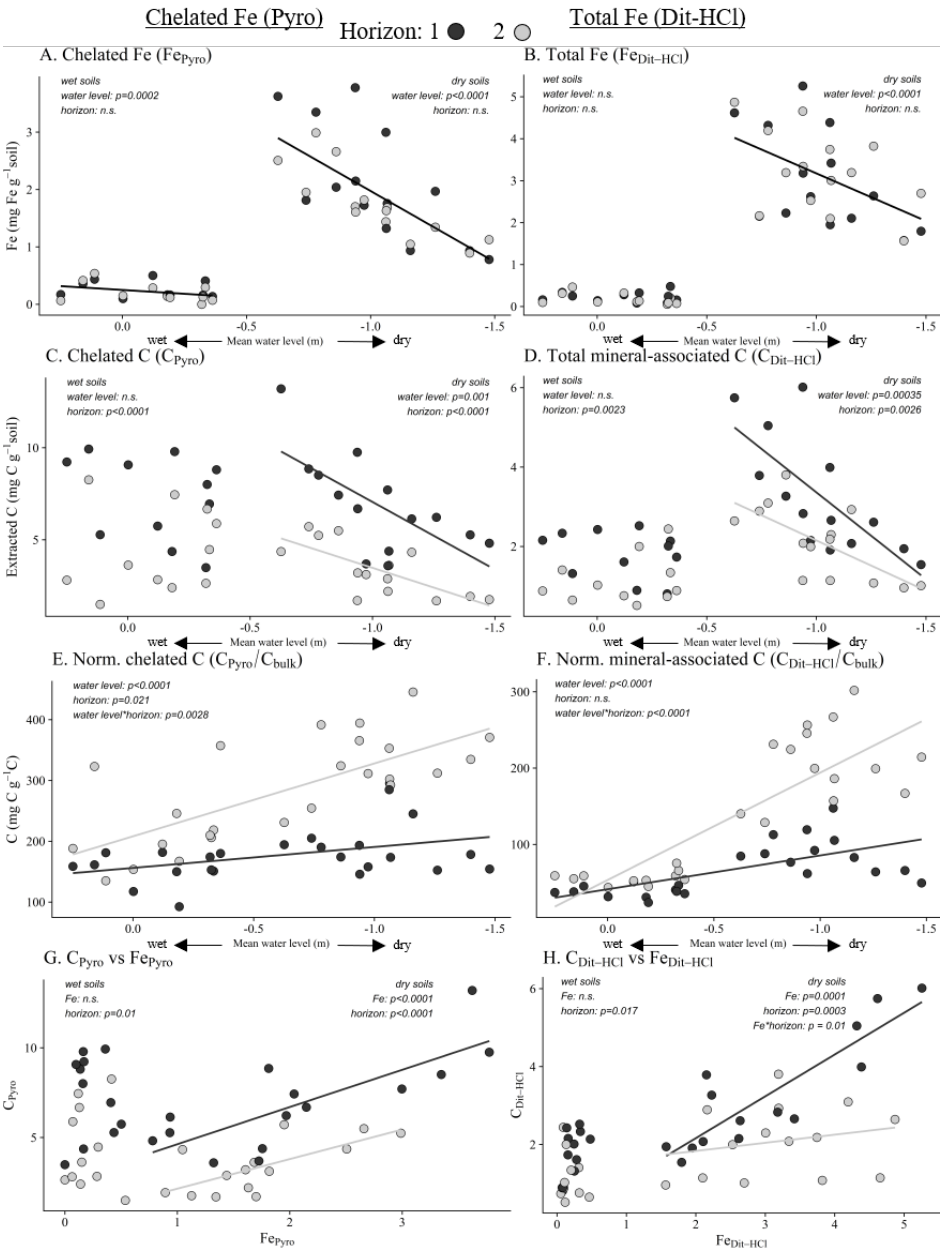

Figure 1.4. Properties of the organo-mineral associations for upper mineral horizons (1 and 2) for sodium pyrophosphate (left) and dithionite-HCl (right). Solid lines represent LME models where mean water level is significant. Only one line is shown for the LME model where differences between horizon (e.g., horizon 1 and 2) are not significant. Panels A–D and G–H are separated at a mean water level of -0.5 m into wet upper soils and dry upper soils.

Figure 1.5

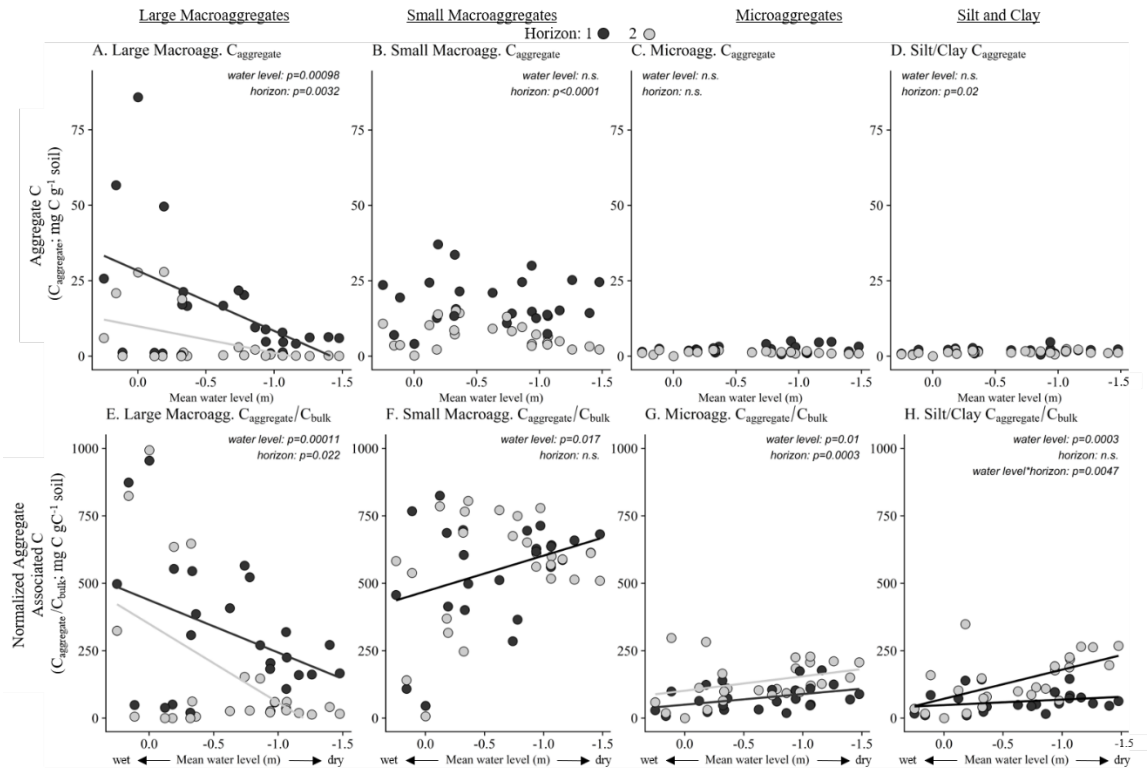

Figure 1.5. Aggregate C ($C_{aggregate}$) and Normalized Aggregate-Associated C ($C_{aggregate}/C_{bulk}$) vs. mean water level in upper soil horizons, by aggregate size class. Solid lines represent significant differences across mean water level in the LME models. Where differences between horizons were not significant, only one line is shown for interpretation.

Supplemental materials

S1.

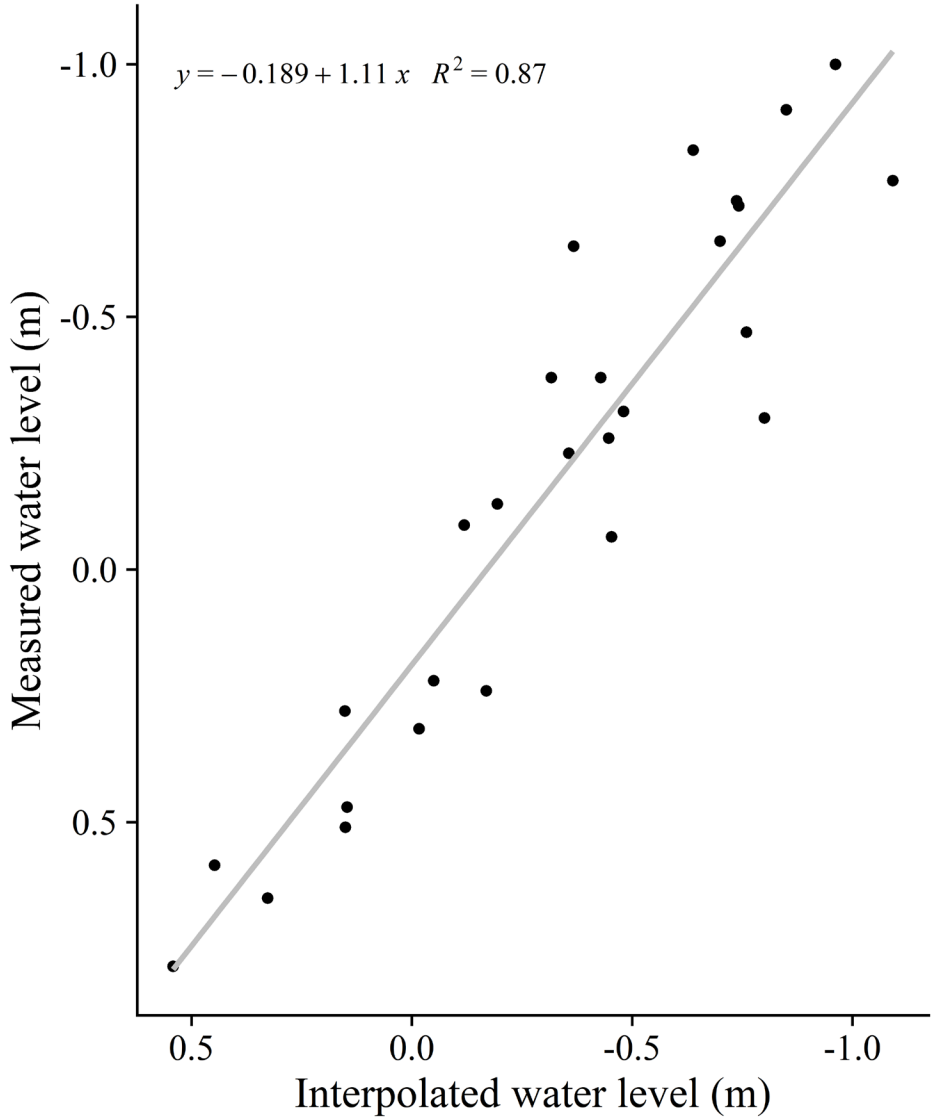

Supplemental S1. Simple linear regression of water level measured at transect points biweekly from May to August 2018 and interpolated daily water levels to validate mean water level interpolation (Simple linear regression, $F(1,25)=174$, $P = 9.0 \cdot 10^{-13}$).

S2.

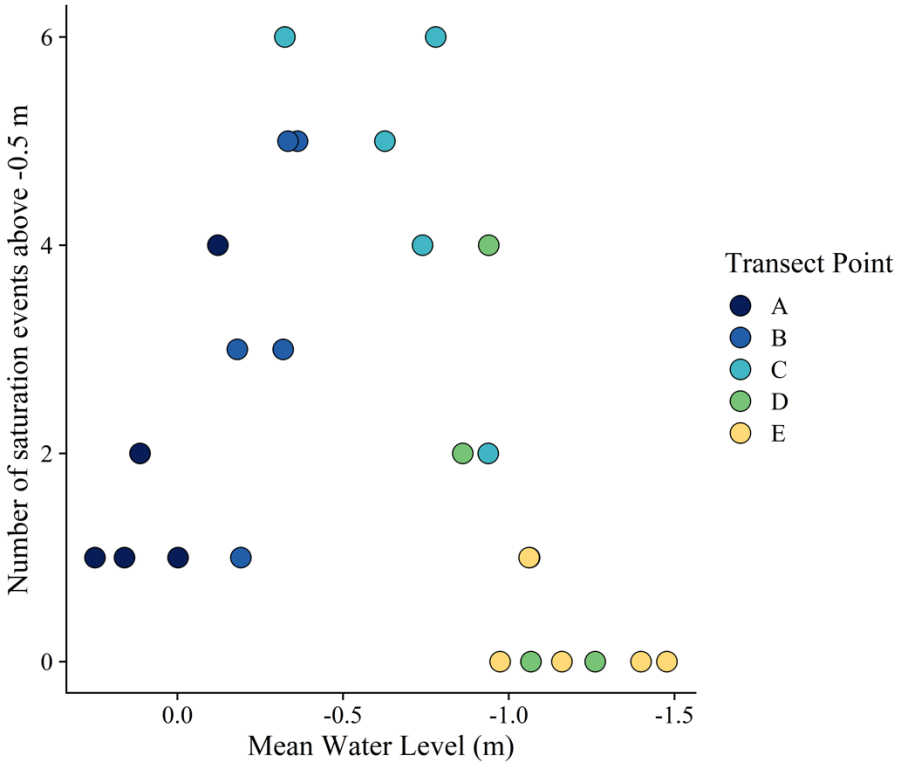

Supplemental S2. Number of saturation events above -0.5 m vs mean water level during water year 2018. Number of saturation events above -0.5 m is calculated as the number of times water level rose from below -0.5 m depth to above -0.5 m depth (i.e., the number of times that soil within the upper 0.5 m switched from being unsaturated to saturated), and is an indicator of hydrologic across transect points and mean water level.

S3.

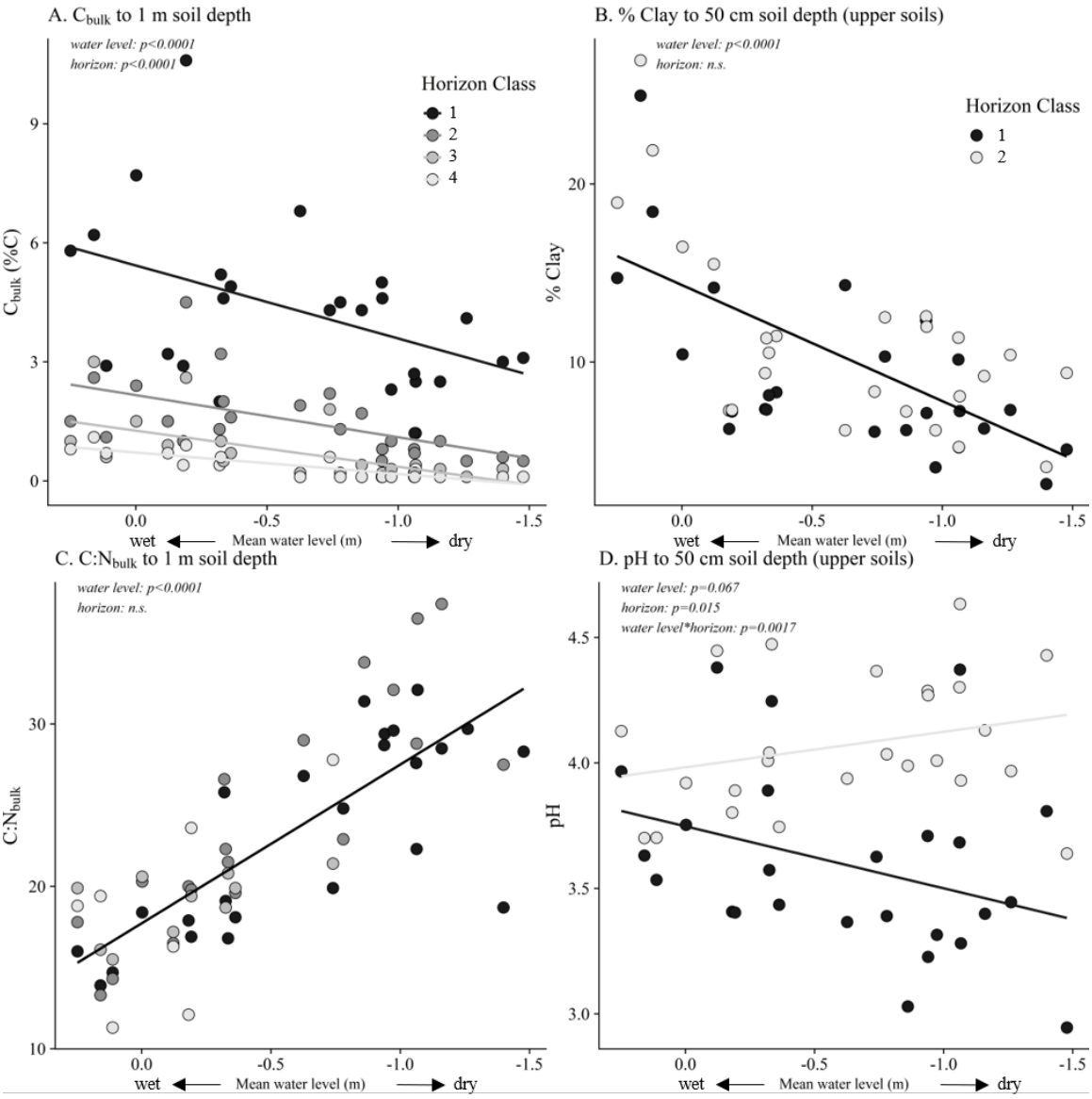

Supplemental S3. Soil properties by horizon vs. mean water level for Cbulk (A) and C:Nbulk (C) to 1 m soil depth and for % clay (B) and pH (D) to 50 cm soil depth (upper soils). Horizon class is ordered by depth within a core to compare pedogenic horizons across different soil types. Significant models are presented as solid lines (P <0.05). Where horizon class was not significant, only one model is presented (black line)

S4.

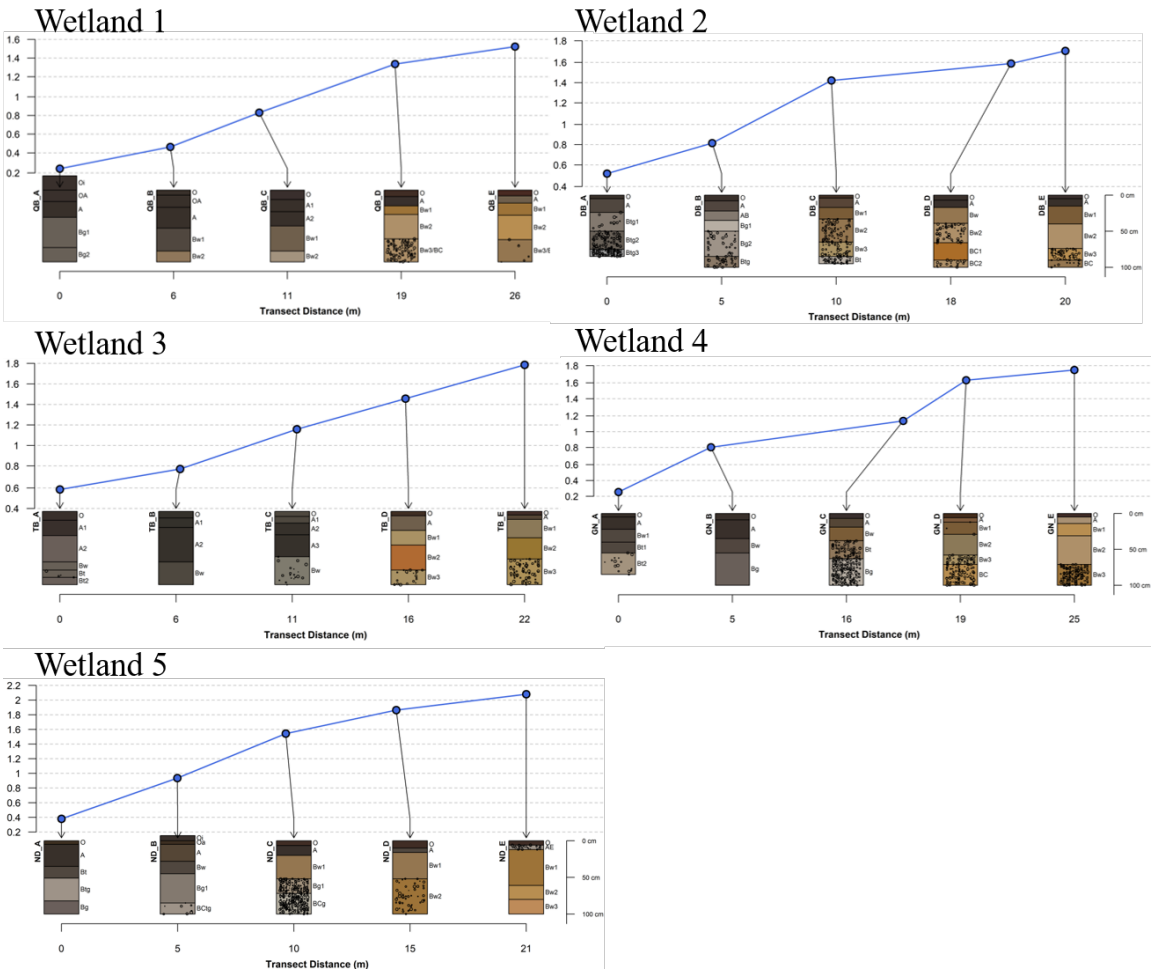

Supplemental S4. Soil colors and elevations relative to wetland center. Blue dots represent soil sample relative elevation on transect. Horizon designations, colors, and percent redoximorphic concentrations are indicated below each transect point

S5.

Supplemental S5. We compared Fe and C removal across extractions on upper soils to better understand extraction efficiency. A paired t-test between $Fe_{Dit\text{-}HCl}$ and Fe_{DCB} revealed no significant difference in Fe extracted by the inorganic (Dit-HCl) and organic (DCB) extractions (paired t-test, t(97.6)=-0.51, P=0.61). The mean extraction efficiency for total Fe ($Fe_{Dit\text{-}HCl}/Fe_{DCB}$) was 88.9% (standard error=2.3), with a median of 99.4%.

Between the organo-mineral extractions, Dit-HCl extracted more Fe but less C in each sample than Pyro. $Fe_{Pyro}/Fe_{Dit\text{-}HCl}$ was 79.7%. The proportion of $Fe_{Dit\text{-}HCl}$ that was extractable by Pyro ($Fe_{Pyro}/Fe_{Dit\text{-}HCl}$) decreases linearly with decreasing water level, falling by over half across the sampled range of water levels (simple linear regression, F(1,48)=21.2, $P=3.0\cdot10^{-5}$). C_{Pyro} was much greater than $C_{Dit\text{-}HCl}$, as the mean percent of $C_{Pyro}/C_{Dit\text{-}HCl}$ was 284.7% (18.06). Similar to $Fe_{Pyro}/Fe_{Dit\text{-}HCl}$, $C_{Pyro}/C_{Dit\text{-}HCl}$ also decreased significantly with decreasing water level (simple linear regression, F(1,48)=37.5, $P=1.6\cdot10^{-7}$).

S6.

Supplemental S6. Statistical models: Parameters, F statistics, p values, and degrees of freedom (Kenworth-Rogers approximation) for the global model (left) and the reduced model (right) for all mixed effects linear models. Standard error (se) and standard deviation (sd) are presented with parameter estimates, as indicated. "Upper horizons" are in the top 0–50 cm of the soil profile and are comparisons among horizon 1 and horizon 2.

S6A. LME model of C_{bulk} on mineral soil horizons to 1 m depth

	LME Model of C_{bulk} on mineral soil horizons to 1 m depth							
	Global model				Reduced model			
Fixed effects	Beta (se)	F-statistic	P	df	Beta (se)	F-statistic	P	df
Intercept	5.4 (0.4)				4.9 (0.3)			
Mean water level (m)	1.8 (0.4)	23.3	6.00E-06	(1, 85.4)	1.0 (0.2)	23.8	4.70E-06	(1,88.4)
Horizon class (1, 2, 3, 4)	2:3 = -3.3 (0.5) 2:4 = -4.2 (0.5) 2:5= -4.7(0.5)	39.5	5.00E-16	(3,84.1)	2:3 = -2.8 (0.3) 2:4 = -3.5 (0.3) 2:5 = -3.9 (0.3)	71.4	2.20E-16	(3,87.0)
Mean water level*horizon class		1.6	0.20	(3,84.1)				
n = 96	Residual Variance (sd)	Between Wetland Variance (sd)	Conditional r^2		Residual Variance (sd)	Between Wetland Variance (sd)	Conditional r^2	
groups = 5	1.0 (1.0)	0.16 (0.41)	0.74		1.06 (1.03)	0.17 (0.41)	0.73	

S6B. LME model of $C:N_{bulk}$ on mineral soil horizons to 1 m depth

	LME Model of $C:N_{bulk}$ on mineral soil horizons to 1 m depth							
	Global model				Reduced model			
Fixed effects	Beta (se)	F-statistic	P	df	Beta (se)	F-statistic	P	df
Intercept	17.2 (1.4)				17.6 (1.1)			
Mean water level (m)	-9.0 (1.2)	55.02	1.10E-09	(1, 52.0)	-10.3 (0.89)	130.1	2.52E-16	(1, 56.9)
Horizon class (1, 2, 3, 4)	2:3 = 0.42 (1.3) 2:4 = 0.83 (1.4) 2:5= 0.39 (1.5)	0.10	9.60E-01	(3, 50.1)				
Mean water level*horizon class		2.25	0.09	(3, 50.69)				
n = 96	Residual Variance (sd)	Between Wetland Variance (sd)	Conditional r^2		Residual Variance (sd)	Between Wetland Variance (sd)	Conditional r^2	
groups = 5	9.7 (3.1)	6.2 (2.5)	0.78		11.4 (3.4)	4.8 (2.2)	0.73	

S6C. LME model of % Clay on upper horizons

	LME Model of %clay (upper horizons)							
	Global model				Reduced model			
Fixed effects	Beta (se)	F-statistic	P	df	Beta (se)	F-statistic	P	df
Intercept	13.3 (1.4)				14.5 (1.2)			
Mean water level (m)	6.4 (1.5)	40.8	9.90E-08	(1, 43.1)	6.7 (1.1)	39.4	1.20E-07	(1,45.2)
Horizon class (1, 2)	2.3 (1.7)	2.0	1.70E-01	(1, 42)				
Mean water level*horizon class		0.1	7.50E-01	(1, 42)				
n = 50	Residual Variance (sd)	Between Wetland Variance (sd)	Conditional r^2		Residual Variance (sd)	Between Wetland Variance (sd)	Conditional r^2	
groups = 5	13.3 (3.7)	3.1 (1.8)	0.54		13.8 (3.7)	3.0 (1.7)	0.52	

S6D. LME model of pH on upper horizons

LME model of pH (upper horizons)				
	Global model			
Fixed effects	Beta (se)	F-statistic	P	df
Intercept	3.8 (0.1)			
Mean water level (m)	0.31 (0.08)	3.5	0.067	(1, 42.2)
Horizon class (1:2)	0.23 (0.09)	6.4	0.015	(1, 42.0)
Mean water level*horizon class	0.039 (0.12)	11.2	0.0017	(1, 42.0)
n = 50	Residual Variance (sd)	Between Wetland Variance (sd)	Conditional r^2	
groups = 5	0.04 (0.20)	0.065(0.26)	0.76	

S6E. LME global model of Fe_{DCB} on upper horizons, separated by mean water level of -0.5 m

Global LME Model of Fe_{DCB} (upper horizons)								
	Wet upper soils (mean water level > -0.5 m)				Dry upper soils (mean water level ≤ -0.5 m)			
Fixed effects	Beta (se)	F-statistic	P	df	Beta (se)	F-statistic	P	df
Intercept	0.37 (0.12)				4.3 (0.9)			
Mean water level (m)	0.14 (0.12)	1.4	0.30	(1, 18.2)	2.5 (0.6)	17.81	3.4E-04	(1, 22.5)
Horizon class (1, 2)	-0.05 (0.05)	1.0	0.30	(1, 16.6)	0.66 (0.24)	7.69	1.1E-02	(1, 21.0)
	Residual Variance (sd)	Between Wetland Variance (sd)	Conditional r^2	n	Residual Variance (sd)	Between Wetland Variance (sd)	Conditional r^2	n
groups = 5	0.14 (0.11)	0.008 (0.09)	0.40	22	0.39 (0.63)	0.56 (0.74)	0.72	28

*this model failed to converge, so Maximum Likelihood was used with Satterthwaite Approximation

S6F. LME global model of Fe_{AAO} on upper horizons, separated by mean water level of -0.5 m

Global LME Model of Fe_{AAO} (upper horizons)								
	Wet upper soils (mean water level > -0.5 m)				Dry upper soils (mean water level ≤ -0.5 m)			
Fixed effects	Beta (se)	F-statistic	P	df	Beta (se)	F-statistic	P	df
Intercept	0.32 (0.11)				4.9 (0.6)			
Mean water level (m)	0.20 (0.10)	3.6	0.076	(1, 16.9)	2.1 (0.4)	27.74	1.9E-05	(1, 25.0)
Horizon class (1, 2)	-0.04 (0.04)	1.1	0.30	(1, 15.0)	-0.51 (0.16)	9.69	5.3E-03	(1, 21.0)
	Residual Variance (sd)	Between Wetland Variance (sd)	Conditional r^2	n	Residual Variance (sd)	Between Wetland Variance (sd)	Conditional r^2	n
groups = 5	0.010 (0.10)	0.002 (0.05)	0.33	22	0.19 (0.44)	0.031 (0.18)	0.65	28

S6G. LME global model of Fe_{AAO}/Fe_{DCB} in upper horizons

Global LME Model of Fe_{AAO}/Fe_{DCB} (upper horizons)				
	All soils together			
Fixed effects	Beta (se)	F-statistic	P	df
Intercept	117.5 (12.1)			
Mean water level (m)	33.9 (4.3)	61.6	7.0E-10	(1, 43.6)
Horizon class (1, 2)	-15.2 (4.2)	13.0	8.1E-04	(1, 43.0)
n = 50	Residual Variance (sd)	Between Wetland Variance (sd)	Conditional r^2	
groups = 5	223.8 (15.0)	111.9 (10.6)	0.68	

S6H. LME of Fe_{Pyro} and $Fe_{Dit\text{-}HCl}$ on upper horizons, separated by mean water level -0.5 m

LME Model of Fe_{Pyro} (wet upper horizons, mean water level > -0.5 m)

	Global Model				Reduced Model			
Fixed effects	Beta (se)	F-statistic	P	df	Beta (se)	F-statistic	P	df
Intercept	0.28 (0.07)				0.27 (0.07)			
Mean water level (m)	0.30 (0.14)	12.2	0.003	(1, 14.4)	0.37 (0.10)	13.0	0.002	(1, 16.5)
Horizon class (1, 2)	-0.02 (0.05)	0.21	0.66	(1, 14.0)				
Mean water level*horizon class	0.12 (0.19)	0.39	0.54	(1, 14.0)				
	Residual Variance (sd)	Between Wetland Variance (sd)	Conditional r^2	n	Residual Variance (sd)	Between Wetland Variance (sd)	Conditional r^2	n
groups = 5	0.0009 (0.09)	0.018 (0.14)	0.74	22	0.008 (0.09)	0.018 (0.14)	0.74	22

LME Model of Fe_{Pyro} (dry upper horizons, mean water level ≤ -0.5 m)

	Global Model				Reduced Model			
Fixed effects	Beta (se)	F-statistic	P	df	Beta (se)	F-statistic	P	df
Intercept	5.1 (0.7)				4.6 (0.5)			
Mean water level (m)	3.0 (0.6)	27.1	2.5E-05	(1, 23.9)	2.6 (0.5)	25.2	3.2E-05	(1, 26.0)
Horizon class (1, 2)	-1.1 (0.9)	1.4	0.23	(1, 20.0)				
Mean water level*horizon class	-0.7 (0.9)	0.75	0.40	(1, 20.0)				
	Residual Variance (sd)	Between Wetland Variance (sd)	Conditional r^2	n	Residual Variance (sd)	Between Wetland Variance (sd)	Conditional r^2	n
groups = 5	0.19 (0.53)	0.06 (0.25)	0.63	28	0.31 (0.55)	0.06 (0.24)	0.59	28

LME Model of $Fe_{Dit\text{-}HCl}$ (wet upper horizons, mean water level > -0.5 m)

	Global Model			
Fixed effects	Beta (se)	F-statistic	P	df
Intercept	0.23 (0.05)			
Mean water level (m)	0.05 (0.15)	3.2	0.09	(1, 15.1)
Horizon class (1, 2)	-0.01 (0.05)	0.09	0.77	(1, 14.0)
Mean water level*horizon class	0.30 (0.21)	2.1	0.16	(1, 14.0)
	Residual Variance (sd)	Between Wetland Variance (sd)	Conditional r^2	n
groups = 5	0.0009 (0.09)	0.018 (0.14)	0.74	22

LME Model of $Fe_{Dit\text{-}HCl}$ (dry upper horizons, mean water level ≤ -0.5 m)

	Global Model				Reduced Model			
Fixed effects	Beta (se)	F-statistic	P	df	Beta (se)	F-statistic	P	df
Intercept	6.2 (0.8)				5.9 (0.7)			
Mean water level (m)	3.1 (0.7)	24.3	7.2 E-05	(1, 21.1)	2.7 (0.5)	24.9	4.7E-05	(1, 23.2)
Horizon class (1, 2)	-0.6 (1.0)	0.4	0.55	(1, 20.0)				
Mean water level*horizon class	-0.8 (1.0)	0.69	0.41	(1, 20.0)				
	Residual Variance (sd)	Between Wetland Variance (sd)	Conditional r^2	n	Residual Variance (sd)	Between Wetland Variance (sd)	Conditional r^2	n
groups = 5	0.65 (0.81)	0.35 (0.59)	0.76	28	0.34 (0.58)	0.66 (0.81)	0.76	28

S6I. LME model of C_{Pyro} and $C_{Dit\text{-}HCl}$ on upper horizons, separated by mean water level -0.5 m

LME Model of C_{Pyro} (wet upper horizons, mean water level > -0.5 m)

	Global Model				Reduced Model			
Fixed effects	Beta (se)	F-statistic	P	df	Beta (se)	F-statistic	P	df
Intercept	7.7 (1.0)				7.2 (0.9)			
Mean water level (m)	4.6 (1.9)	2.3	0.200	(1, 14.4)				
Horizon class (1, 2)	-3.5 (0.6)	30.7	0.00	(1, 14.0)	-2.9 (0.6)	22.3	2.20E-04	
Mean water level * horizon class	-4.9 (2.6)	3.5	0.08	(1, 14.0)				
	Residual Variance (sd)	Between Wetland Variance (sd)	Conditional r^2	n	Residual Variance (sd)	Between Wetland Variance (sd)	Conditional r^2	n
groups = 5	1.7 (1.3)	4.1 (2.0)	0.80	22	2.1 (1.4)	3.6 (1.9)	0.74	22

LME Model of C_{Pyro} (dry upper horizons, mean water level≤ -0.5 m)

	Global Model				Reduced Model			
Fixed effects	Beta (se)	F-statistic	P	df	Beta (se)	F-statistic	P	df
Intercept	14.3 (1.9)				12.8 (1.4)			
Mean water level (m)	7.3 (1.8)	15.5	0.001	(1, 22.0)	5.9 (1.3)	15.3	0.001	(1, 22.6)
Horizon class (1, 2)	-6.6 (2.7)	5.8	0.03	(1, 20.1)	-3.5 (0.6)	32.3	1.20E-05	(1, 21.1)
Mean water level * horizon class	-3.1 (2.6)	1.4	0.26	(1, 20.1)				
	Residual Variance (sd)	Between Wetland Variance (sd)	Conditional r^2	n	Residual Variance (sd)	Between Wetland Variance (sd)	Conditional r^2	n
groups = 5	2.6 (1.6)	0 (0)	0.65	28	2.7 (1.6)	0 (0)	0.65	28

*wetland variance=0, adjusted R^2 approximated from linear model

LME Model of $C_{Dit\text{-}HCl}$ (wet upper horizons, mean water level > -0.5 m)

	Global Model				Reduced Model			
Fixed effects	Beta (se)	F-statistic	P	df	Beta (se)	F-statistic	P	df
Intercept	1.9 (0.25)				1.8 (0.2)			
Mean water level (m)	1.2 (0.6)	1.4	0.25	(1, 14.6)				
Horizon class (1, 2)	-0.84 (0.19)	18.7	0.00	(1, 14.0)	-0.66 (0.18)	13.1	2.3E-03	(1, 16.0)
Mean water level * horizon class	-1.4 (0.80)	3.2	0.09	(1, 14.0)				
	Residual Variance (sd)	Between Wetland Variance (sd)	Conditional r^2	n	Residual Variance (sd)	Between Wetland Variance (sd)	Conditional r^2	n
groups = 5	0.15 (0.39)	0.22 (0.47)	0.71	22	0.18 (0.43)	0.18 (0.43)	0.62	22

LME Model of $C_{Dit\text{-}HCl}$ (dry upper horizons,mean water level≤ -0.5 m)

	Global Model				Reduced Model			
Fixed effects	Beta (se)	F-statistic	P	df	Beta (se)	F-statistic	P	df
Intercept	7.7 (1.1)				6.8 (0.8)			
Mean water level (m)	4.4 (1.0)	18.1	3.3E-04	(1, 22.0)	3.5 (0.7)	17.7	3.5E-04	(1, 22.7)
Horizon class (1, 2)	-3.1 (1.5)	4.1	0.06	(1, 20.1)	-1.1 (0.34)	11.6	2.6E-03	(1, 21.1)
Mean water level * horizon class	-1.8 (1.4)	1.6	0.21	(1, 20.1)				
	Residual Variance (sd)	Between Wetland Variance (sd)	Conditional r^2	n	Residual Variance (sd)	Between Wetland Variance (sd)	Conditional r^2	n
groups = 5	0.80 (0.9)	0 (0)	0.55	28	0.82 (0.9)	0 (0)	0.54	28

*wetland variance=0, adjusted R^2 approximated from linear model

S6J. LME model of C_{Pyro}/C_{bulk} and $C_{Dit\text{-}HCl}/C_{bulk}$ on upper horizons

LME Model of C_{Pyro}/C_{bulk} (upper horizons)				
	Global Model			
Fixed effects	Beta (se)	F-statistic	P	df
Intercept	156.7 (18.0)			
Mean water level (m)	-33.8 (19.2)	30.9	1.6E-06	(1, 43.2)
Horizon class (1, 2)	52.0 (21.6)	5.8	0.021	(1, 42.0)
Mean water level * horizon class	-85.4 (26.9)	10.1	-0.0028	(1, 42.0)
n=50	Residual Variance (sd)	Between Wetland Variance (sd)	Conditional r^2	
groups = 5	2275 (48)	442 (21)	0.70	

LME Model of $C_{Dit\text{-}HCl}/C_{bulk}$ (upper horizons)				
	Global Model			
Fixed effects	Beta (se)	F-statistic	P	df
Intercept	40.4 (13.3)			
Mean water level (m)	-45.6 (15.3)	73.1	7.0E-11	(1, 43.7)
Horizon class (1, 2)	12.2 (17.2)	0.50	0.48	(1, 42.0)
Mean water level * horizon class	-96.4 (21.5)	20.2	-0.000054	(1, 42.0)
n=50	Residual Variance (sd)	Between Wetland Variance (sd)	Conditional r^2	
groups = 5	1447 (38)	136 (12)	0.75	

S6K. Simple linear regression between C_{Pyro} and Fe_{Pyro} for upper soils, separated by mean water level of -0.5 m

Simple linear regression for C_{Pyro} (wet upper soils, mean water level >0.5 m)						
	Global model			Reduced		
Fixed effects	Beta (se)	F-statistic	P	Beta (se)	F-statistic	P
intercept	7.5 (.13)			7.3 (0.7)		
Fe_{Pyro} (mg Fe g^{-1} soil)	-0.8 (4.7)	0.01	0.90			
horizon class (1 or 2)	-30 (1.7)	8.1	0.01	-2.9 (0.98)	8.90	0.01
Fe*horizon class	0.2 (6.6)	0.00	0.98			
	n = 21			n = 21		
	Adjusted R^2 = 0.19			Adjusted R^2 = 0.27		
	df = 3,18			df =1,20		

Simple linear regression for C_{Pyro} (dry upper soils, mean water level ≤ -0.5 m)						
	Global model			Reduced		
Fixed effects	Beta (se)	F-statistic	P	Beta (se)	F-statistic	P
intercept	2.5 (0.9)			2.8 (0.8)		
Fe_{Pyro} (mg Fe g^{-1} soil)	2.1(0.4)	48.7	3.3E-07	2.0 (0.3)	50.1	2.0E-07
horizon class (1 or 2)	-2.1 (1.5)	26.1	3.1E-05	2.8 (0.5)	26.9	2.3E-05
Fe*horizon class	-0.4 (0.8)	0.30	0.60			
	n = 28			n = 28		
	Adjusted R^2 = 0.73			Adjusted R^2 = 0.73		
	df = 3, 24			df = 2, 25		

S6L. Simple linear regression between $C_{Dit\text{-}HCl}$ and $Fe_{Dit\text{-}HCl}$ for upper soils, separated by mean water level of -0.5 m

Simple linear regression for C_{DitHCl} (wet upper soils, mean water level >0.5 m)

	Wet upper soils (depth to water table <0.5 m)					
	Global model			Reduced		
Fixed effects	Beta (se)	F-statistic	P	Beta (se)	F-statistic	P
intercept	1.2 (0.4)			1.8 (0.2)		
$Fe_{Dit\text{-}HCl}$ (mg Fe g^{-1} soil)	2.7 (1.5)	1.60	0.22			
horizon class (1 or 2)	0.13 (0.5)	6.30	0.02	-0.66 (0.23)	6.8	0.017
Fe*horizon class	3.6 (2.0)	3.20	0.09			
	n = 21			n = 21		
	Adjusted R^2 = 0.28			Adjusted R^2 = 0.21		
	df = 3, 18			df=1,20		

Simple linear regression for $C_{Dit\text{-}HCl}$ (dry upper soils, mean water level ≤ -0.5 m)

	Global model		
Fixed effects	Beta (se)	F-statistic	P
intercept	0.02 (0.6)		
$Fe_{Dit\text{-}HCl}$ (mg Fe g^{-1} soil)	1.1 (0.20)	19.8	0.0001
horizon class (1 or 2)	1.4 (1.0)	17.0	0.0003
Fe*horizon class	-0.86 (03.1)	7.80	0.01
	n = 28		
	Adjusted R^2 = 0.61		
	df = 3, 24		

S6M. LME model of C:$N_{aggregate}$ for upper soils, by aggregate size class

LME model on Large Macroagg. $CN_{aggregate}$ (upper soils)

	Global model				Reduced model			
Fixed effects	Beta (se)	F-statistic	P	df	Beta (se)	F-statistic	P	df
Intercept	15.9 (1.8)				15.8 (1.6)			
Mean water level (m)	-6.8 (1.4)	39.3	2.02E-07	(1, 39.6)	-6.5 (1.0)	41.0	1.10E-07	(1, 41.6)
Horizon class (1, 2)	-0.20 (1.7)	0.91	0.91	(1, 39.1)				
Mean water level * horizon class	0.66 (2.0)	0.74	0.74	(1, 39.0)				
n = 50	Residual Variance (sd)	Between Wetland Variance (sd)	Conditional r^2		Residual Variance (sd)	Between Wetland Variance (sd)	Conditional r^2	
groups = 5	11.9 (3.5)	9.2 (3.0)	0.63		11.5 (3.4)	9.1 (3.0)	0.64	

LME model on Small Macroagg. $CN_{aggregate}$ (upper soils)

	Global model				Reduced model			
Fixed effects	Beta (se)	F-statistic	P	df	Beta (se)	F-statistic	P	df
Intercept	16.2 (1.6)				16.1 (1.4)			
Mean water level (m)	-6.1 (1.1)	46.8	3.10E-08		-5.9 (0.8)	50.6	9.80E-09	(1, 42.2)
Horizon class (1, 2)	-0.28 (1.3)	0.05	0.83					
Mean water level * horizon class	0.66 (1.7)	0.15	0.70					
n = 50	Residual Variance (sd)	Between Wetland Variance (sd)	Conditional r^2		Residual Variance (sd)	Between Wetland Variance (sd)	Conditional r^2	
groups = 5	7.8 (2.8)	8.2 (2.3)	0.68		7.5 (2.7)	8.4 (2.9)	0.69	

LME model on Microagg. $CN_{aggregate}$ (upper soils)

	Global model				Reduced model			
Fixed effects	Beta (se)	F-statistic	P	df	Beta (se)	F-statistic	P	df
Intercept	15.8 (1.7)				16.7 (1.6)			
Mean water level (m)	-6.1 (1.3)	27.6	5.20E-06	(1, 40.2)	-4.8 (0.9)	26.8	6.20E-06	(1, 41.2)
Horizon class (1, 2)	-0.90 (1.5)	0.38	4.00E-01	(1, 40.0)	-2.6 (0.9)	8.4	6.00E-03	(1, 41.0)
Mean water level * horizon class	2.6 (1.8)	2.12	0.15	(1, 40.0)				
n = 50	Residual Variance (sd)	Between Wetland Variance (sd)	Conditional r^2		Residual Variance (sd)	Between Wetland Variance (sd)	Conditional r^2	
groups = 5	9.5 (3.1)	9.6 (3.1)	0.65		9.8 (3.1)	9.6 (3.1)	0.64	

LME model on Silt/Clay $CN_{aggregate}$ (upper soils)

	Global model			
Fixed effects	Beta (se)	F-statistic	P	df
Intercept	13.8 (1.2)			
Mean water level (m)	-4.7 (0.95)	18.9	9.10E-05	(1, 40.2)
Horizon class (1, 2)	-0.86 (1.1)	0.62	4.40E-01	(1, 40.0)
Mean water level * horizon class	3.4 (1.3)	6.4	0.015	(1, 40.0)
n = 50	Residual Variance (sd)	Between Wetland Variance (sd)	Conditional r^2	
groups = 5			0.64	

S6N. LME model of $C_{aggregate}$ for upper soils, by aggregate size class

LME model on Large Macroagg. $C_{aggregate}$ (upper soils)

	Global model				Reduced model			
Fixed effects	Beta (se)	F-statistic	P	df	Beta (se)	F-statistic	P	df
Intercept	27.6 (4.9)				24.1 (4.42)			
Mean water level (m)	18.7 (5.1)	12.85	8.5E-04	(1, 43.1)	13.2 (3.7)	12.48	9.8E-04	(1, 44.1)
Horizon class (1, 2)	-18.4 (5.8)	10.22	0.0026	(1, 42.0)	-11.4 (3.7)	9.73	3.2E-03	(1, 43.0)
Mean water level * horizon class	-11.2 (7.2)	2.52	0.13	(1, 42.0)				
n = 50	Residual Variance (sd)	Between Wetland Variance (sd)	Conditional r^2		Residual Variance (sd)	Between Wetland Variance (sd)	Conditional r^2	
groups = 5	161.5 (12.7)	38.1 (6.2)	0.43		166.8 (12.9)	37.6 (6.1)	0.41	

LME model on Small Macroagg. $C_{aggregate}$ (upper soils)

	Global model				Reduced model			
Fixed effects	Beta (se)	F-statistic	P	df	Beta (se)	F-statistic	P	df
Intercept	18.5 (2.1)				18.18 (1.34)			
Mean water level (m)	0.5 (2.6)	0.60	0.44	(1, 44.8)				
Horizon class (1, 2)	-10.0 (3.0)	11.2	0.0017	(1, 42.0)	-11.30 (1.85)	37.2	2.4E-07	(1, 44.0)
Mean water level * horizon class	2.0 (3.7)	0.28	0.60	(1, 42.0)				
n = 50	Residual Variance (sd)	Between Wetland Variance (sd)	Conditional r^2		Residual Variance (sd)	Between Wetland Variance (sd)	Conditional r^2	
groups = 5	43.92 (6.63)	0.31 (0.55)	0.43		42.85 (6.55)	0.38 (0.62)	0.43	

LME model on Microagg. $C_{aggregate}$ (upper soils)

	Global model			
Fixed effects	Beta (se)	F-statistic	P	df
Intercept	1.6 (0.3)			
Mean water level (m)	-0.94 (0.39)	2.06	0.16	(1, 44.8)
Horizon class (1, 2)	-0.25 (0.44)	0.32	0.57	(1, 42.0)
Mean water level * horizon class	1.07 (0.55)	3.83	0.057	(1, 42.0)
n = 50	Residual Variance (sd)	Between Wetland Variance (sd)	Conditional r^2	
groups = 5	0.95 (0.97)	0.0056 (0.075)	0.26	

LME model on silt/clay $C_{aggregate}$ (upper soils)

	Global model				Reduced model			
Fixed effects	Beta (se)	F-statistic	P	df	Beta (se)	F-statistic	P	df
Intercept	1.51 (0.26)				1.76 (0.20)			
Mean water level (m)	-0.39 (0.28)	3.27	0.08	(1, 43.3)				
Horizon class (1, 2)	-0.44 (0.32)	1.96	0.17	(1, 42.0)	-0.47 (0.20)	5.65	0.02	(1, 44.0)
Mean water level * horizon class	0.049 (0.39)	0.015	0.90	(1, 42.0)				
n = 50	Residual Variance (sd)	Between Wetland Variance (sd)	Conditional r^2		Residual Variance (sd)	Between Wetland Variance (sd)	Conditional r^2	
groups = 5	0.49 (0.70)	0.082 (0.29)	0.26		0.50 (0.70)	0.10 (0.32)	0.24	

S6O. LME model of $C_{aggregate}/C_{bulk}$ for upper soils, by aggregate size class

LME model on Large Macroagg. $C_{aggregate}/C_{bulk}$ (upper soils)

	Global model				Reduced model			
Fixed effects	Beta (se)	F-statistic	P	df	Beta (se)	F-statistic	P	df
Intercept	0.43 (0.085)				0.46 (0.075)			
Mean water level (m)	0.18 (0.090)	12.2	0.0011	(1, 43.1)	0.22 (0.063)	12.3	0.0011	(1, 44.2)
Horizon class (1, 2)	-0.009 (0.10)	0.76	0.38	(1, 43.1)	-0.15 (0.062)	5.7	0.022	(1, 43.0)
Mean water level * horizon class	0.097 (0.13)	0.60	0.44	(1, 43.1)				
n = 50	Residual Variance (sd)	Between Wetland Variance (sd)	Conditional r^2		Residual Variance (sd)	Between Wetland Variance (sd)	Conditional r^2	
groups = 5	0.050 (0.22)	0.010 (0.10)	0.37		0.049 (0.22)	0.010 (0.10)	0.37	

LME model on Small Macroagg. $C_{aggregate}/C_{bulk}$ (upper soils)

	Global model				Reduced model			
Fixed effects	Beta (se)	F-statistic	P	df	Beta (se)	F-statistic	P	df
Intercept	0.46 (0.061)				0.47 (0.042)			
Mean water level (m)	-0.13 (0.076)	5.8	0.02	(1, 44.9)	-0.13 (0.053)	6.1	0.017	(1, 47.0)
Horizon class (1, 2)	0.013 (0.086)	0.023	0.88	(1, 42.0)				
Mean water level * horizon class	-0.004 (0.11)	0.0017	0.97	(1, 42.0)				
n = 50	Residual Variance (sd)	Between Wetland Variance (sd)	Adjusted R^2		Residual Variance (sd)	Between Wetland Variance (sd)	Adjusted R^2	
groups = 5	0.036 (0.19)	0 (0)	0.06		0.035 (0.19)	0 (0)	0.1	

*wetland variance=0, adjusted R^2 approximated from linear model

LME model on Microagg. $C_{aggregate}/C_{bulk}$ (upper soils)

	Global model				Reduced model			
Fixed effects	Beta (se)	F-statistic	P	df	Beta (se)	F-statistic	P	df
Intercept	0.053 (0.023)				0.049 (0.020)			
Mean water level (m)	-0.035 (0.02)	7.03	0.011	(1, 42.8)	-0.042 (0.02)	7.2	0.010	(1, 43.84)
Horizon class (1, 2)	0.052 (0.03)	4.33	0.043	(1, 42.0)	0.061 (0.02)	15.5	0.0003	(1, 43.0)
Mean water level * horizon class	-0.014 (0.03)	0.21	0.65	(1, 42.0)				
n = 50	Residual Variance (sd)	Between Wetland Variance (sd)	Conditional r^2		Residual Variance (sd)	Between Wetland Variance (sd)	Conditional r^2	
groups = 5	0.003 (0.06)	0.001 (0.03)	0.44		0.003 (0.05)	0.001 (0.03)	0.45	

LME model on silt/clay $C_{aggregate}/C_{bulk}$ (upper soils)

	Global model			
Fixed effects	Beta (se)	F-statistic	P	df
Intercept	0.052 (0.023)			
Mean water level (m)	-0.015 (0.02)	15.5	0.0003	(1, 42.7)
Horizon class (1, 2)	0.023 (0.02)	1.00	0.32	(1, 42.0)
Mean water level * horizon class	-0.087 (0.03)	8.94	0.0047	(1, 42.0)
n = 50	Residual Variance (sd)	Between Wetland Variance (sd)	Conditional r^2	
groups = 5	0.003 (0.05)	0.001 (0.03)	0.60	

S6P. ANOVA test on C:$N_{aggregate}$, $C_{aggregate}$, and $C_{aggregate}/C_{bulk}$ for upper soils, by size class

	Aggregate Size Class Property				
	Large Macroagg.	Small Macroagg.	Microagg.	Silt/Clay	ANOVA, Tukey's HSD
C:$N_{aggregate}$	20.1 (0.8)^a	19.5 (0.7)^a	18.3 (0.7)^a	15.2 (0.4)^b	F(3, 187)=10.9, P <0.0001
$C_{aggregate}$	10.1 (2.4)^a	12.5 (1.2)^a	1.8 (0.2)^b	1.5 (0.1)^b	F(3, 196)=18.3, P <0.0001
$C_{aggregate}/C_{bulk}$	0.24 (0.04)^b	0.55 (0.03)^a	0.11 (0.01)^c	0.10 (0.01)^c	F(3, 196)=71.1, P <0.0001

Chapter 2: Soil organic carbon stocks are more related to metrics of wetland drying than inundation duration in seasonally flooded freshwater mineral wetlands

Abstract

Wetlands store significant soil organic carbon (SOC) globally. Freshwater mineral wetlands are less studied than peatlands but are highly susceptible to hydrologic alteration. We explore the relationship between SOC stocks and hydrologic regime in seasonally flooded freshwater mineral wetlands, both within and across wetlands. We measured SOC stocks, clay content, and Fe concentration to a depth of 100 cm at the center of 19 wetlands. At a subset of 12 wetlands, we recorded daily water level to calculate metrics of hydrologic regime (e.g., mean water level, minimum water level, inundation duration, water level coefficient of variation, inundation recession rate). At a further subset of 5 wetlands, we measured SOC stocks to 50 cm across a transect from wetland edge to upland. Our findings suggest stronger associations between SOC stocks from 10–100 cm with hydrologic metrics of dryness (e.g., minimum water level, inundation recession rate) than wetness (e.g., mean water level, inundation duration). We also found high SOC stocks below 50 cm in the soil profile and depth-dependent relationships between SOC stocks, hydrology, and soil characteristics, indicating that large, deep SOC stocks may respond differently to change than shallow organic soils. Finally, we found generalizable relationships between SOC stocks and hydrologic indicators across the transect, which may be useful in modeling SOC stocks on the landscape scale. Overall, our study suggests that drying is a strong control on SOC stocks in seasonally flooded depressional wetlands, and we expect future increases in wetland drying to stimulate C loss and emissions from freshwater mineral wetlands.

1. Introduction

Wetland soils contribute approximately 22% of soil organic carbon (SOC) storage in the conterminous United States despite comprising only 5% of the total land area (Lajtha et al. 2018). While wetland research focuses extensively on SOC storage in peatlands (Villa and Bernal 2018), freshwater mineral wetlands make up the majority of wetland area and account for one-quarter of wetland SOC storage in the conterminous U.S. (Bridgham et al., 2006). Freshwater mineral wetlands are vulnerable to agriculture and development, as 80% of wetland loss worldwide is from these ecosystems (Bridgham et al. 2006). As such, there is considerable interest in conservation and restoration of wetlands for SOC storage (Griscom et al. 2017), and quantifying controls on SOC storage is critical to wetland conservation and modeling. Previous research has documented large regional variability in wetland SOC storage across the U.S. (Nahlik and Fennessy 2016), among ecoregions and along disturbance gradients (e.g., Ballantine & Schneider, 2009; Fennessy et al., 2018; Mitsch et al., 2013), and among wetlands of different types within a region (e.g., Bernal & Mitsch, 2012; Moreno-Casasola, Hernández, & Campos, 2017). However, due to the broad spatial scale of studies exploring SOC in wetlands of different types and disturbance levels, multiple factors controlling wetland SOC storage vary simultaneously among sites and present a challenge to elucidating the relative importance of each factor.

At large spatial scales, SOC storage in wetlands is controlled by plant C inputs (Trettin et al., 2001), microbial communities (Yarwood 2018), climate (Osland et al. 2018), redox conditions (Chapman et al., 2019; LaCroix et al., 2019; McLatchey & Reddy, 1998), and soil properties such as parent material and texture (Angst et al. 2018). Hydrology, specifically wetland saturation and inundation, is considered a master variable that influences each of these factors by altering biotic communities, oxygen (O_2) concentrations, and decomposition rates (Day and Megonigal 1993, Tarr et al. 2005, Mitsch and Gosselink 2015). Soils with a longer duration of saturation or inundation are assumed to contain more SOC due to anoxic conditions, which suppresses C

decomposition rates; however, to date surprisingly few studies have explicitly tested this hypothesis in freshwater mineral wetlands (e.g., Fennessy et al., 2018; Lewis & Feit, 2015).

At a smaller spatial scale, several studies focus within individual wetlands to isolate the importance of hydrology (e.g., mean water level, duration of inundation) or landscape position on SOC dynamics (e.g., LaCroix et al., 2019; Pearse et al., 2018; Webster et al., 2011). These studies develop relationships between hydrology and SOC stocks across wetland–upland transects within individual wetlands, which can then be used to predict SOC stocks at the landscape scale (e.g., Webster et al., 2011). Studies across wetland–upland transects indicate that wetland perimeters contribute substantially to landscape-scale SOC stocks, even though these edge areas may not fall under the regulatory definition of wetlands due to insufficiently saturated conditions (Tiner 1996). However, studies focused solely on SOC stocks within individual wetlands may not capture variation in SOC across wetlands (e.g., Pearse et al., 2018) and factors relevant to SOC storage (e.g., physiochemical stabilization) may vary in addition to hydrology across the wetland–upland gradient. Therefore, sampling both within and among wetlands that vary hydrologically but are otherwise similar with respect to other drivers of C storage is needed for a more complete understanding of hydrologic controls on SOC than sampling across transects alone.

Rather than focus only on duration of inundation or saturation, we examine multiple aspects of the hydrologic regime that may be important for oxic conditions and therefore SOC dynamics in freshwater mineral wetlands. Hydrologic regime (e.g., magnitude, frequency, duration, and timing) has long been the focus of riverine ecology, where biotic, sediment, and biogeochemical dynamics are known to be influenced by multiple aspects of the flow regime ((Poff et al. 1997, Palmer and Ruhi 2019). Hydrologic regime is a strong control on wetland biotic communities and gas fluxes, which often depend on the magnitude and timing of hydrologic events (e.g., Crawford, 2003; Semlitsch & Bodie, 1998; Tangen & Bansal, 2019; Zedler, 2003), but few studies explore the relationship between wetland soil biogeochemistry and multiple aspects of hydrologic regime. We focus on indicators of hydrologic regime that describe

the seasonal variability and magnitude of wetland wetting and drying (e.g., inundation duration, mean and minimum water level, coefficient of variation, summertime inundation recession rate), which are likely to influence SOC processing in seasonal wetlands, including depressional wetlands and floodplain wetlands. Specifically, we expect these aspects of hydrologic regime to indicate relative differences in anoxic conditions across wetlands that influence wetland SOC decomposition and production (Reddy and Patrick 1975, McLatchey and Reddy 1998, Chapman et al. 2019).

Seasonally flooded wetlands are a unique type of freshwater mineral wetland with hydrologic regimes that vary both spatially (i.e., among wetlands and across a gradient from wetland to upland) and temporally (i.e., seasonal drying and wetting). Due to their hydrologic variability, seasonally flooded wetlands are an ideal study unit to address the knowledge gap regarding hydrologic regime and wetland SOC stocks. Our first objective was to determine the relationship between hydrologic regime and SOC stocks across wetlands to determine which aspects of hydrologic regime might have the most predictive power and may be most useful for wetland C modeling. Our second objective was to quantify SOC stocks along a hydrologic gradient from wetland to upland to determine the importance of hydrologic regime across the landscape. We sampled soils to 1.0 m depth at 19 seasonally flooded wetlands less than 8 km apart to calculate SOC stocks and measured daily water level at a subset of 12 wetlands to characterize hydrologic regime. Additionally, we sampled SOC stocks to 0.5 m depth across a wetland–upland transect at a subset of five transect wetlands. We hypothesize that SOC stocks across wetlands will be higher in areas with longer duration of inundation and higher mean water level and will be lower in areas with a lower minimum water level, faster summertime recession rate, and higher coefficient of variation in water level. We also hypothesize that SOC stocks will decline across the wetland–upland gradient. This research explores relationships between SOC stocks and hydrologic regime that could be used to improve SOC stock models.

2. Methods

2.1 Study sites and climate

The Delmarva Peninsula is a low-relief (<30 m elevation) region of the Eastern U.S.A. bordered by the Chesapeake Bay and the Atlantic Ocean. The climate of the Delmarva Peninsula is humid and temperate. Mean monthly temperatures range from 1.3 °C (January) to 25.1 °C (July; PRISM average 1981–2010; Oregon State University 2019). Annual precipitation is 1105 mm on average and is typically distributed evenly throughout the year (PRISM average 1981–2010; Oregon State University 2019). Hydrology in the region is driven largely by the combined effects of seasonal increases in evapotranspiration during the growing season (May–September), connections to groundwater and local streams, and topography (Brooks 2005). The Delmarva Peninsula contains an abundance of wetlands, though many of the historic wetlands have been drained for agriculture (Fenstermacher et al., 2014).

We sampled soils at the center of 19 seasonally flooded freshwater mineral wetlands located within 8 km distance of each other and ranging in depressional area from 500–1100 m^2 (Fig. 2.1B). Study wetlands have also been called natural Delmarva Bays (Fenstermacher et al., 2014; Stolt & Rabenhorst, 1987), geographically isolated wetlands (Tiner 2003), freshwater depressional wetlands (Jones et al. 2018), and Coastal Plain forested wetlands (Epting et al., 2018; Lang et al., 2013). Study wetlands are located adjacent to large open-canopy wetlands with emergent vegetation that The Nature Conservancy began restoring in 2003. Study wetlands range from temporarily flooded to semipermanently flooded (Cowardin et al., 2005). Soils are acidic to very acidic (pH ~4). Typical soil series is the Hammonton-Fallsington-Corsica complex, though some soils are as Lenni loams or Corsica mucky loams (Soil Survey Staff, Natural Resources Conservation Service). Study wetlands were intentionally selected to lack emergent vegetation to isolate the impacts of hydrologic regime on SOC, and are surrounded by upland forests of *Acer rubrum*, *Quercus phellos, Liquidambar styraciflua*, and *Nyssa sylvatica* overstory with *Ilex opaca, Magnolia virginianica, Clethra alnifolia,* and *Vaccinium corymbosum* understory.

A subset of 12 from the 19 total wetlands were selected for hydrologic analysis by installing wells, as described below (hereafter, "well wetlands"). Out of the 12 well wetlands, a further subset of five wetlands were selected for intensive study of SOC stocks across an elevational gradient from wetland edge to upland forest (hereafter, "transect wetlands"). In addition to sampling at the center of each transect wetland, we established transects of five evenly-spaced points spanning 20–25 m from the edge of the wetland as observed during low hydrologic expression in November 2017, to a higher elevation upland point with understory vegetation where no hydromorphic soil features were present in the upper 50 cm (e.g., depletions, concentrations, thick organic layer, etc.). Total length from wetland's center well to upland transect point ranged from 29 m to 54 m.

2.2 Hydrologic variables

In September 2017, we installed surface wells in each of the 12 well wetlands at the deepest point to a depth of 1 m to record water level in 5 min intervals (HOBO water level loggers; Onset Computer Corporation, Bourne, MA). Water levels of each well wetland were aggregated to daily timesteps to calculate water level metrics for water year 2018 (October 1, 2017–September 31, 2018), including mean, minimum (5^{th} percentile), maximum (95^{th} percentile), range (maximum–minimum), and coefficient of variation, and percent of year inundated (Table 2.1). Due to dynamic water levels during the growing season, we also calculated summertime inundation recession rate as the linear change in inundation (i.e., water level above wetland soil surface) during the period in the growing season (May–September) where daily rain was <0.01 cm. For water year 2018, the largest recession event occurred June 11–July 18 (Fig. 2.2B). In wetlands where water level fell below the soil surface during this period (n=4), we stopped calculating recession rate once water level was <0 m due to the differences in specific yield above and below the soil surface. Gaps in water level data were filled by creating linear models with water levels from wells in nearby wetlands, which were not part of the 12 well wetlands studied here (i.e., wells were only used for gap-filling; Jones, 2019).

At the five transect wetlands selected for intensive study of SOC stocks from wetland to upland, we also installed an upland well to a depth of 1 m. Water levels from the wetland and upland wells were used to interpolate water level at each transect point, assuming linear change in water table altitude from the point where water level intersected with ground surface to the upland well (Jones, 2019). While seasonally flooded wetlands may experience groundwater mounding throughout the year (Phillips and Shedlock 1993, Rosenberry and Winter 1997), we assumed that water table altitude changes linearly across the transect due to the short transect distance and low-relief landscape. We surveyed each transect point to measure elevation relative to the central wetland well.

2.3 Field methods in wetland center and across transects

At the center of each of the 19 total study wetlands, we collected two replicate soil cores to a depth of 1.0 m in August 2018. For well wetlands (n=12), samples were randomly located within 2.5 m of the well. Wetlands without a well were randomly sampled within 2.5 m of the deepest point in the wetland (n=7). Briefly, two replicate soil cores from 0–50 cm depth were collected in the center of each wetland depression by pushing a 5.08 cm diameter sharpened aluminum core into the organic soil, plugging the top of the core to create suction and prevent soil from falling out of the bottom of the core, and extracting the core from the soil. Compaction of each sample core was recorded to the nearest centimeter. Cores were sealed, transported to the lab, and frozen whole for sample processing.

To collect soil from 50–100 cm, a McCauley peat sampler (Eijkelkamp Soil & Water, Morrisville, SC) was inserted into the same hole in two 25 cm depth increments (50–75 cm and 75–100 cm). Depth increments were transferred into pre-weighed aluminum tins and transferred in coolers to the lab for processing within 24 hours. Where soil was too dense to sample with the peat sampler, we used an open-faced bucket auger to collect soils from 50–100 cm to determine C concentration.

At the five transect wetlands, samples were collected across the five transect points to calculate SOC stocks from 0–50 cm. At the two points closer to the wetland center a McCauley peat sampler was used to collect samples from 0–50 cm. Samples from the peat sampler were separated into increments of 0–10 cm, 10–30 cm, and 30–50 cm in the field, transported to the lab in coolers for processing within 24 h. At the three furthest upland points where sampling with the peat sampler was not possible, intact cores were collected from 0–50 cm with a sharpened aluminum core, as above. Cores were sealed, transported to the lab, and frozen whole for sample processing.

2.4 Lab methods

The following measurements and analyses are for all 19 wetlands unless specified otherwise.

2.4.1 Bulk density

We calculated bulk density for two replicates at each wetland center from 0–100 cm depth to constrain the well-known spatial heterogeneity in bulk density (Walter et al., 2016) and limit the potential for compaction to bias results. For soil cores from 0–50 cm, the frozen intact cores were thawed for 1 min under running water and extruded. We conducted a soil profile description for each core including horizonation, soil color, and hydromorphic features (e.g., depletions, concentrations). Cores were separated into the following depth increments: 0–10 cm, 10–30 cm, and 30–50 cm. Intervals for depth increments were corrected for compaction using a simple linear correction shown in Equation 1, where $l_{increment}$ is the length of the uncompacted depth increment (i.e., 10 cm for the 0–10 cm depth increment) and $l_{compacted}$ is the length of the compacted depth increment. Linear correction assumes that compaction is evenly distributed across the core (Walter et al. 2016), which is less accurate than bulk density corrections that account for horizon differences in compaction. However, we believe this method is appropriate due to high organic matter in the upper 50 cm of soils, which indicates that compaction may occur throughout the entire 50 cm profile.

$$l_{compacted} = \frac{total\ core\ length\ (50\ cm) - compaction\ (cm)}{total\ core\ length\ (50\ cm)} \times l_{increment} \quad \text{Eq. 1}$$

We measured bulk density for all depth increments (e.g., 0–10, 10–30, 30–50 cm from the cores and 50–75, 75–100 cm from the peat sampler). First, samples were dried in clean, pre-weighed aluminum tins in a 65 °C drying oven for >7 days or until no further mass loss, and then weighed for dry soil mass ($Mass_{dry}$; Collins & Kuehl, 2001). We removed rocks and roots with volume >0.1 cm^3 or mass >0.1 g. Bulk density was calculated by dividing soil dry mass by core volume for each sample increment, accounting for roots and rocks (Poeplau et al. 2017).

For wetlands in which we could not collect any soil for bulk density below 50 cm (n=5 wetlands) we used average bulk density from the Web Soil Survey (Soil Survey Staff, Natural Resources Conservation Service). For wetlands in which we could only collect one profile sample from 50–100 cm due to high soil density, the bulk density value from the single profile sample was used (n=3 samples). In wetlands where high bulk density prevented us from collecting the full sample from 75–100 cm, C concentration and bulk density were assumed to continue to the full depth of the increment.

2.4.2 Soil C concentrations, Fe concentrations, and clay content

Mass loss on ignition (LOI) was determined for all soil samples by weighing three replicates of 5 g oven-dry ground soil into crucibles and placing in a muffle furnace for 16 hours at 400 °C (Nelson and Sommers 1996). Samples were cooled to 65 °C and then immediately re-weighed to determine mass loss, which is equal to the amount of soil organic matter. Soil C concentration was measured on a subset of 90 samples that spanned the entire range of measured sample values for mass LOI using dry combustion on a LECO elemental analyzer (LECO Corp, St. Joseph, MI). We developed two separate linear regressions between mass LOI and C concentration separately for soil horizons above and below 50 cm (R^2=0.987 and R^2=0.981, respectively) to predict SOC for all soils (Fig S3).

Soil texture analysis was conducted to estimate clay content in mineral soil horizons (30–50, 50–75, 75–100 cm) on a composite sample at each wetland using the hydrometer method (Gee and Bauder, 1986). We measured total Fe (hydr)oxides (Fe_{Total}) in dried, ground (<2 mm) soils in depth increments of 10–30, 30–50, 50–75, and 75–100 cm. Briefly, Fe_{Total} was extracted from 0.8 g subsamples using dithionite-citrate-bicarbonate (Darke and Walbridge 1994). Supernatant Fe_{Total} was analyzed on an atomic absorption spectrometer on an air-acetylene flame (Perkin Elmer, Waltham, MA).

2.5 SOC stock calculations

Mean SOC stocks (kg C m^{-2}) were calculated by multiplying the C concentration in each depth increment by the bulk density and sample length, as in Eq. 2, where C is in g C g^{-1} soil and bulk density is in g cm^{-3}. We summed stocks for all depth increments of interest in each soil profile and took the mean of the two replicate cores for total SOC stocks.

$$SOC\ stock = C * bulk\ density * l_{increment} * 10 \quad \text{Eq. 2}$$

To compare SOC stocks of depth increments which differ in length, we also calculated normalized SOC stocks accounting for the length of the increment (i.e., g C cm^{-2} in 1 cm soil increment) by dividing SOC stock of each depth increment by the length of the increment.

2.6 Statistical methods

We conducted an initial analysis to test spatial autocorrelation between wetlands in close proximity with the Global Test for Spatial Autocorrelation using the R packages *sp* and *spdep* (Bivand, Pebesma, & Gomez-Rubio, 2013; Bivand & Wong, 2018; Pebesma & Bivand, 2005). This analysis showed no evidence of spatial autocorrelation in SOC stocks from 0–100 cm (Fig S2, Moran's I=-0.0049 (0.19), p=0.42), we therefore proceeded with linear regressions on the assumption that SOC stocks were randomly distributed through the study area.

We tested differences in soil characteristics (e.g., C concentration, SOC stock, bulk density, clay content, and Fe_{Total} concentration) across depth increments at all 19 wetlands with an analysis of variance (ANOVA) test and *post-hoc* comparisons with Tukey's honestly significant

differences (HSD; Supplemental S4B). We used simple linear regression to test the relationship between basic soil characteristics (e.g., bulk density, clay content, and Fe concentration) and C concentration separately for each depth increment (Supplemental S4C). We similarly tested the relationship between clay content and SOC stock and between clay content and bulk density using simple linear regression by depth increment (Supplemental S4C).

To test the relationship between SOC stocks and water level metrics across wetlands by depth increment, we conducted individual linear regressions for each predictor and corrected p-values for multiple tests using the Holm adjustment (Holm 1979). Our predictor variables were water level metrics of percent of year inundated, mean water level, minimum water level, water level coefficient of variation, and summertime recession rate (Table 2.1). Predictors were centered around 0 and scaled to +/- 2 before analysis to correct for differences in scale among metrics. To account for similarities among depth increments from the same wetland, we specified a first-order autocorrelation structure and corrected each model with the autocorrelation function, following Mangiafico (2016). Adjusted R^2 was approximated by the Nagelkerke pseudo R^2 (Nagelkerke 1991). Upon exploratory analysis of our data, we determined that SOC stocks in the 0–10 cm depth increment (organic horizon) showed no trends with water level metrics; therefore, we proceeded with analysis with SOC stocks from depth increments below 10 cm. Following our analysis of SOC stocks and water level metrics among depth increments, we conducted simple linear regressions with total SOC stocks from 10–100 cm using only significant predictors from the depth-specific analyses. We again applied the Holm p-value correction for multiple tests.

Finally, we used simple linear regression to test the relationship between SOC stocks and hydrologic variables across a hydrologic gradient (i.e., center well and five transect points) at the five transect wetlands. Initial data exploration showed differences between 0–10 cm depth increment and 10–50 cm depth increment; therefore, we separated our analysis into SOC stocks from 0–10 cm and 10–50 cm. We conducted two separate analyses with the predictor variables of water level and elevation relative to the center of the wetland. Initially, we conducted a linear

mixed effects model with wetland as a random effect to account for the differences in SOC stocks (intercept) across wetlands using the *lmer* R package (Bates et al. 2015). However, the log-likelihood ratio test showed that including wetland as a random variable did not significantly improve either model (Zuur et al. 2009; Supplemental S4D; Supplemental S5). Therefore, we removed the random term for wetland and instead conducted a separate simple linear model for each predictor variable (Table 2.3).

All analyses and graphing were conducted in R with the package *tidyr*, *sf*, *raster*, *nlme, rcompanion, ggpmisc*, *cowplot*, and *gridExtra* (Aphalo, 2016; Auguie, 2017; Hijmans, 2019; Pebesma, 2018; Wickham, 2017; Wilke, 2019).

3. Results

3.1 Wetland hydrology

Water levels were seasonally dynamic in water year 2018 (Fig. 2.2B). Water levels rose January–February and remained high February–May. Water levels declined as temperatures rose from 5 °C (March) to 20 °C (May) at the beginning of the growing season. Water levels continued to decline linearly as temperatures rose to 20–30 °C during the rain-free period in June and July, with water level at four wetlands dropping below the soil surface in mid-July. Water levels rose in response to a large storm event in July, but low rain in August caused water levels to fall to their lowest point in the year.

Precipitation was 1366 mm during water year 2018, which is higher than the average annual precipitation from the 30-year mean (1105 mm; Oregon State University, 2019). Total precipitation was 1169 mm in the prior water year 2017, which is closer to the average annual precipitation (PRISM, Oregon State University, 2019). Temperature followed typical seasonal patterns during water year 2018 (Fig. 2.2A).

All wetlands were inundated at their center (water level >0 m) for >80% of the water year (Table 2.1). Water levels were dynamic and ranged by 0.70 m over the year, on average (Table 2.1). Summertime recession rates ranged from -1.1 cm day^{-1} to -2.0 cm day^{-1}. Wetlands with a

wider annual range in water levels also experienced more rapid summertime recession, indicating that summertime drawdown is related to the magnitude of annual hydrologic fluctuation (P=0.006, Supplemental S4A).

3.2 How do C, bulk density, clay content, and Fe change throughout the soil profile?

We observed a nearly tenfold decline in C concentration from surface soils (0–10 cm) to deep soils (75–100 cm; P <0.0001; Fig. 2.3A; Supplemental S4B). In contrast, bulk density increased with depth, ranging from 0.27 g cm^{-3} in surface soils to 1.30 g cm^{-3} in deep soils (P <0.0001; Fig. 2.3C; Supplemental S4B). Soil texture changed with depth, but the difference varied widely between wetlands (Fig. 2.3E). Soil texture classes in the wetland center were mostly clay loams, silty clay loams, silty clays, and clays. Fewer than 10 samples were loams or sandy loams. Mean clay was 40% in the 30–50 cm depth increment and was lower in deep soils (P=0.003; Supplemental S4B). There were no significant differences in SOC stocks (kg C m^{-2}) between 0–10 cm, 10–30 cm, and 30–50 cm. However, SOC stocks were significantly higher in the 50–75 cm depth increment than all other increments (P<0.0001; Fig. 2.3B; Supplemental S4B). Because the length of depth increments varied, we also normalized SOC stock to the length of each increment. Normalized SOC stock (i.e., g C cm^{-2} in 1 cm increment) was high in the 0–10 cm and 50–75 cm depth increment and was lowest in the deepest soils (75-100 cm), though the only significantly different segment was the upper 0-10 cm zone (P<0.0001; Supplemental S4B).

We found high Fe_{Total} concentrations at depth (>50 cm) for several wetlands, though most Fe_{Total} concentrations were <5 mg Fe g^{-1} soil. Mean Fe_{Total} concentrations increased with depth from 1.3 mg Fe g^{-1} soil at 10–30 cm to 7.2 mg Fe g^{-1} soil in deep soils (75–100 cm; P=0.0007; Fig. 2.3G; Supplemental S5B).

We examined relationships between basic soil characteristics (bulk density, clay, and Fe_{Total}) and SOC within each depth increment. The relationship between bulk density and C concentration followed expected patterns, as C concentration declined with increasing bulk density in each depth increment (P <0.0001; Fig. 2.3D; Supplemental S4C). Concentrations of C

declined with increasing clay in the 30–50 cm depth increment (P=0.001; Supplemental S5C). In contrast, C concentrations increased with increasing clay in the 75–100 cm depth increment (P=0.024; Supplemental S4C). Similarly, SOC stocks increased significantly with increasing clay only in the 75–100 cm depth increment (P=0.0002; Fig. 2.3F, Supplemental S4C). There was no statistically significant relationship between Fe_{Total} and C concentration; however, we observed the highest C concentration in samples with low Fe_{Total} (10–30 cm depth increment) and the lowest concentrations of C in deep samples with high Fe_{Total} (below 50 cm; Fig. 2.4H).

3.3 How are SOC stocks across wetlands related to water level metrics?

Across wetlands, mean SOC stock from 0–100 cm was 32.2 kg C m^{-2}. For each horizon increment, the mean standard error of between SOC stocks of replicate cores was 0.2 kg C m^{-2}. We first examined the relationship between SOC stocks and water level metrics across depth increments, thus only wetlands with wells were used in this analysis (n=12 of the 19). Upon initial data exploration, we found that SOC stocks in the 0–10 cm depth increment did not respond to any water level metrics (Fig. 2.4). Therefore, we excluded 0–10 cm from our analysis of SOC stocks to account for the interaction effect and hereafter focus on SOC stocks in soil depth increments from 10–100 cm.

Across depth increments, we found a significant linear relationship between minimum water level and SOC stocks, as wetlands with a lower minimum water level contained lower SOC stocks in each depth increment (P=0.03; Fig. 2.4C; Table 2.2). We also found a significant linear relationship between summertime inundation recession rate and SOC stocks, where wetlands with faster recession rates had lower SOC stocks in each depth increment (P=0.04; Fig. 2.4E; Table 2.2). There were no significant relationships between SOC stocks in each depth increment and percent of year inundated, mean water level, and coefficient of variation in water level (Fig. 2.4A, 2.4B, and 2.4D; Table 2.2).

We selected only significant models (minimum water level and summertime recession rate) from the multiple linear regression across depth increments to scale up to the soil profile

from 10–100 cm. Both minimum water level and summertime recession rate were significantly related to SOC stocks from 10–100 cm (P=0.03 both tests; Table 2.2). Overall, minimum water level explained 41% of the variation in SOC stocks, as wetlands with lower minimum water level contained lower SOC stocks (Fig. 2.5A). Wetlands with faster summertime recession rates also contained lower SOC stocks (R^2=0.38; Fig. 2.5B).

3.4 How do SOC stocks within transect wetlands vary in response to water level and relative elevation?

We compared SOC stocks across the transect from wetland center to upland at the five transect wetlands, again separating our analysis at 10 cm into 0–10 cm and 10–50 cm depth increments. In the top 0–10 cm, SOC stocks increased with decreasing mean water level (i.e., drier soils; P=0.0003; Table 2.3; Fig. 2.6A). Conversely, in the 10–50 cm depth increment, SOC stocks decreased with decreasing mean water level (i.e., drier soils; P<0.0001; Table 2.3; Fig. 2.6C). We also tested the relationship between SOC stocks and elevation relative to the center of the wetland. Again, in surface soils (0–10 cm), SOC stocks increased with increasing relative elevation (i.e., drier soils; P=0.0001; Table 2.3; Fig. 2.6B). In deeper soils (from 10–50 cm), SOC stocks decreased with increasing elevation (P<0.0001; Table 2.3; Fig. 2.6D).

4. Discussion

This study is one of few to directly link wetland SOC stocks to metrics of hydrologic regime, such as water level magnitude, frequency, duration, and timing in freshwater mineral wetlands. First, we demonstrated that indicators of wetland drying, particularly minimum annual water levels and the rate at which inundation declines seasonally (i.e., summertime recession), were significantly correlated with SOC across our 12 wetland sites while the amount of time wetlands are inundated (often called, “hydroperiod”) was not. Although it was outside the scope of this study to measure C fluxes or soil O_2 availability, our findings corroborate studies indicating that wetland SOC is controlled by increased decomposition associated with oxic conditions (e.g., Bernal & Mitsch, 2008; Spivak et al., 2019); however, this hypothesis requires

further study. Second, we found depth-dependent relationships between hydrology, soil characteristics, and SOC stocks as well as high SOC stocks at depth (>50 cm deep), which may represent an understudied but significant component of SOC storage in freshwater mineral wetlands. Finally, we found strong trends in SOC stocks across wetland–upland gradients within wetlands that reflect the influence of decreasing mean water level and increasing elevation on SOC stocks, which may be used to improve landscape-scale SOC models in wet forested areas. Overall, our research suggests that the magnitude and rate of drying are more strongly correlated with SOC than inundation duration in seasonally flooded wetlands. As methods to detect the presence of saturated or inundated conditions advance via remote sensing, understanding the relationship between SOC and wetland drying could improve models of wetland SOC.

4.1 Indicators of drying were related to SOC stocks across wetlands more than inundation duration

Our results indicate that metrics of wetland soil drying correlate more strongly to SOC stocks than inundation duration (Fig. 2.4; Fig. 2.5). We anticipate that wetlands with lower minimum water level and faster summertime recession rates become drier and experience more rapid fluctuations in wet-dry conditions, which would increase O_2 availability as soils dry (Skopp et al. 1990, Moyano et al. 2013). Numerous studies have demonstrated that wetland soil drying increases C respiration, which may lead to a loss of SOC. First, wetland drying increases the rate of O_2 diffusion into soils, causing oxic conditions that stimulate respiration and decomposition (Chapman et al., 2019; Davidson, Belk, & Boone, 1998; Fenner & Freeman, 2011; Inglett et al., 2012; Morse, Ardón, & Bernhardt, 2012). Dry conditions also promote decomposition of C inputs to wetlands during leaf-off (September–October), reducing plant C inputs that might have otherwise contributed to SOC accumulation in wet soils (Day et al., 1988; but see Neckles & Neill, 1994). In contrast to drying soils, saturated or flooded soils are typically anoxic, which is linked to slower decomposition rates due to the reduced metabolic efficiency of anaerobic respiration (e.g., Day & Megonigal, 1993; Gingerich, Merovich, & Anderson, 2014; Hervé et al.,

2019; McLatchey & Reddy, 1998; Wright et al., 2013; but see Stagg et al. 2018). Second, the temperature response of respiration is higher in oxic soils than anoxic soils (Chapman et al., 2019; Chen et al., 2018), indicating that drying soils may experience further increases in respiration with warming in spring and summer. Third, fluctuating wet-dry conditions stimulate SOC and leaf litter decomposition (Reddy and Patrick 1975, Battle and Golladay 2001, Borken and Matzner 2009, Capps et al. 2014). Overall, we expect that the correlation between wetland SOC and indicators of wetland drying is due to the relationships between soil drying and respiration. Therefore, we anticipate that drying-induced decomposition is a control on SOC in these systems, though this hypothesis necessitates further testing.

In contrast to the well-documented relationship between wetland soil drying and decomposition, our results indicate a more complex influence of saturation and inundation on SOC production in mineral wetlands. Several studies suggest that SOC inputs via root growth and aquatic primary productivity are enhanced under optimally flooded conditions (e.g., Cronk & Mitsch, 1994; Day & Megonigal, 1993; Watt & Golladay, 1999). Alternatively, others have suggested that C production is lower in saturated or inundated soils due to suppressed plant abundance, root growth, and microbial biomass (e.g., Dwire, Kauffman, & Baham, 2006; Ma et al., 2018; McLatchey & Reddy, 1998). We anticipate that primary productivity plays less of a role in SOC dynamics of studied wetlands because the wetlands studied here were purposely selected for their lack of emergent vegetation to better isolate the role of hydrology on soils; therefore, we expect that leaf litter inputs from the surrounding forest are a significant allochthonous C source to the soils of studied wetlands (Rubbo et al. 2006). While our results indicate that drying is associated with SOC in the wetlands studied here, relationships between hydrologic regime and SOC may be less strong than implied by our results in wetlands with herbaceous vegetation due to the variable influence of hydrology on autochthonous productivity.

The hydrologic regime of seasonally flooded wetlands is sensitive to climate change, which is likely to impact wetland SOC (Fay et al., 2016; Johnson et al., 2005; McCauley et al.,

2015). While the study period was wetter than average, we expect the metrics of hydrologic regime studied here to represent relative historic differences across wetlands that have influenced the formation of SOC for decades, and these relative differences would persist or be accentuated during drier years. However, as climate change is expected to cause more extreme, episodic precipitation and warmer temperatures in the northeastern U.S. (*Climate Science Special Report: Fourth National Climate Assessment, Volume I* 2017), shifts in the average hydrologic regime of seasonally flooded wetlands is likely to shape wetland SOC over time. For instance, longer, warmer growing seasons and longer rain-free periods between extreme precipitation events may increase summertime recession rates and cause minimum water levels to fall further below the soil surface, which we speculate could lead to increased decomposition, higher C emissions, and reduced wetland SOC over time. Previous research has shown significant, rapid impacts of decreased water tables and increased temperatures on peatland SOC (Koven, Lawrence, & Riley, 2015; Schuur et al., 2015; Webster et al., 2014; Bridgham et al., 2008), but little is known about how climate change will impact freshwater mineral wetlands (Kolka et al. 2018). Freshwater mineral wetlands are important components of the global C cycle, emitting up to 70% more methane but sequestering C at approximately equivalent rates to peatlands across North America (Bridgham et al. 2006). Therefore, the implications of a drier, more episodic hydrologic regime of seasonally flooded wetlands with climate change is likely to have significant impacts on the global carbon cycle.

4.2 The importance of deep SOC and depth-dependent controls on wetland C

SOC stocks fell within the range for temperate freshwater wetlands reported by Pearse et al. (2018; ~30–120 kg C m^{-2}). However, mean SOC stocks from 0–100 cm (32.2 ±1.9 kg C m^{-2}) were higher than previously reported stocks for natural wetlands in the mid-Atlantic (21.5 kg C m^{-2} to 100 cm; Fenstermacher et al., 2016) and higher than SOC stocks for similar wetlands in the U.S (Bridgham et al. 2006, Nahlik and Fennessy 2016, Kolka et al. 2018). While we did not measure sequestration, depressional wetlands are known to have high SOC sequestration rates

(e.g., Bernal & Mitsch, 2012) and SOC stocks that increase with depth (Bernal and Mitsch 2008) even up to depths of 2 m (Fenstermacher 2012). Deep soil C may, in part, be caused by water rich in dissolved organic C moving down the soil profile, which would cause C to translocate from surface soils and be stabilized deeper in the soil profile, as proposed by Kaiser and Kalbitz (2012). Overall, we expect that the low topographic relief, generally shallow water tables, and depressional shape of our study wetlands contributes to relatively high C concentrations throughout the soil profile, especially at depths below 30 cm (Fig. 2.3).

Our findings indicate that relationships between wetland SOC and other soil characteristics vary with depth in the soil profile. We found depth-dependent relationships between SOC stocks and hydrologic indicators (Fig. 2.4; Fig. 2.6), which suggests that other factors control SOC more than hydrology in surface soils. Such factors may include primary production, the composition and amount of water column dissolved organic C, and root or litter inputs. We also observed that the correlation between SOC and clay varied with depth, as SOC stocks increased with clay content only in the deepest soils (75–100 cm; Fig. 2.3F). In deep soils, clay content is indicative of fine sediment, which may indicate C translocation and stabilization in soils comprised of fine basin fill. Overall, our findings corroborate other recent studies identifying varying mechanisms of carbon preservation throughout the soil profile, whereby organic matter inputs and biology influence SOC in surface soils, but in deeper mineral layers, slower processes dominate and mineral surfaces become more important for SOC storage (Angst et al. 2018, Matteodo et al. 2018, Cagnarini et al. 2019). For instance, we found sharp increases in soil Fe concentrations below 50 cm depth at several wetlands (Fig. 2.3G), suggesting that potentially stabilizing interactions between SOC and Fe are most dominant in deep soils. Interactions between SOC and Fe (hydr)oxides stabilize SOC in terrestrial soils for centuries (von Lützow et al. 2006, Wagai and Mayer 2007, Kögel-Knabner et al. 2008); however, in wetlands, Fe may be solubilized and translocated illuvially down the soil profile, leaving SOC in wetland surface soils relatively vulnerable to decomposition under oxic conditions but increasing organo-

mineral associations in deep soils. Further, these results further underscore the importance of examining deep soils (>50 cm) in wetland studies. The majority of SOC stocks in North American wetlands are deeper than 30 cm (Nahlik and Fennessy 2016), but most wetland soil studies overlook these deep SOC stocks by only examining surface soils in the upper 15 to 30 cm (e.g., Ballantine et al., 2012; Ballantine & Schneider, 2009; Bernal & Mitsch, 2008; Fennessy et al., 2018; Kim & Grunwald, 2016; Lewis & Feit, 2015). Our results indicate that studies focused only on shallow wetland soils may fail to capture the dynamics of significant amounts of SOC.

4.3 Scaling up: changes in SOC across the wetland–upland gradient

Within wetlands, we found generalizable, but contrasting trends in SOC stocks across the hydrologic gradient between the organic 0–10 cm depth increment and the mineral 10–50 cm depth increment (Fig. 2.6), further demonstrating that the response of SOC to hydrology varies throughout the soil profile. As expected, wetland SOC stocks from 10–50 cm decreased from wetland center to upland, which is likely caused by oxic conditions and faster decomposition rates in upland soils (Mitsch and Gosselink 2015). However, SOC stocks from 0–10 cm increased from wetland center to upland, which we expect is due to higher root growth in shallow upland soils than in shallow wetland soils, as has been found across wetland–upland transects in similar wetland systems (LaCroix et al. 2019). Our work identifies continuous-variable relationships that can be used to model landscape-scale wetland SOC stocks, building on prior studies showing significant differences in SOC stocks across topographic categories such as basin, transition, and upland (e.g.,Webster et al., 2011). Low relief, wet forests are ubiquitous throughout the northeastern U.S. but have previously been neglected in forest C models (e.g., Hurtt et al., 2019) and are poorly represented by upland SOC models (Trettin, Song, Jurgensen, & Li, 2001). As remote sensing and geospatial methods improve wetland inundation detection (e.g., Evenson et al., 2018; Lang, McCarty, Oesterling, & Yeo, 2013; Lang & McCarty, 2009), relationships between SOC and hydrologic regime may lead to more accurate, comprehensive models of SOC stocks in wet forests.

Overall, our results indicate that the relationship between hydrology and SOC is a continuum and not a binary (e.g., wetland vs. upland). We found soils at the wetland perimeter contained higher SOC stocks than upland forest soils (Fig. 2.6), even though they are rarely saturated and do not meet the regulatory definition of a wetland (Tiner 1996). However, soils at the wetland perimeter may not receive the same jurisdictional protection as wetlands and may therefore be vulnerable to loss or degradation due to development. On the global scale, these wet-but-not-wetland soils may contribute significantly to terrestrial SOC stocks, but are underrepresented in global wetland SOC estimates (Bridgham et al. 2006). A broader understanding of how hydrologic regime controls SOC stocks across the wetland–upland gradient could both improve SOC models and expand targets of wetland conservation for SOC storage.

5. Conclusions

This work highlights the importance of freshwater mineral wetlands in SOC storage and demonstrates that aspects of hydrologic regime related to wetland drying (i.e., minimum water level and summertime inundation recession rate) are correlated to SOC storage among seasonally flooded mineral wetlands. We found depth-dependent responses of SOC to hydrologic regime and soil characteristics, indicating the importance of studying SOC stocks below 30 cm to more fully understand the dynamics of the majority of wetland SOC stocks. We also found strong trends in SOC stocks across a hydrologic gradient within wetlands, suggesting that wetland perimeters contribute substantially to forest SOC storage despite not falling under the regulatory definition of a "wetland soil."

Freshwater mineral wetlands make up nearly 80% of all wetlands in the conterminous U.S. and forested wetlands have a high potential to act as a SOC sink, but are also vulnerable to SOC loss and C emissions as a result of climate change (Kolka et al. 2018). A more nuanced understanding of the role of hydrologic regime in wetland SOC storage may inform models of wetland SOC stocks over space across landscapes and over time with climate change. Overall, we demonstrate that hydrologic regime is a useful framework to study wetland SOC, and our results

suggest that changes to hydrologic regime, such as increased wetland drying, may have implications for SOC storage in seasonally flooded mineral wetlands.

Acknowledgements

We thank Dr. C. Nathan Jones for collecting, maintaining, and processing water level data at wetland sites as well as for his insight and thoughtful suggestions throughout the writing process. We also thank Graham Stewart, Alec Armstrong, Kelly Hondula, and Dr. Christine Maietta for their support and suggestions throughout the research process. We also thank Bianca Noveno and Maggie Tan, without whom this work would not be possible, for their indefatigable spirits during fieldwork as well as their independence and attention to detail in the lab.

Tables

Table 2.1

Table 2.1. Water level metrics show that while all wetlands were inundated for most of the year, there was variation in the characteristics of soil saturation across wetlands.

Variable (unit)	Description	Mean	Minimum	Maximum	Standard Error
Percent of year inundated (%)	Percent of the year with water level >0 m.	94.0	83.8	100.0	1.8
Mean water level (m)	Mean water level relative to the soil surface.	0.41	0.23	0.64	0.04
Maximum water level (m)	95^{th} percentile of water level relative to the soil surface.	0.71	0.43	1.08	0.06
Minimum water level (m)	5^{th} percentile of water level relative to the soil surface.	0.00	-0.22	0.19	0.04
Coefficient of variation (%)	The coefficient of variation for daily water level over the entire water year.	62.9	42.1	86.7	5.2
Range (m)	Maximum - Minimum water level	0.70	0.50	1.14	0.06
Summertime recession rate (cm day^{-1})	Rate of water level change during rain-free summertime recession, from June 11-July 18, 2018. Where water level fell below soil surface (<0 m), rate only calculated for period where water levels were >0 m (see text).	-1.5	-1.1	-2.0	0.1

Table 2.2

Table 2.2. Results from multiple linear regression of SOC stocks and water level metrics across depth increments (excluding 0–10 cm) and from simple linear regression of SOC stocks and water level metrics from 10–100 cm. Only significant models from the multiple linear regression were carried forward to simple linear regression. Minimum water level and summertime recession rate have the strongest relationship with SOC stocks from 10–100 cm.

Multiple regression of C stocks from 10-100 cm vs water level metrics by depth increment							
	Metric	Beta	95% Confidence Interval	F	Corrected P-value	Degrees of Freedom	Adj. R^2
n=48	Percent of year inundated (%)	1.2	0.033, 2.4	4.3	0.16	(3, 45)	0.09
	Mean water level (m)	0.36	-0.95, 1.7	0.3	0.58	(3, 45)	<0.01
	Minimum water level (m)	1.5	0.44, 2.6	8.1	0.03	(3, 45)	0.15
	Coefficient of variation (%)	-1.2	-2.4, -0.063	4.5	0.16	(3, 45)	0.09
	Summertime recession rate (m day^{-1})	-1.4	-2.5, 0.35	7.1	0.04	(3, 45)	0.13
Simple linear regression of C stocks from 10-100 cm vs water level metrics							
	Metric	Beta	Confidence Interval	F	Corrected P-value	Degrees of Freedom	Adj. R^2
n=12	Minimum water level (m)	6.0	1.5, 10.5	8.7	0.03	(1, 10)	0.41
	Summertime recession rate (m day^{-1})	-5.8	-10.5, -1.1	7.6	0.03	(1, 10)	0.38

Table 2.3

Table 2.3. Simple linear regression of SOC stocks across the transect, separated into 0–10 cm and 10–50 cm, by either water level or relative elevation.

A. C stocks 0-10 cm, Water Level

Fixed effect	Beta	95% Confidence Interval	F	P-value	Degrees of freedom	Adjusted R^2
Intercept	3.8	1.9, 5.6				
Water Level (m)	-3.7	-6.1, -1.3	10.1	3.70E-03	(1, 28)	0.24

B. C stocks 0-10 cm, Relative Elevation

Fixed Effect	Beta	95% Confidence Interval	F	P-value	Degrees of freedom	Adjusted R^2
Intercept	1.7	-0.91, 4.3				
Relative Elevation	3.4	1.6, 6.1	12.6	1.00E-03	(1, 28)	0.29

C. C stocks 10-50 cm, Water Level

Fixed effect	Beta	95% Confidence Interval	F	P-value	Degrees of freedom	Adjusted R^2
Intercept	13.1	11.3, 14.9				
Water Level (m)	6.7	4.4, 9.0	34.9	2.30E-06	(1, 28)	0.54

D. C stocks 10-50 cm, Relative Elevation

Fixed Effect	Beta	95% Confidence Interval	F	P-value	Degrees of freedom	Adjusted R^2
Intercept	16.5	14.1, 19.0				
Relative Elevation	-6.7	-8.8, -4.6	42.2	4.90E-07	(1, 28)	0.59

Figures

Figure 2.1

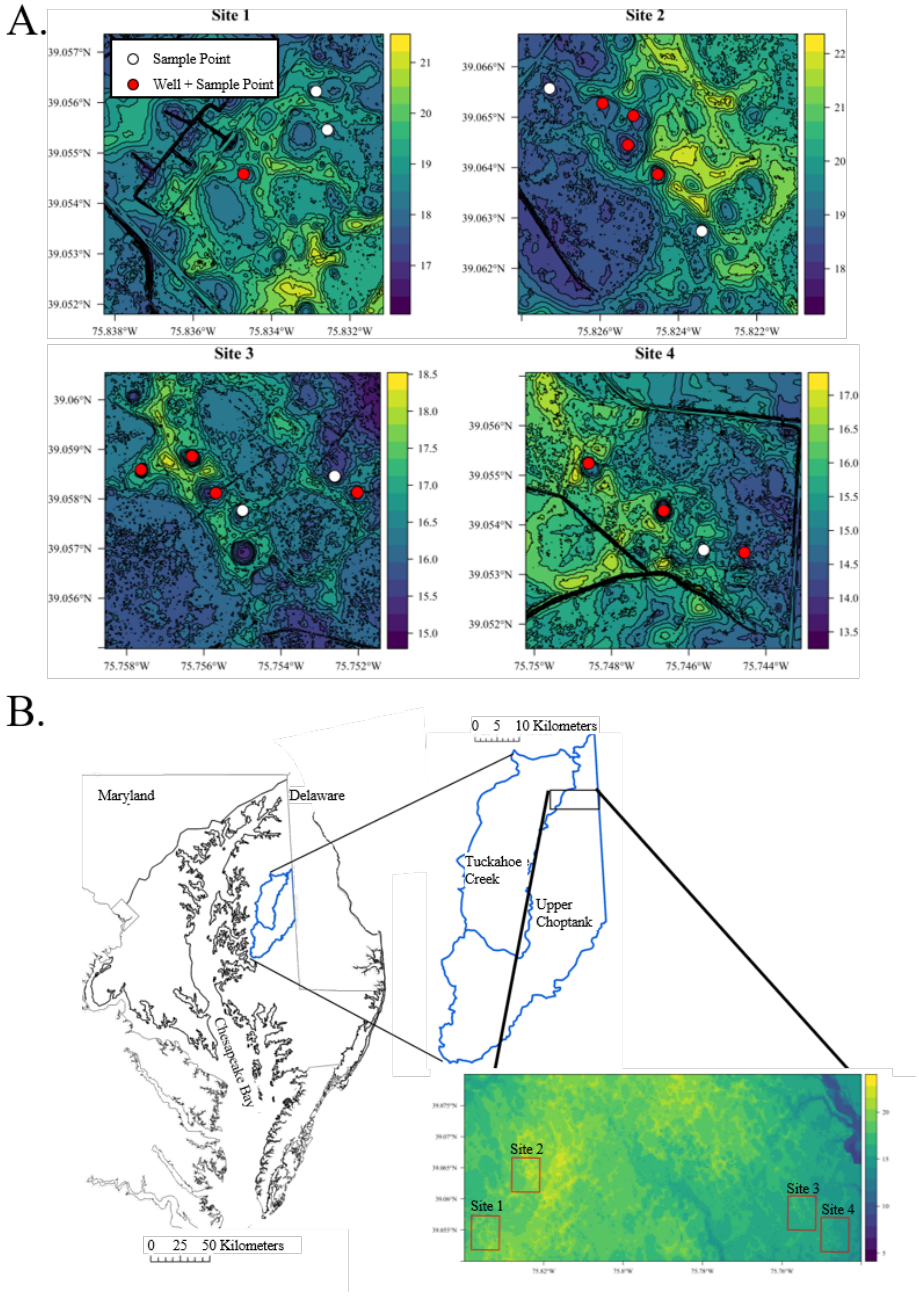

Figure 2.1. Sampling locations in individual wetlands on the DEM (Panel A), where darker colors on the DEM indicate lower elevations of depressions. Wetlands are spread across four sites of varying elevation in the Upper Choptank and Tuckahoe Creek watersheds (Panel B).

Figure 2.2

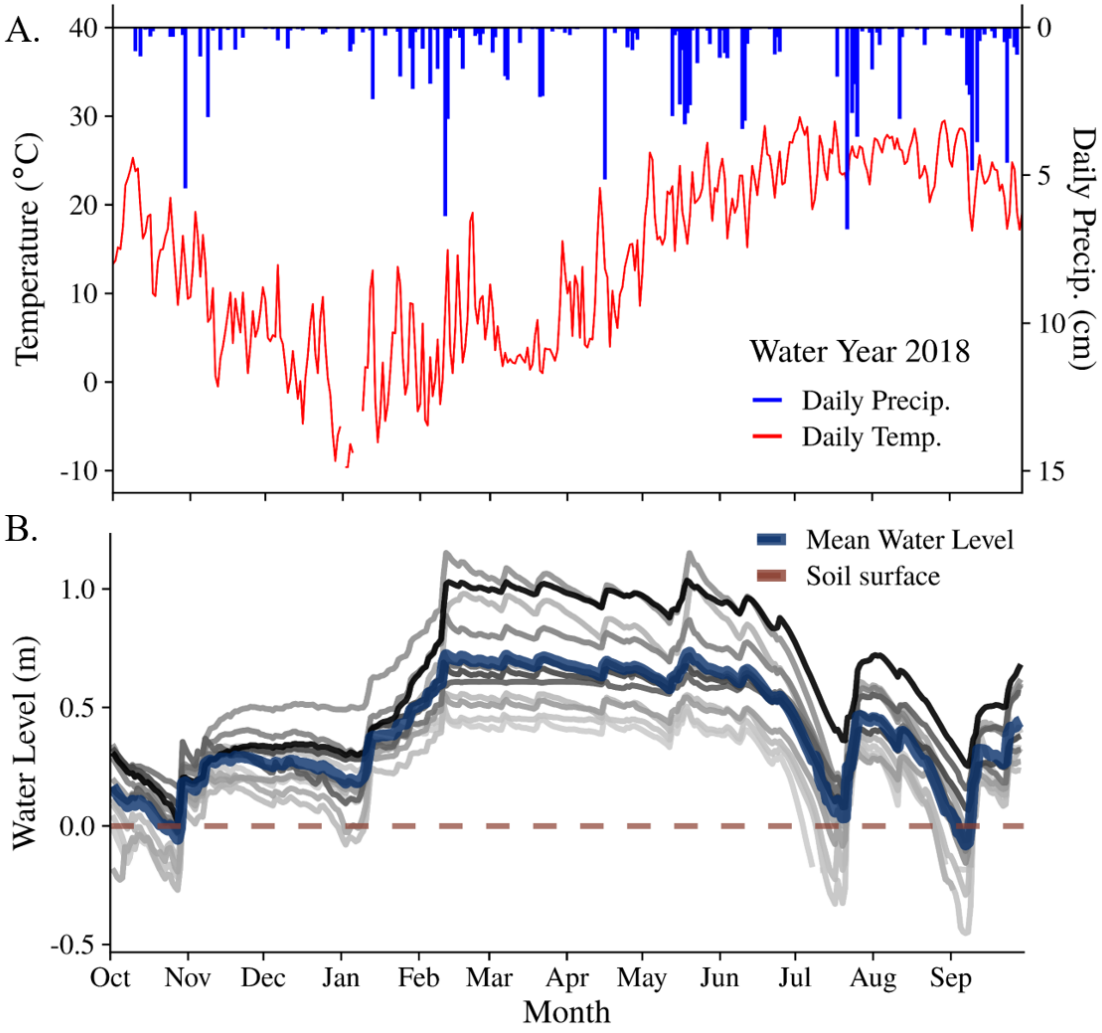

Figure 2.2. Temperature, precipitation, and water level data for water year 2018 (Panel A). Panel B depicts the mean daily water level, where positive water level indicates inundation above the soil surface. Wetlands are sorted in order of increasing duration of inundation, wetlands that were inundated for a longer percent of the year represented by darker lines on the hydrograph.

Figure 2.3

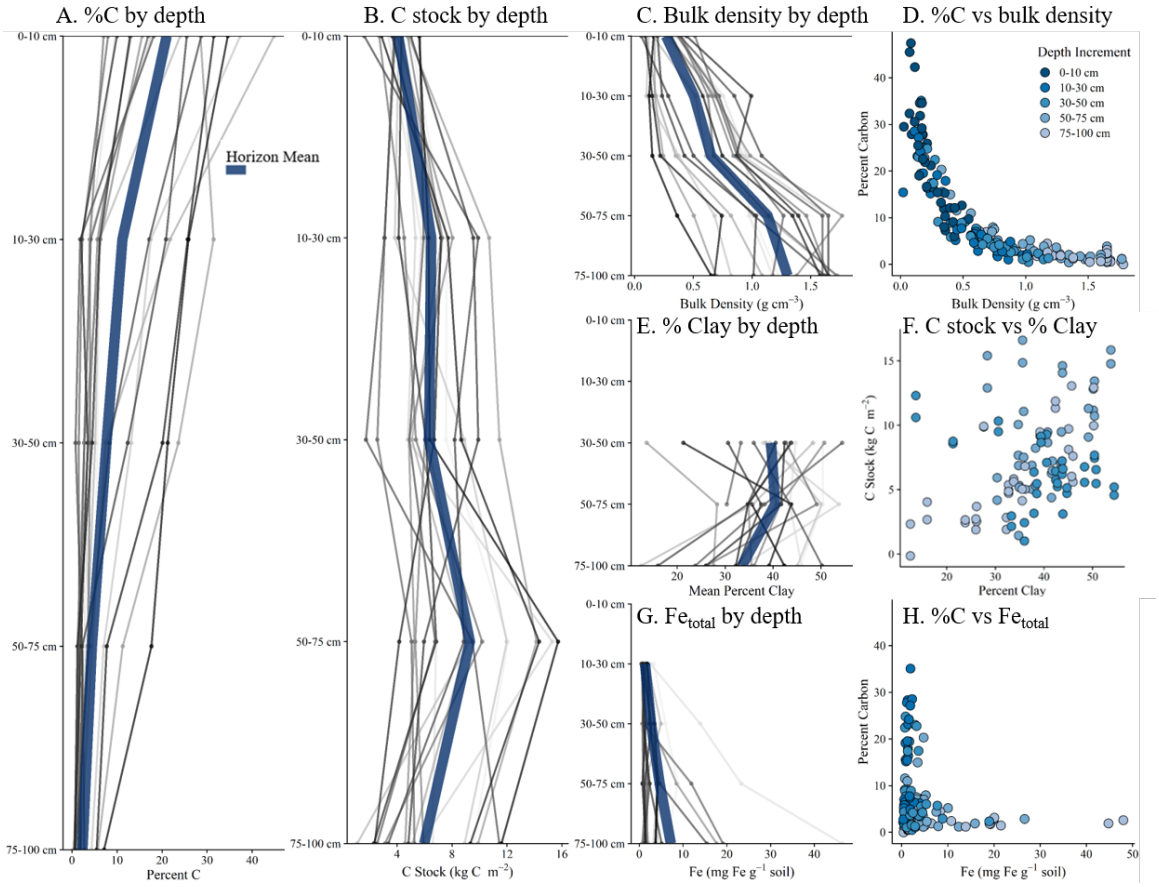

Figure 2.3. Horizon characteristics by depth increment for each wetland, with mean depth trend in blue (Panels A, B, C, D, and G). Line colors represent wetland volume, which is arranged from wetlands with smaller volume (light gray) to wetlands with larger volume (dark gray). Relationships between physiochemical properties C within a sample show different relationships in each depth increment (Panel D, F, and H).

Figure 2.4

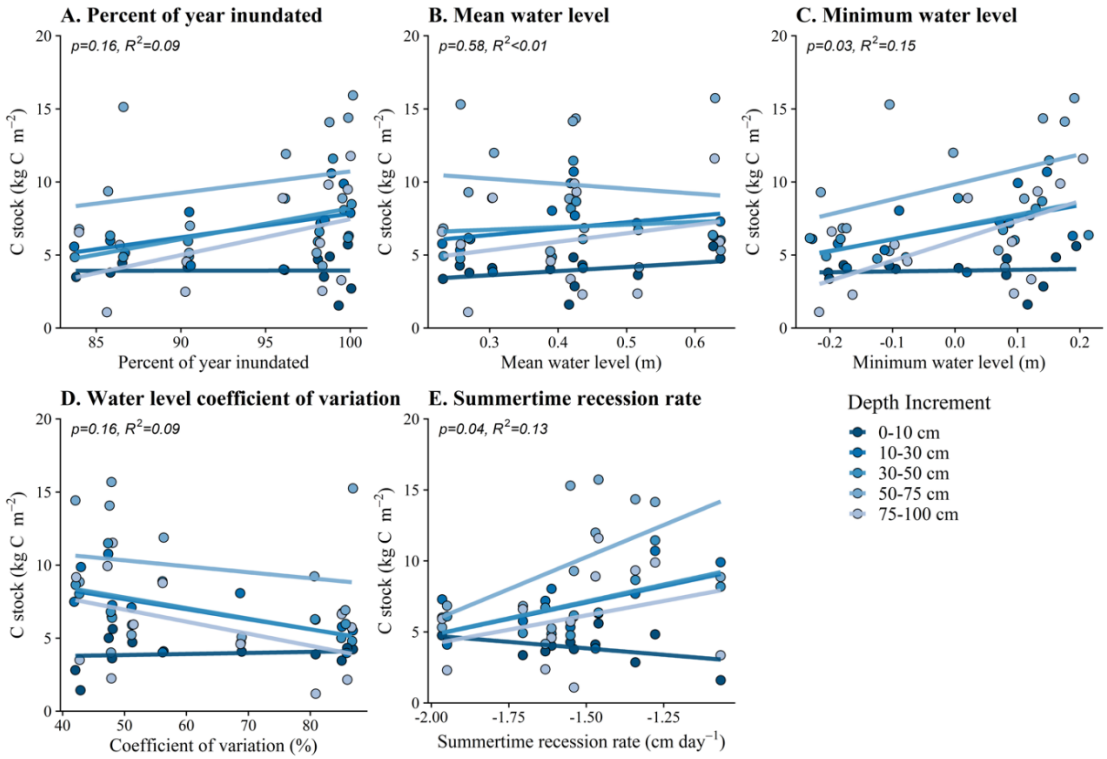

Figure 2.4. Results from multiple linear regression of C stocks and individual water level metrics by depth increment, including p-values after Holm correction and adjusted R^2. Relationships in the 0–10 cm increment were not significant and were removed for further modeling and analysis; linear models are depicted here to illustrate lack of response. Statistical results in Table 2.2.

Figure 2.5

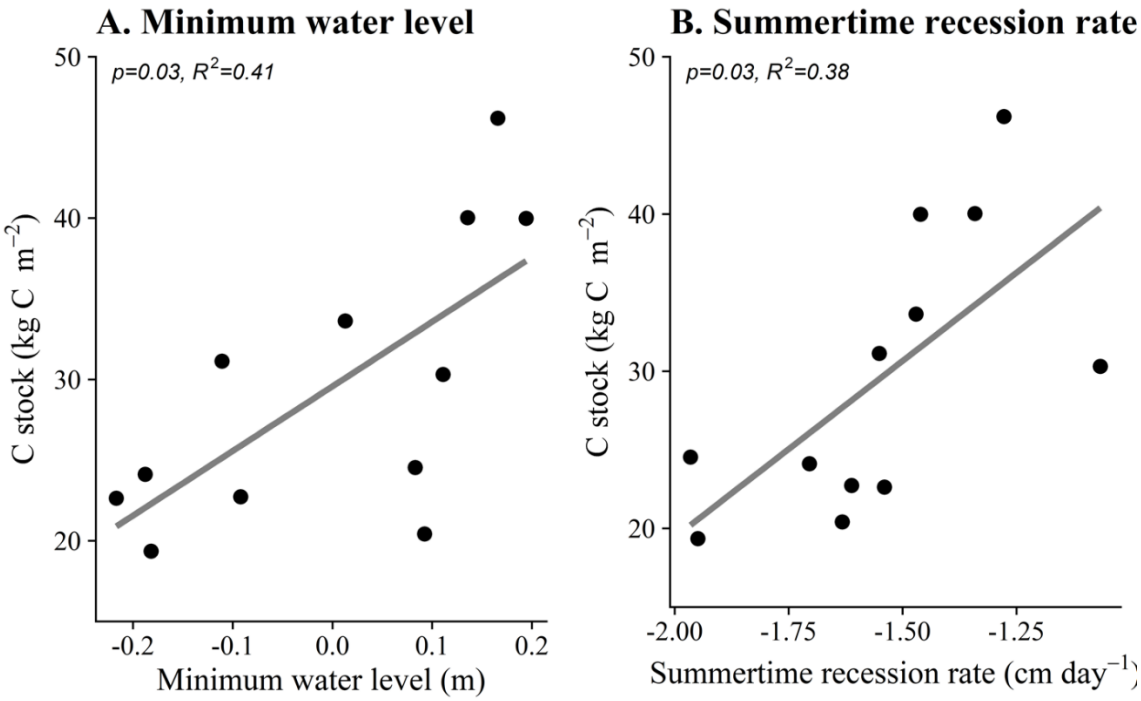

Figure 2.5. Model results for simple linear regression between C stocks from 10–100 cm and water level metrics. Statistical results in Table 2.2.

Figure 2.6

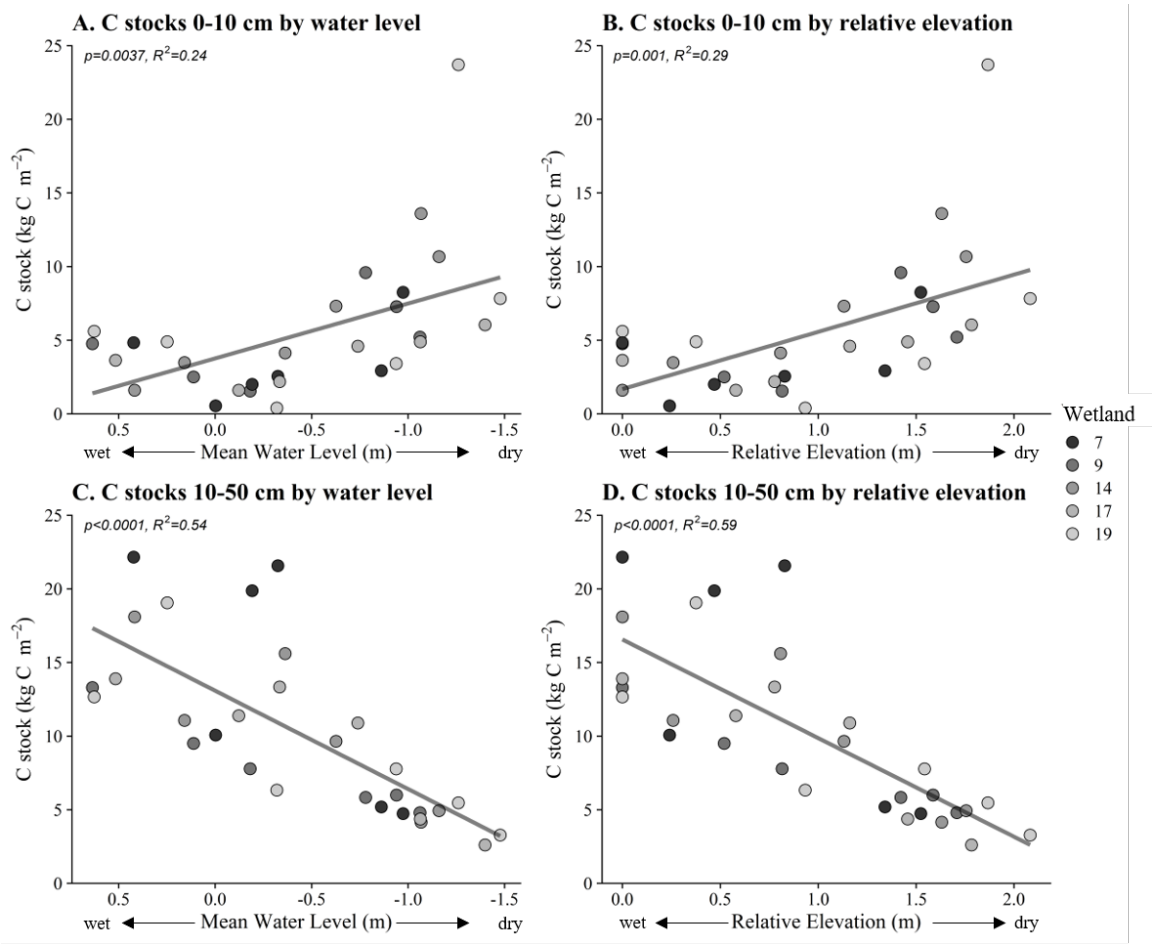

Figure 2.6. Stocks of C across the transect from wetland center to upland, at a subset of five wetlands. Models were conducted with mean water level for water year 2018 (left) and by elevation relative to wetland center (right). Stocks were separated into 0–10 cm (top) and 10–50 cm (bottom) due to differences in C stock response. Statistical results in Table 2.3.

Supplemental Materials

S1

Supplemental S1. Water level metrics and soil properties at each wetland.

	Water Level Metrics						Soil		
Wetland Number	Percent of Year Inundated	Mean Water Level (m)	Minimum water level (m)	Maximum water level (m)	Coefficient of Variation (%)	Summer Recession Rate (m day^{-1})	C stocks 0-100 cm (kg m^{-2})	Fe stocks 10-100 cm (kg m^{-2})	Mean % Clay
1							41.8	5.3	49
2	83.8	0.23	-0.19	0.43	0.85	-0.017	27.5	22.5	44
3	86.5	0.26	-0.11	0.55	0.87	-0.016	35.4	3.9	43
4	96.2	0.31	0.01	0.52	0.56	-0.015	37.7	1.5	45
5	85.7	0.27	-0.22	0.46	0.81	-0.015	26.4	1.5	36
6							30.9	0.8	37
7	98.9	0.42	0.17	0.69	0.47	-0.013	51.0	0.5	23
8	90.4	0.39	-0.09	0.68	0.69	-0.016	26.8	10.6	39
9	98.1	0.64	0.08	1.08	0.51	-0.020	29.3	1.7	43
10							25.9	1.1	42
11							19.7	9.6	32
12							25.8	1.3	42
13							29.6	9.0	43
14	99.5	0.42	0.11	0.61	0.43	-0.011	31.9	1.1	30
15							35.2	2.0	34
16	90.4	0.44	-0.18	0.96	0.86	-0.019	23.7	1.6	38
17	98.4	0.52	0.09	0.82	0.48	-0.016	24.0	1.1	39
18	100	0.43	0.14	0.65	0.42	-0.013	42.9	1.6	35
19	100	0.63	0.19	1.01	0.48	-0.015	45.6	1.1	39

S2

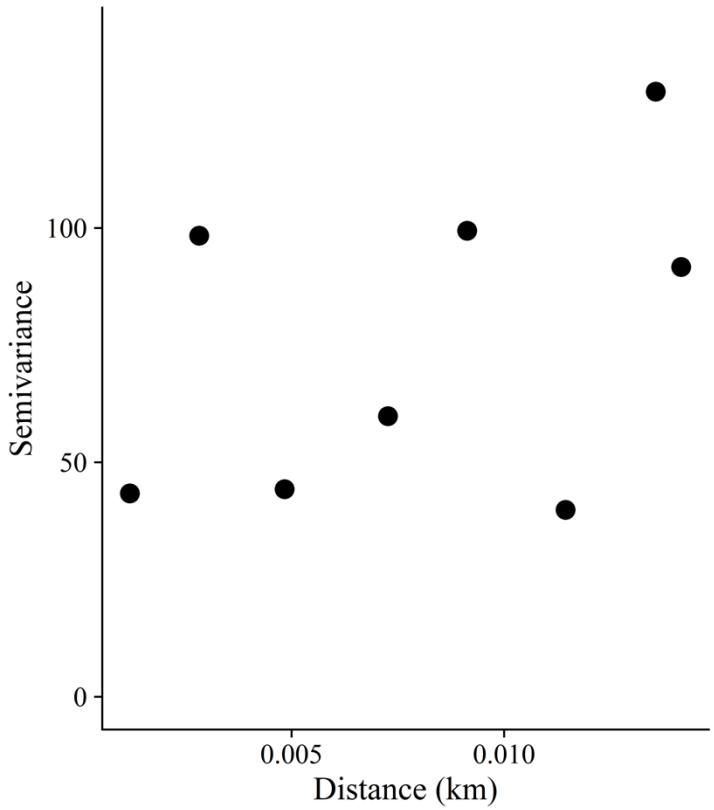

Supplemental S2. Semi-Variogram of global autocorrelation for C stocks, showing no spatial autocorrelation (Moran's I = -0.0049(0.19), P=0.42).

S3

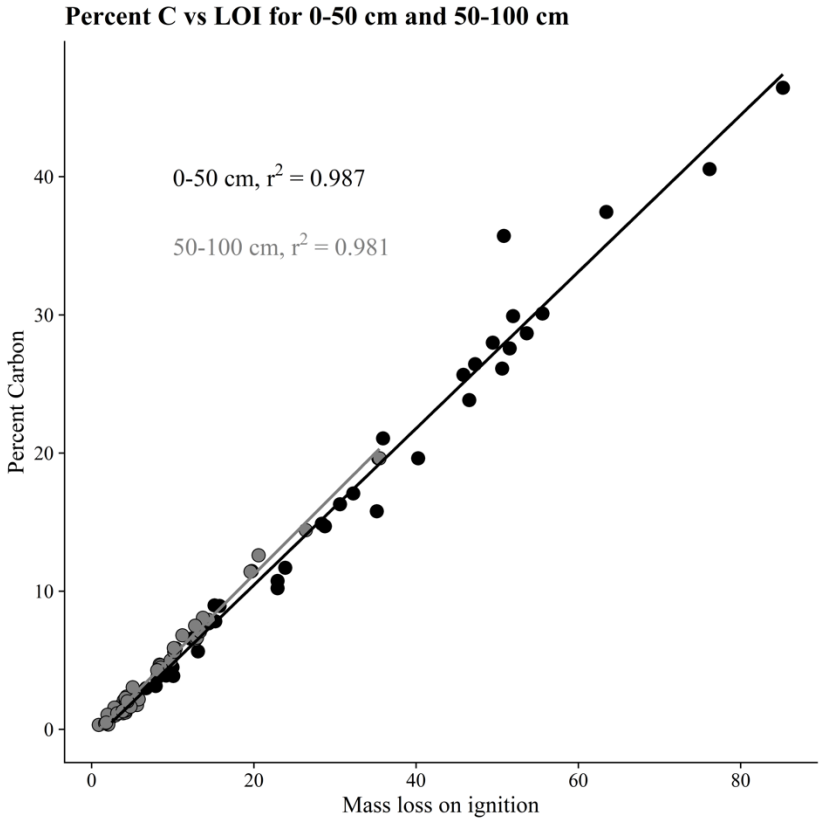

Supplemental S3. Simple linear regression between percent C and LOI for soil samples from 0-50 cm (upper soil horizons) and 50-100 cm (lower soil horizons), with adjusted R^2 for each model. The relationship between C and LOI is highly significant for the upper soil horizons ($F(2, 41) = 2216$, $P=2.6\cdot10^{-37}$). The relationship between C and LOI is also highly significant for lower soil horizons ($F(2, 42) = 3221$, $P=2.5\cdot10^{-41}$).

S4.

Supplemental S4. Statistical results.

S4A. Simple linear model to test the relationship between range in water level during water year 2018 with summertime recession rate (n=12).

Response	Predictor	F	P-value	Degrees of Freedom	Adjusted R^2
Summertime recession (m day^{-1})	Range (m)	23.7	0.0006	(1, 10)	0.67

S4B. Mean (standard error) soil properties by depth increment, with results from ANOVA of soil property by depth increment. Letters indicate significant differences between depth increments (Tukey's HSD, P <0.05).

Response	0-10 cm	10-30 cm	30-50 cm	50-75 cm	75-100 cm	F	P-value	Degrees of Freedom
% C	21.0 (1.8)^{a}	11.2 (1.6)^{b}	7.67 (1.2)^{bc}	4.4 (0.7)^{cd}	2.3 (0.3)^{d}	33.9	<0.0001	(4,185)
Bulk density (g cm^{-3})	0.27 (0.03)^{a}	0.51 (0.05)^{b}	0.65 (0.05)^{b}	1.13 (0.07)^{c}	1.30 (0.06)^{c}	70.2	<0.0001	(4,185)
C stock (kg C m^{-2})	4.1 (0.2)^{b}	6.5 (0.5)^{b}	6.3 (0.5)^{b}	9.3 (0.9)^{a}	6.0 (0.7)^{b}	9.2	<0.0001	(4, 90)
Normalized C stock (g C cm^{-2} in 1 cm)	0.041 (0.002)^{a}	0.032 (0.002)^{b}	0.032 (0.002)^{bc}	0.037 (0.002)^{ab}	0.024 (0.002)^{b}	9.0	<0.0001	(4, 185)
Fe_{total} (mg Fe g^{-1} soil)		1.3 (0.4)^{b}	2.7 (0.5)^{b}	4.6 (0.9)^{ab}	7.2 (1.8)^{a}	6.01	0.0007	(3,148)
% Clay			39.6 (1.6)^{a}	40.5 (1.1)^{a}	33.5 (1.6)^{b}	6.2	0.003	(2,107)

S4C. Simple linear regression results between Percent C and soil properties, with separate models for each depth increment.

Response	Predictor	Depth Increment	F	P-value	Degrees of Freedom
% C	% Clay	30-50 cm	23.4	0.0001	(2, 16)
		50-75 cm	0.2	0.66	(2, 17)
		75-100 cm	6.2	0.024	(2, 16)
% C	Fe_{total} (mg Fe g^{-1} soil)	10-30 cm	1.23	0.28	(2, 36)
		30-50 cm	0.98	0.33	(2, 36)
		50-75 cm	0.30	0.56	(2, 36)
		75-100 cm	0.011	0.92	(2, 36)
% C	Bulk density (g cm^{-3})	0-10 cm	95.6	<0.0001	(2, 36)
		10-30 cm	129	<0.0001	(2, 36)
		30-50 cm	133	<0.0001	(2, 36)
		50-75 cm	60.4	<0.0001	(2, 36)
		75-100 cm	104	<0.0001	(2, 36)
C stock (kg C m^{-2})	% Clay	30-50 cm	4	0.063	(2, 16)
		50-75 cm	2.5	0.14	(2, 17)
		75-100 cm	23.4	0.00018	(2, 16)
Bulk density (g cm^{-3})	% Clay	30-50 cm	7.9	0.012	(2, 16)
		50-75 cm	0.33	0.57	(2, 17)
		75-100 cm	3.6	0.077	(2, 16)

S4D. Linear Mixed Effects Model of C stocks from center of wetland to upland, for C stocks from 0-10 cm and 10-50 cm. Separate analyses were conducted for the fixed effects of mean water level and elevation relative to wetland center. Likelihood ratio test is the result of the Chi-Squared Likelihood Ratio test on the goodness-of-fit between the model with the random effect (wetland) and the model without the random effect. For both metrics, the model with wetland as a random intercept is not significantly better than the simple linear model; therefore we proceeded with the simple linear model.

A. C stocks 0-10 cm, Water Level

Fixed Effect	Parameter (standard error)	F	P-value	Degrees of freedom	Conditional R^2
Intercept	3.8 (0.9)				
Water Level (m)	-3.7 (1.2)	9.9	0.004	(1, 24.7)	0.26

Random Effect	Wetland variance (sd)	Residual variance (sd)	Likelihood Ratio	P-value	groups
	0.14 (0.38)	16.2 (4.0)	0.005	0.47	

B. C stocks 0-10 cm, Relative Elevation

Fixed Effect	Parameter (standard error)	F	P-value	Degrees of freedom	Conditional R^2
Intercept	1.7 (1.3)				
Relative Elevation (m)	3.9 (1.1)	12.1	1.80E-03	(1, 25.7)	NA

Random Effect	Wetland variance (sd)	Residual variance (sd)	Likelihood Ratio	P-value	groups
	0 (0)	15.29 (3.91)	<0.0001	0.50	5

C. C stocks 10-50 cm, Water Level Metric

Fixed effect	Parameter (standard error)	F	P-value	Degrees of freedom	Conditional R^2
Intercept	13.1 (1.0)				
Water Level (m)	6.6 (1.1)	38.5	1.90E-06	(1, 24.4)	0.60

Random Effect	Wetland variance (sd)	Residual variance (sd)	Likelihood Ratio	P-value	groups
	2.0 (1.4)	13.3 (3.7)	0.82	0.18	5

D. C stocks 10-50 cm, Relative Elevation

Geospatial Fixed Effect	Parameter (standard error)	F	P-value	Degrees of freedom	Conditional R^2
Intercept	16.5 (1.2)				
Relative Elevation (m)	-6.7 (1.0)	40.6	1.01E-06	(1, 25.6)	0.59

Random Effect	Wetland variance (sd)	Residual variance (sd)	Likelihood Ratio	P-value	groups
	0.2 (0.4)	13.4 (3.7)	0.01	0.46	5

S5

S5. Results from regression of individual wetlands with mean water level (left) and elevation relative to center of wetland (right), to show variation in intercept between wetland when wetland is included as a random variable (Supplemental S4D). Differences among wetlands were not significant, so wetland variation was collapsed into a single regression (Table 2.3; Fig. 2.6).

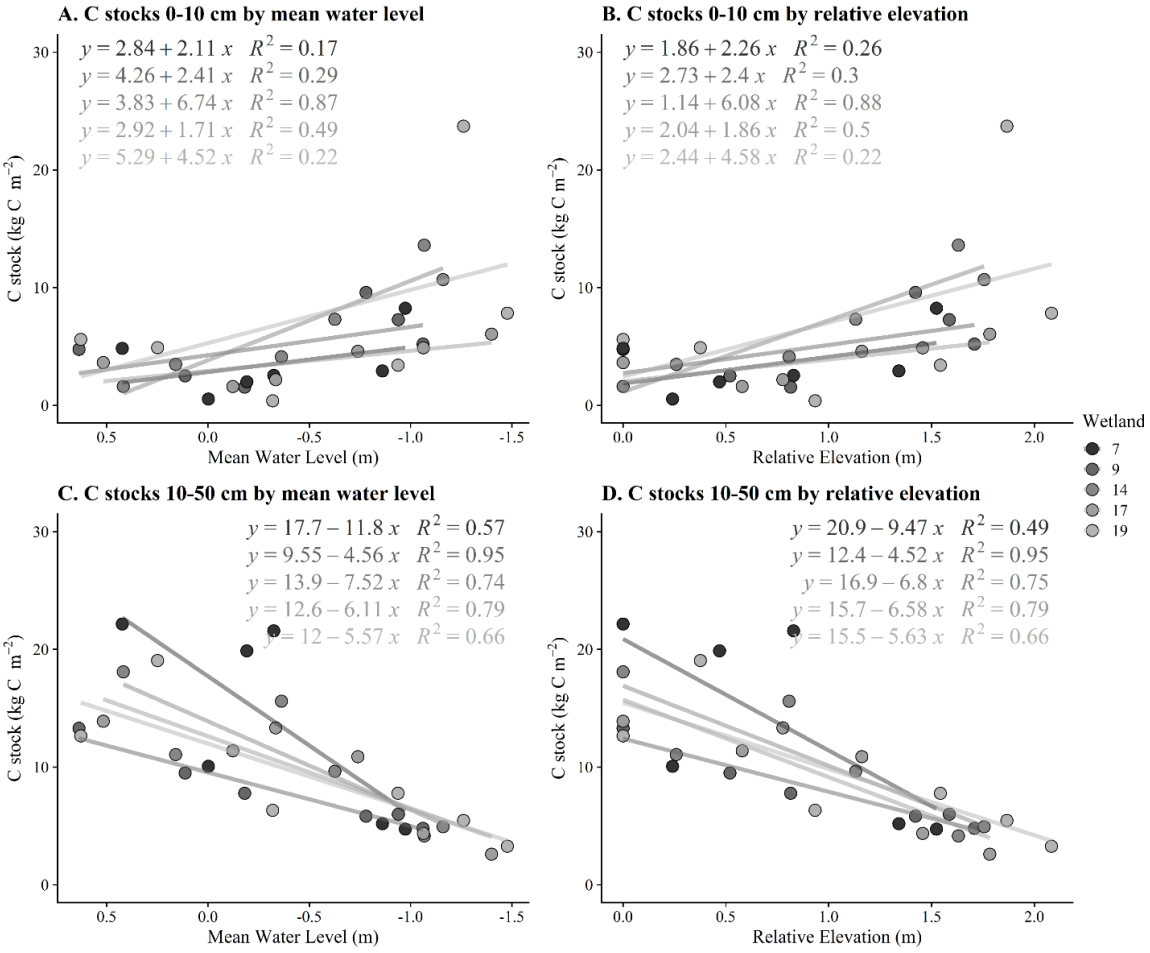

References

Angst, G., J. Messinger, M. Greiner, W. Häusler, D. Hertel, K. Kirfel, I. Kögel-Knabner, C. Leuschner, J. Rethemeyer, and C. W. Mueller. 2018. Soil organic carbon stocks in topsoil and subsoil controlled by parent material, carbon input in the rhizosphere, and microbial-derived compounds. Soil Biology and Biochemistry 122:19–30.

Aphalo, P. J. 2016. Learn R... as you learnt your mother tongue. Leanpub, Helsinki.

Arachchige, P. S. P., G. M. Hettiarachchi, C. W. Rice, J. J. Dynes, L. Maurmann, J. Wang, C. Karunakaran, A. L. D. Kilcoyne, C. P. Attanayake, T. J. C. Amado, and J. E. Fiorin. 2018. Sub-micron level investigation reveals the inaccessibility of stabilized carbon in soil microaggregates. Scientific Reports 8.

Armstrong, A. 2019. Dissertation in preparation: Hydrologic connectivity and dissolved organic carbon in depressional freshwater wetlands on the Delmarva Peninsula.

Arndt, J. L., R. E. Emanuel, and J. L. Richardson. 2016. Hydrology of Wetland and Related Soils. Pages 40–106 Wetland Soils: Genesis, Morphology, Hydrology, Landscapes, and Classification. First. CRC Press, Boca Raton, Florida.

Auguie, B. 2017. gridExtra: Miscellaneous Funcntions for "Grid" Graphics. R package version 2.3.

Ballantine, K., and R. Schneider. 2009. Fifty-five years of soil development in restored freshwater depressional wetlands. Ecological Applications 19:1467–1480.

Ballantine, K., R. Schneider, P. Groffman, and J. Lehmann. 2012. Soil Properties and Vegetative Development in Four Restored Freshwater Depressional Wetlands. Soil Science Society of America Journal 76:1482.

Barr, D. J., R. Levy, C. Scheepers, and H. J. Tily. 2013. Random effects structure for confirmatory hypothesis testing: Keep it maximal. Journal of Memory and Language 68:255–278.

Bates, D., M. Mächler, B. Bolker, and S. Walker. 2015. Fitting Linear Mixed-Effects Models Using lme4. Journal of Statistical Software 67:1–48.

Battle, J. M., and S. W. Golladay. 2001. Hydroperiod Influence on Breakdown of Leaf Litter in Cypress-gum Wetlands. The American Midland Naturalist 146:128–145.

Beare, M. H., and R. R. Bruce. 1993. a Comparison of Methods for Measuring Water-Stable Aggregates - Implications for Determining Environmental-Effects on Soil Structure. Geoderma 56:87–104.

Bernal, B., and W. J. Mitsch. 2008. A comparison of soil carbon pools and profiles in wetlands in Costa Rica and Ohio. Ecological Engineering 34:311–323.

Bernal, B., and W. J. Mitsch. 2012. Comparing carbon sequestration in temperate freshwater wetland communities. Global Change Biology 18:1636–1647.

Bivand, R. S., E. Pebesma, and V. Gomez-Rubio. 2013. Applied spatial data analysis with R. Second. Springer, NY.

Bivand, R. S., and D. W. S. Wong. 2018. Comparing implementations of global and local indicators of spatial association. TEST 27:716–748.

Blankinship, J. C., S. J. Fonte, J. Six, and J. P. Schimel. 2016. Plant versus microbial controls on soil aggregate stability in a seasonally dry ecosystem. Geoderma 272:39–50.

Blankinship, J., and J. Schimel. 2018. Biotic versus Abiotic Controls on Bioavailable Soil Organic Carbon. Soil Systems 2:10.

Boesch, D. F., F. Dawson, R. Summers, W. Boicourt, A. Busalacchi, D. Cahoon, F. Coale, V. Coles, R. Dickerson, W. Eichbaum, B. Fath, R. Hoff, D. Kimmel, C. Larsen, A. Miller, M. Palmer, L. Pitelka, S. Prince, B. Schwartz, D. Secor, T. Warman, and C. Welty. 2015. Chapter 2: Comprehensive Assessment of Climate Change Impacts in Maryland. Maryland Commission on Climate Change.

Borken, W., and E. Matzner. 2009. Reappraisal of drying and wetting effects on C and N mineralization and fluxes in soils. Global Change Biology 15:808–824.

Bridgham, S. D., J. P. Megonigal, J. K. Keller, N. B. Bliss, and C. Trettin. 2006. The carbon balance of North American wetlands. Wetlands 26:889–916.

Bridgham, S. D., J. Pastor, B. Dewey, J. F. Weltzin, and K. Updegraff. 2008. Rapid Carbon Response of Peatlands to Climate Change. Ecology 89:3041–3048.

Brooks, R. T. 2005. A review of basin morphology and pool hydrology of isolated ponded wetlands: implications for seasonal forest pools of the northeastern United States. Wetlands Ecology and Management 13:335–348.

Cagnarini, C., E. Blyth, B. A. Emmett, C. D. Evans, R. I. Griffiths, A. Keith, L. Jones, I. Lebron, N. P. McNamara, J. Puissant, S. Reinsch, D. A. Robinson, E. C. Rowe, A. R. C. Thomas, S. M. Smart, J. Whitaker, and B. J. Cosby. 2019. Zones of influence for soil organic matter dynamics: A conceptual framework for data and models. Global Change Biology 0.

Capps, K. A., R. Rancatti, N. Tomczyk, T. B. Parr, A. J. K. Calhoun, and M. Hunter. 2014. Biogeochemical Hotspots in Forested Landscapes: The Role of Vernal Pools in Denitrification and Organic Matter Processing. Ecosystems 17:1455–1468.

Castenson, K. L., and M. C. Rabenhorst. 2006. Indicator of Reduction in Soil (IRIS). Soil Science Society of America Journal 70:1222.

Chapman, S. K., M. A. Hayes, B. Kelly, and J. A. Langley. 2019. Exploring the oxygen sensitivity of wetland soil carbon mineralization. Biology Letters 15:20180407.

Chen, C., R. K. Kukkadapu, O. Lazareva, and D. L. Sparks. 2017. Solid-Phase Fe Speciation along the Vertical Redox Gradients in Floodplains using XAS and Mössbauer Spectroscopies. Environmental Science & Technology 51:7903–7912.

Chen, H., J. Zou, J. Cui, M. Nie, and C. Fang. 2018. Wetland drying increases the temperature sensitivity of soil respiration. Soil Biology and Biochemistry 120:24–27.

Climate Science Special Report: Fourth National Climate Assessment, Volume I. 2017. . Page 470. U.S. Global Change Research Program, Washington, DC, USA.

Cloy, J. M., C. A. Wilson, and M. C. Graham. 2014. Stabilization of Organic Carbon via Chemical Interactions with Fe and Al Oxides in Gley Soils: Soil Science 179:547–560.

Collins, M. E., and R. J. Kuehl. 2001. Organic matter accumulation in organic soils. Pages 137–162 *in* J. L. Richardson and M. J. Vepraskas, editors. Wetland Soils. Genesis, hydrology, landscapes, and classification. Lewis Publishers, CRC Press, Boca Raton, Florida.

Coward, E. K., A. T. Thompson, and A. F. Plante. 2017. Iron-mediated mineralogical control of organic matter accumulation in tropical soils. Geoderma 306:206–216.

Cowardin, L. M., V. Carter, F. C. Golet, and E. T. Laroe. 2005. Classification of Wetlands and Deepwater Habitats of the United States. Page *in* J. H. Lehr and J. Keeley, editors. Water Encyclopedia. John Wiley & Sons, Inc., Hoboken, NJ, USA.

Crawford, R. M. 2003. Seasonal differences in plant responses to flooding and anoxia. Canadian Journal of Botany 81:1224–1246.

Creed, I. F., J. Miller, D. Aldred, J. K. Adams, S. Spitale, and R. A. Bourbonniere. 2013. Hydrologic profiling for greenhouse gas effluxes from natural grasslands in the prairie pothole region of Canada. Journal of Geophysical Research: Biogeosciences 118:680–697.

Cronk, J. K., and W. J. Mitsch. 1994. Aquatic metabolism in four newly constructed freshwater wetlands with different hydrologic inputs. Ecological Engineering 3:449–468.

Dahl, T. E. 2011. Status and Trends of Wetlands in the Conterminous United States 2004 to 2009. Page 108. U.S. Department of the Interior; Fish and Wildlife Service, Washington, D.C.

Darke, A. K., and M. R. Walbridge. 1994. Estimating non-crystalline and crystalline aluminum and iron by selective dissolution in a riparian forest soil. Communications in Soil Science and Plant Analysis 25:2089–2101.

Davidson, E. A., E. Belk, and R. D. Boone. 1998. Soil water content and temperature as independent or confounded factors controlling soil respiration in a temperate mixed hardwood forest. Global Change Biology 4:217–227.

Day, F. P., and J. P. Megonigal. 1993. The relationship between variable hydroperiod, production allocation, and belowground organic turnover in forested wetlands. Wetlands 13:115–121.

Day, F. P., S. K. West, and E. G. Tupacz. 1988. The influence of ground-water dynamics in a periodically flooded ecosystem, the Great Dismal Swamp. Wetlands 8:1–13.

Denef, K., J. Six, H. Bossuyt, S. D. Frey, E. T. Elliott, R. Merckx, and K. Paustian. 2001. Influence of dry-wet cycles on the interrelationship between aggregate, particulate organic matter, and microbial community dynamics. Soil Biology:13.

Dwire, K. A., J. B. Kauffman, and J. E. Baham. 2006. Plant species distribution in relation to water-table depth and soil redox potential in montane riparian meadows. Wetlands 26:131–146.

Ebrahimi, A., and D. Or. 2016. Microbial community dynamics in soil aggregates shape biogeochemical gas fluxes from soil profiles - upscaling an aggregate biophysical model. Global Change Biology 22:3141–3156.

Elliott, E. T., C. A. Palm, D. E. Reuss, and C. A. Monz. 1991. Organic matter contained in soil aggregates from a tropical chronosequence: correction for sand and light fraction. Agriculture, Ecosystems & Environment 34:443–451.

Epting, S. M., J. D. Hosen, L. C. Alexander, M. W. Lang, A. W. Armstrong, and M. A. Palmer. 2018. Landscape metrics as predictors of hydrologic connectivity between Coastal Plain forested wetlands and streams. Hydrological Processes 32:516–532.

Evenson, G. R., C. N. Jones, D. L. McLaughlin, H. E. Golden, C. R. Lane, B. DeVries, L. C. Alexander, M. W. Lang, G. W. McCarty, and A. Sharifi. 2018. A watershed-scale model for depressional wetland-rich landscapes. Journal of Hydrology X 1:100002.

Fay, P. A., G. R. Guntenspergen, J. H. Olker, and W. C. Johnson. 2016. Climate change impacts on freshwater wetland hydrology and vegetation cover cycling along a regional aridity gradient. Ecosphere 7:e01504.

Fenner, N., and C. Freeman. 2011. Drought-induced carbon loss in peatlands. Nature Geoscience 4:895–900.

Fennessy, M. S., D. H. Wardrop, J. B. Moon, S. Wilson, and C. Craft. 2018. Soil carbon sequestration in freshwater wetlands varies across a gradient of ecological condition and by ecoregion. Ecological Engineering 114:129–136.

Fenstermacher, D. 2012. Carbon storage and potential carbon sequestration in depressional wetlands of the Mid-Atlantic region.

Fenstermacher, D. E., M. C. Rabenhorst, M. W. Lang, G. W. McCarty, and B. A. Needelman. 2014. Distribution, Morphometry, and Land Use of Delmarva Bays. Wetlands 34:1219–1228.

Fenstermacher, D. E., M. C. Rabenhorst, M. W. Lang, G. W. McCarty, and B. A. Needelman. 2016. Carbon in Natural, Cultivated, and Restored Depressional Wetlands in the Mid-Atlantic Coastal Plain. Journal of Environment Quality 45:743-.

Fiedler, S., and M. Sommer. 2004. Water and Redox Conditions in Wetland Soils—Their Influence on Pedogenic Oxides and Morphology. Soil Science Society of America Journal 68:326–335.

Fissore, C., C. P. Giardina, R. K. Kolka, and C. C. Trettin. 2009. Soil organic carbon quality in forested mineral wetlands at different mean annual temperature. Soil Biology and Biochemistry 41:458–466.

Gee, GW, and Bauder, JW. 1986. Particle-size analysis. Pages 383–411 *in* Klute, A, editor. Methods of soil analysis. Part 1. Physical and mineralogical methods. Soil Science Socitey of America, Madison, WI.

Gingerich, R. T., G. Merovich, and J. T. Anderson. 2014. Influence of environmental parameters on litter decomposition in wetlands in West Virginia, USA. Journal of Freshwater Ecology 29:535–549.

Gollany, H. T., T. E. Schumacher, P. D. Evenson, M. J. Lindstrom, and G. D. Lemme. 1991. Aggregate Stability of an Eroded and Desurfaced Typic Argiustoll. Soil Science Society of America Journal 55:811.

Grandy, A. S., and G. P. Robertson. 2007. Land-Use Intensity Effects on Soil Organic Carbon Accumulation Rates and Mechanisms. Ecosystems 10:59–74.

Griscom, B. W., J. Adams, P. W. Ellis, R. A. Houghton, G. Lomax, D. A. Miteva, W. H. Schlesinger, D. Shoch, J. V. Siikamäki, P. Smith, P. Woodbury, C. Zganjar, A. Blackman, J. Campari, R. T. Conant, C. Delgado, P. Elias, T. Gopalakrishna, M. R. Hamsik, M. Herrero, J. Kiesecker, E. Landis, L. Laestadius, S. M. Leavitt, S. Minnemeyer, S. Polasky, P. Potapov, F. E. Putz, J. Sanderman, M. Silvius, E. Wollenberg, and J. Fargione. 2017. Natural climate solutions. Proceedings of the National Academy of Sciences 114:11645–11650.

Halekoh, U., and S. Højsgaard. 2014. A Kenward-Roger Approximation and Parametric Bootstrap Methods for Tests in Linear Mixed Models – The R Package pbkrtest. Journal of Statistical Software 59:1–32.

Hall, S. J., A. A. Berhe, and A. Thompson. 2018. Order from disorder: do soil organic matter composition and turnover co-vary with iron phase crystallinity? Biogeochemistry 140:93–110.

Heckman, K., C. R. Lawrence, and J. W. Harden. 2018. A sequential selective dissolution method to quantify storage and stability of organic carbon associated with Al and Fe hydroxide phases. Geoderma 312:24–35.

Hefting, M., J. C. Clément, D. Dowrick, A. C. Cosandey, S. Bernal, C. Cimpian, A. Tatur, T. P. Burt, and G. Pinay. 2004. Water table elevation controls on soil nitrogen cycling in riparian wetlands along a European climatic gradient. Biogeochemistry 67:113–134.

Herndon, E., A. AlBashaireh, D. Singer, T. Roy Chowdhury, B. Gu, and D. Graham. 2017. Influence of iron redox cycling on organo-mineral associations in Arctic tundra soil. Geochimica et Cosmochimica Acta 207:210–231.

Hervé, P., S. D. Tiegs, S. Grellier, K. M. Wantzen, and F. Isselin-Nondedeu. 2019. Combined Effects of Vegetation and Drought on Organic-Matter Decomposition in Vernal Pool Soils. Wetlands 39:321–327.

Hijmans, R. J. 2019. raster: Geographic Data Analysis and Modeling. R package version 2.9-5.

Holm, S. 1979. A Simple Sequentially Rejective Multiple Test Procedure. Scandinavian Journal of Statistics 6:65–70.

Hossler, K., and V. Bouchard. 2010. Soil development and establishment of carbon-based properties in created freshwater marshes. Ecological Applications 20:539–553.

Hurtt, G., M. Zhao, R. Sahajpal, A. Armstrong, R. Birdsey, E. Campbell, K. A. Dolan, R. Dubayah, J. P. Fisk, S. A. Flanagan, C. Huang, W. Huang, K. D. Johnson, R. Lamb, L. Ma, R. Marks, D. O'Leary, J. O'Neil-Dunne, A. Swatantran, and H. Tang. 2019. Beyond MRV: High-resolution forest carbon modeling for climate mitigation planning over Maryland, USA. Environmental Research Letters.

Inglett, K. S., P. W. Inglett, K. R. Reddy, and T. Z. Osborne. 2012. Temperature sensitivity of greenhouse gas production in wetland soils of different vegetation. Biogeochemistry 108:77–90.

Johnson, W. C., B. V. Millett, T. Gilmanov, R. A. Voldseth, G. R. Guntenspergen, and D. E. Naugle. 2005. Vulnerability of Northern Prairie Wetlands to Climate Change. BioScience 55:863.

Jones, C. N. 2019. Depth_To_Water_Table. https://github.com/FloodHydrology/Depth_To_Water_Table.

Jones, C. N., G. R. Evenson, D. L. McLaughlin, M. K. Vanderhoof, M. W. Lang, G. W. McCarty, H. E. Golden, C. R. Lane, and L. C. Alexander. 2018. Estimating restorable wetland water storage at landscape scales. Hydrological Processes 32:305–313.

Kaiser, and G. Guggenberger. 2007. Sorptive stabilization of organic matter by microporous goethite: sorption into small pores vs. surface complexation. European Journal of Soil Science 58:45–59.

Kaiser, K., and G. Guggenberger. 2000. The role of DOM sorption to mineral surfaces in the preservation of organic matter in soils. Organic Geochemistry 31:711–725.

Kaiser, K., and K. Kalbitz. 2012. Cycling downwards – dissolved organic matter in soils. Soil Biology and Biochemistry 52:29–32.

Kaiser, M., M. Kleber, and A. A. Berhe. 2015. How air-drying and rewetting modify soil organic matter characteristics: An assessment to improve data interpretation and inference. Soil Biology and Biochemistry 80:324–340.

Keiluweit, M., K. Gee, A. Denney, and S. Fendorf. 2018. Anoxic microsites in upland soils dominantly controlled by clay content. Soil Biology and Biochemistry 118:42–50.

Kemper, W. D., and R. C. Rosenau. 1984. Soil cohesion as affected by time and water content. Soil Science Society of America Journal 48:1001–1006.

Kim, J., and S. Grunwald. 2016. Assessment of Carbon Stocks in the Topsoil Using Random Forest and Remote Sensing Images. Journal of Environment Quality 45:1910.

Kleber, M., R. Mikutta, M. S. Torn, and R. Jahn. 2005. Poorly crystalline mineral phases protect organic matter in acid subsoil horizons. European Journal of Soil Science 0:050912034650054.

Kögel-Knabner, I., G. Guggenberger, M. Kleber, E. Kandeler, K. Kalbitz, S. Scheu, K. Eusterhues, and P. Leinweber. 2008. Organo-mineral associations in temperate soils: Integrating biology, mineralogy, and organic matter chemistry. Journal of Plant Nutrition and Soil Science 171:61–82.

Kolka, R. K., C. Trettin, W. Tang, K. Krauss, S. Bansal, J. Drexler, K. Wickland, R. Chimner, D. Hogan, E. J. Pindilli, B. Benscoter, B. Tangen, E. Kane, S. Bridgham, and C. Richardson. 2018. Chapter 13: Terrestrial Wetlands. In Second State of the Carbon Cycle Report (SOCCR2): A Sustained Assessment Report. Pages 507–567. U.S. Global Change Research Program, Washington, DC, USA.

Koven, C. D., D. M. Lawrence, and W. J. Riley. 2015. Permafrost carbon−climate feedback is sensitive to deep soil carbon decomposability but not deep soil nitrogen dynamics. Proceedings of the National Academy of Sciences 112:3752–3757.

Krause, S., J. Lewandowski, N. B. Grimm, D. M. Hannah, G. Pinay, K. McDonald, E. Martí, A. Argerich, L. Pfister, J. Klaus, T. Battin, S. T. Larned, J. Schelker, J. Fleckenstein, C. Schmidt, M. O. Rivett, G. Watts, F. Sabater, A. Sorolla, and V. Turk. 2017. Ecohydrological interfaces as hot spots of ecosystem processes: ECOHYDROLOGICAL INTERFACES AS HOT SPOTS. Water Resources Research 53:6359–6376.

Kuznetsova, A., P. B. Brockhoff, and R. H. B. Christensen. 2017. lmerTest Package: Tests in Linear Mixed Effects Models. Journal of Statistical Software 82:1–26.

LaCroix, R. E., M. M. Tfaily, M. McCreight, M. E. Jones, L. Spokas, and M. Keiluweit. 2019. Shifting mineral and redox controls on carbon cycling in seasonally flooded mineral soils. Biogeosciences 16:2573–2589.

Lajtha, K., V. Bailey, K. McFarlane, K. Paustian, D. Bachelet, R. Abramoff, D. Angers, S. A. Billings, D. Cerkowniak, Y. G. Dialynas, A. Finzi, N. French, S. Frey, N. Gurwick, J. Harden, J. M. F. Johnson, K. Johnson, J. Lehmann, S. (Leo) Liu, B. McConkey, U. Mishra, S. Ollinger, D. Paré, F. Paz, D. deB. Richter, S. M. Schaeffer, J. Schimel, C. Shaw, J. Tang, K. Todd-Brown, C. Trettin, M. Waldrop, T. Whitman, and K. Wickland. 2018. Chapter 12: Soils. In Second State of the Carbon Cycle Report (SOCCR2): A Sustained Assessment Report. U.S. Global Change Research Program, Wsahington, DC.

Lang, M., G. McCarty, R. Oesterling, and I.-Y. Yeo. 2013. Topographic Metrics for Improved Mapping of Forested Wetlands. Wetlands 33:141–155.

Lang, M. W., and G. W. McCarty. 2009. Lidar intensity for improved detection of inundation below the forest canopy. Wetlands 29:1166–1178.

Lehmann, J., and M. Kleber. 2015. The contentious nature of soil organic matter. Nature.

Lewis, D. B., and S. J. Feit. 2015. Connecting carbon and nitrogen storage in rural wetland soil to groundwater abstraction for urban water supply. Global Change Biology 21:1704–1714.

Ligi, T., M. Truu, J. Truu, H. Nõlvak, A. Kaasik, W. J. Mitsch, and Ü. Mander. 2014. Effects of soil chemical characteristics and water regime on denitrification genes (nirS, nirK, and nosZ) abundances in a created riverine wetland complex. Ecological Engineering 72:47–55.

Lopez-Sangil, L., and P. Rovira. 2013. Sequential chemical extractions of the mineral-associated soil organic matter: An integrated approach for the fractionation of organo-mineral complexes. Soil Biology and Biochemistry 62:57–67.

von Lützow, M., I. Kögel-Knabner, K. Ekschmitt, H. Flessa, G. Guggenberger, E. Matzner, and B. Marschner. 2007. SOM fractionation methods: Relevance to functional pools and to stabilization mechanisms. Soil Biology and Biochemistry 39:2183–2207.

von Lützow, M., I. Kogel-Knabner, K. Ekschmitt, E. Matzner, G. Guggenberger, B. Marschner, and H. Flessa. 2006. Stabilization of organic matter in temperate soils: mechanisms and their relevance under different soil conditions - a review. European Journal of Soil Science 57:426–445.

Ma, Y., J. Li, J. Wu, Z. Kong, L. M. Feinstein, X. Ding, G. Ge, and L. Wu. 2018. Bacterial and Fungal Community Composition and Functional Activity Associated with Lake Wetland Water Level Gradients. Scientific Reports 8:1–12.

Maietta, C. E., Z. A. Bernstein, J. R. Gaimaro, J. S. Buyer, M. C. Rabenhorst, V. L. Monsaint-Queeney, A. H. Baldwin, and S. A. Yarwood. 2019. Aggregation but Not Organo-Metal Complexes Contributed to C Storage in Tidal Freshwater Wetland Soils. Soil Science Society of America Journal 83:252.

Mangiafico, S. S. 2016. Summary and Analysis of Extension Program Evaluation in R. 1.18.1. Web.

Márquez, C. O., V. J. Garcia, C. A. Cambardella, R. C. Schultz, and T. M. Isenhart. 2004. Aggregate-Size Stability Distribution and Soil Stability. Soil Science Society of America Journal 68:725.

Matteodo, M., S. Grand, D. Sebag, M. C. Rowley, P. Vittoz, and E. P. Verrecchia. 2018. Decoupling of topsoil and subsoil controls on organic matter dynamics in the Swiss Alps. Geoderma 330:41–51.

McCauley, L. A., M. J. Anteau, M. P. van der Burg, and M. T. Wiltermuth. 2015. Land use and wetland drainage affect water levels and dynamics of remaining wetlands. Ecosphere 6:art92.

McLatchey, G. P., and K. R. Reddy. 1998. Regulation of Organic Matter Decomposition and Nutrient Release in a Wetland Soil. Journal of Environment Quality 27:1268.

Mikutta, R., M. Kleber, M. S. Torn, and R. Jahn. 2006. Stabilization of Soil Organic Matter: Association with Minerals or Chemical Recalcitrance? Biogeochemistry 77:25–56.

Mikutta, R., D. Lorenz, G. Guggenberger, L. Haumaier, and A. Freund. 2014. Properties and reactivity of Fe-organic matter associations formed by coprecipitation versus adsorption: Clues from arsenate batch adsorption. Geochimica et Cosmochimica Acta 144:258–276.

Mitsch, W. J., B. Bernal, A. M. Nahlik, Ü. Mander, L. Zhang, C. J. Anderson, S. E. Jørgensen, and H. Brix. 2013. Wetlands, carbon, and climate change. Landscape Ecology 28:583–597.

Mitsch, W. J., and J. G. Gosselink. 2015. Wetlands. 5. ed. John Wiley and Sons, Inc, Hoboken, NJ.

Mitsch, W. J., A. Nahlik, P. Wolski, B. Bernal, L. Zhang, and L. Ramberg. 2010. Tropical wetlands: seasonal hydrologic pulsing, carbon sequestration, and methane emissions. Wetlands Ecology and Management 18:573–586.

Moore, T. R., and J. Turunen. 2004. Carbon Accumulation and Storage in Mineral Subsoil beneath Peat. Soil Science Society of America Journal 68:690–696.

Moreno-Casasola, P., M. E. Hernández, and A. Campos C. 2017. Hydrology, Soil Carbon Sequestration and Water Retention along a Coastal Wetland Gradient in the Alvarado Lagoon System, Veracruz, Mexico. Journal of Coastal Research 77:104–115.

Morse, J. L., M. Ardón, and E. S. Bernhardt. 2012. Greenhouse gas fluxes in southeastern U.S. coastal plain wetlands under contrasting land uses. Ecological Applications 22:264–280.

Moyano, F. E., S. Manzoni, and C. Chenu. 2013. Responses of soil heterotrophic respiration to moisture availability: An exploration of processes and models. Soil Biology and Biochemistry 59:72–85.

Nagelkerke, N. J. D. 1991. A note on a general definition of the coefficient of determination. Biometrika 78:691–692.

Nahlik, A. M., and M. S. Fennessy. 2016. Carbon storage in US wetlands. Nature Communications 7.

Neckles, H. A., and C. Neill. 1994. Hydrologic control of litter decomposition in seasonally flooded prairie marshes. Hydrobiologia 286:155–165.

Nelson, D. W., and L. E. Sommers. 1996. Total Carbon, Organic Carbon, and Organic Matter. Pages 961–1010 Methods of Soil Analysis. Part 3. Chemical Methods. Soil Science Society of America and American Society of Agronomy, Madison, WI.

Oades, J. M. 1988. The retention of organic matter in soils. Biogeochemistry 5:35–70.

Oregon State University. 2019. Parameter-elevation Regressions on Independent Slopes Model ("PRISM") Climate Group. http://www.prism.oregonstate.edu/.

Osland, M. J., C. A. Gabler, J. B. Grace, R. H. Day, M. L. McCoy, J. L. McLeod, A. S. From, N. M. Enwright, L. C. Feher, C. L. Stagg, and S. B. Hartley. 2018. Climate and plant controls on soil organic matter in coastal wetlands. Global Change Biology 24:5361–5379.

Palmer, M., and A. Ruhi. 2019. Linkages between flow regime, biota, and ecosystem processes: Implications for river restoration. Science 365:eaaw2087.

Park, E.-J., W. J. Sul, and A. J. M. Smucker. 2007. Glucose additions to aggregates subjected to drying/wetting cycles promote carbon sequestration and aggregate stability. Soil Biology and Biochemistry 39:2758–2768.

Pearse, A. L., J. L. Barton, R. E. Lester, A. Zawadzki, and P. I. Macreadie. 2018. Soil organic carbon variability in Australian temperate freshwater wetlands: Temperate wetland soil organic carbon variability. Limnology and Oceanography 63:S254–S266.

Pebesma, E. 2018. Simple Features for R: Standardized Support for Spatial Vector Data. The R Journal 10:439–446.

Pebesma, E. J., and R. S. Bivand. 2005. Classes and methods for spatial data in R. R News 5.
Phillips, P. J., and R. J. Shedlock. 1993. Hydrology and chemistry of groundwater and seasonal ponds in the Atlantic Coastal Plain in Delaware, USA. Journal of Hydrology 141:157–178.
Poeplau, C., C. Vos, and A. Don. 2017. Soil organic carbon stocks are systematically overestimated by misuse of the parameters bulk density and rock fragment content. SOIL 3:61–66.
Poff, N. L., J. D. Allan, M. B. Bain, J. R. Karr, K. L. Prestegaard, B. D. Richter, R. E. Sparks, and J. C. Stromberg. 1997. The Natural Flow Regime. BioScience 47:769–784.
Puget, P., C. Chenu, and J. Balesdent. 2000. Dynamics of soil organic matter associated with particle-size fractions of water-stable aggregates. European Journal of Soil Science 51:595–605.
R Development Core Team. (n.d.). R: A language and environment for statistical computing. https://www.r-project.org/.
Rabenhorst, M. C. 2018. A System for Making and Deploying Oxide-Coated Plastic Films for Environmental Assessment of Soils. Soil Science Society of America Journal 82:1301.
Rasmussen, C., K. Heckman, W. R. Wieder, M. Keiluweit, C. R. Lawrence, A. A. Berhe, J. C. Blankinship, S. E. Crow, J. L. Druhan, C. E. Hicks Pries, E. Marin-Spiotta, A. F. Plante, C. Schädel, J. P. Schimel, C. A. Sierra, A. Thompson, and R. Wagai. 2018. Beyond clay: towards an improved set of variables for predicting soil organic matter content. Biogeochemistry 137:297–306.
Reddy, K. R., and W. H. Patrick. 1975. Effect of alternate aerobic and anaerobic conditions on redox potential, organic matter decomposition and nitrogen loss in a flooded soil. Soil Biology and Biochemistry 7:87–94.
Riedel, T., D. Zak, H. Biester, and T. Dittmar. 2013. Iron traps terrestrially derived dissolved organic matter at redox interfaces. Proceedings of the National Academy of Sciences 110:10101–10105.
Rosenberry, D. O., and T. C. Winter. 1997. Dynamics of water-table fluctuations in an upland between two prairie-pothole wetlands in North Dakota. Journal of Hydrology 191:266–289.
Rubbo, M. J., J. J. Cole, and J. M. Kiesecker. 2006. Terrestrial Subsidies of Organic Carbon Support Net Ecosystem Production in Temporary Forest Ponds: Evidence from an Ecosystem Experiment. Ecosystems 9:1170–1176.
Scanlon, D., and T. Moore. 2000. CARBON DIOXIDE PRODUCTION FROM PEATLAND SOIL PROFILES: THE INFLUENCE OF TEMPERATURE, OXIC/ANOXIC CONDITIONS AND SUBSTRATE. Soil Science 165:153.
Schmidt, M. W. I., M. S. Torn, S. Abiven, T. Dittmar, G. Guggenberger, I. A. Janssens, M. Kleber, I. Kögel-Knabner, J. Lehmann, D. A. C. Manning, P. Nannipieri, D. P. Rasse, S. Weiner, and S. E. Trumbore. 2011. Persistence of soil organic matter as an ecosystem property. Nature 478:49–56.
Schuur, E. a. G., A. D. McGuire, C. Schädel, G. Grosse, J. W. Harden, D. J. Hayes, G. Hugelius, C. D. Koven, P. Kuhry, D. M. Lawrence, S. M. Natali, D. Olefeldt, V. E. Romanovsky, K. Schaefer, M. R. Turetsky, C. C. Treat, and J. E. Vonk. 2015. Climate change and the permafrost carbon feedback. Nature 520:171–179.

Semlitsch, R. D., and J. R. Bodie. 1998. Are Small, Isolated Wetlands Expendable? Conservation Biology 12:1129–1133.

Six, J., H. Bossuyt, S. Degryze, and K. Denef. 2004. A history of research on the link between (micro)aggregates, soil biota, and soil organic matter dynamics. Soil and Tillage Research 79:7–31.

Six, J., P. Callewaert, S. Lenders, S. De Gryze, S. J. Morris, E. G. Gregorich, E. A. Paul, and K. Paustian. 2002. Measuring and Understanding Carbon Storage in Afforested Soils by Physical Fractionation. Soil Science Society of America Journal 66:1981.

Six, J., E. T. Elliott, and K. Paustian. 2000. Soil macroaggregate turnover and microaggregate formation: a mechanism for C sequestration under no-tillage agriculture. Soil Biology and Biochemistry 32:2099–2103.

Skopp, J. M., M. D. Jawson, and J. W. Doran. 1990. Steady-state aerobic microbial activity as a function of soil water content.

Sodano, M., C. Lerda, R. Nisticò, M. Martin, G. Magnacca, L. Celi, and D. Said-Pullicino. 2017. Dissolved organic carbon retention by coprecipitation during the oxidation of ferrous iron. Geoderma 307:19–29.

Soil Survey Staff, Natural Resources Conservation Service, United States Department of Agriculture. (n.d.). Web Soil Survey. https://websoilsurvey.sc.egov.usda.gov/App/Help/Citation.htm.

Spivak, A. C., J. Sanderman, J. L. Bowen, E. A. Canuel, and C. S. Hopkinson. 2019. Global-change controls on soil-carbon accumulation and loss in coastal vegetated ecosystems. Nature Geoscience 12:685–692.

Stagg, C. L., M. M. Baustian, C. L. Perry, T. J. B. Carruthers, and C. T. Hall. 2018. Direct and indirect controls on organic matter decomposition in four coastal wetland communities along a landscape salinity gradient. Journal of Ecology 106:655–670.

Stolt, M. H., and M. C. Rabenhorst. 1987a. Carolina Bays on the Eastern Shore of Maryland: I. Soil Characterization and Classification1. Soil Science Society of America Journal 51:394.

Stolt, M. H., and M. C. Rabenhorst. 1987b. Carolina Bays on the Eastern Shore of Maryland: II. Distribution and Origin1. Soil Science Society of America Journal 51:399.

Sugimura, Y., and Y. Suzuki. 1988. A high-temperature catalytic oxidation method for the determination of non-volatile dissolved organic carbon in seawater by direct injection of a liquid sample. Marine Chemistry 24:105–131.

Tangen, B. A., and S. Bansal. 2019. Hydrologic Lag Effects on Wetland Greenhouse Gas Fluxes. Atmosphere 10:269.

Tarr, T. L., M. J. Baber, and K. J. Babbitt. 2005. Macroinvertebrate community structure across a wetland hydroperiod gradient in southern New Hampshire, USA. Wetlands Ecology and Management 13:321–334.

Tiner, R. W. 1996. Technical aspects of wetlands: Wetland definitions and classifications in the United States. US Geological Survey.

Tiner, R. W. 2003. Geographically isolated wetlands of the United States. Wetlands 23:494–516.

Torn, M. S., S. E. Trumbore, O. A. Chadwick, P. M. Vitousek, and D. M. Hendricks. 1997. Mineral control of soil organic carbon storage and turnover. Nature 389:170–173.

Totsche, K. U., W. Amelung, M. H. Gerzabek, G. Guggenberger, E. Klumpp, C. Knief, E. Lehndorff, R. Mikutta, S. Peth, A. Prechtel, N. Ray, and I. Kögel-Knabner. 2018. Microaggregates in soils. Journal of Plant Nutrition and Soil Science 181:104–136.

Trettin, C. C., B. Song, M. F. Jurgensen, and C. Li. 2001. Existing Soil Carbon Models Do Not Apply to Forested Wetlands. Gen. Tech. Rep. SRS-46. Asheville, NC: U.S. Department of Agriculture, Forest Service, Southern Research Station. 10 p. 046.

Villa, J. A., and B. Bernal. 2018. Carbon sequestration in wetlands, from science to practice: An overview of the biogeochemical process, measurement methods, and policy framework. Ecological Engineering 114:115–128.

Wagai, R., and L. M. Mayer. 2007. Sorptive stabilization of organic matter in soils by hydrous iron oxides. Geochimica et Cosmochimica Acta 71:25–35.

Wagai, R., L. M. Mayer, K. Kitayama, and Y. Shirato. 2013. Association of organic matter with iron and aluminum across a range of soils determined via selective dissolution techniques coupled with dissolved nitrogen analysis. Biogeochemistry 112:95–109.

Wahid, P. A., and N. V. Kamalam. 1993. Reductive dissolution of crystalline and amorphous Fe(III) oxides by microorganisms in submerged soil. Biology and Fertility of Soils 15:144–148.

Walter, K., A. Don, B. Tiemeyer, and A. Freibauer. 2016. Determining Soil Bulk Density for Carbon Stock Calculations: A Systematic Method Comparison. Soil Science Society of America Journal 80:579.

Watt, K., and S. Golladay. 1999. Organic Matter Dynamics in Seasonally Inundated, Forested Wetlands of the Gulf Coastal Plain. Wetlands 19:139–148.

Webster, K. L., I. F. Creed, F. D. Beall, and R. A. Bourbonnière. 2011. A topographic template for estimating soil carbon pools in forested catchments. Geoderma 160:457–467.

Webster, K. L., I. F. Creed, R. A. Bourbonnière, and F. D. Beall. 2008. Controls on the heterogeneity of soil respiration in a tolerant hardwood forest. Journal of Geophysical Research 113.

Webster, K. L., I. F. Creed, T. Malakoff, and K. Delaney. 2014. Potential Vulnerability of Deep Carbon Deposits of Forested Swamps to Drought. Soil Science Society of America Journal 78:1097.

Wickham, H. 2017. tidyverse: Easily Install and Load the Tidyverse. R package version 1.2.1. https://www.tidyverse.org/.

Wilke, C. 2019. cowplot: Streamlined Plot Theme and Plot Annotations for “ggplot2”. R package version 0.9.4). https://CRAN.R-project.org/package=cowplot.

Wright, A. L., and P. W. Inglett. 2009. Soil Organic Carbon and Nitrogen and Distribution of Carbon-13 and Nitrogen-15 in Aggregates of Everglades Histosols. Soil Science Society of America Journal 73:427.

Wright, E. L., C. R. Black, A. W. Cheesman, B. L. Turner, and S. Sjögersten. 2013. Impact of Simulated Changes in Water Table Depth on Ex Situ Decomposition of Leaf Litter from a Neotropical Peatland. Wetlands 33:217–226.

Yarwood, S. A. 2018. The role of wetland microorganisms in plant-litter decomposition and soil organic matter formation: a critical review. FEMS Microbiology Ecology 94.

Zedler, P. H. 2003. Vernal pools and the concept of “isolated wetlands.” Wetlands 23:597–607.

Zhao, Q., S. R. Poulson, D. Obrist, S. Sumaila, J. J. Dynes, J. M. McBeth, and Y. Yang. 2016. Iron-bound organic carbon in forest soils: quantification and characterization. Biogeosciences 13:4777–4788.

Zuur, A., E. N. Ieno, N. Walker, A. Saveliev, and G. Smith. 2009. Mixed Effects Models and Extensions in Ecology with R. Springer Science and Business Media.